ABSTRACT

Title of Dissertation: MITIGATION OF HIGH ALKALINITY IN LEACHATES OF AGED STEEL SLAG

Enes Özkök, Doctor of Philosophy, 2015

Dissertation directed by: Professor Allen P. Davis
Professor Ahmet H. Aydilek

Steel slag, an abundant by-product of the steel-making industry, after it is aged, has a huge potential for use as an aggregate in road construction. However, the high pH of steel slag seepage (pH≥12) is a major impediment in its beneficial use. Analyses on aged steel slag samples demonstrated that the alkalinity producing capacity of aged steel slag samples strongly correlated to $Ca(OH)_2$ dissolution and that prolonged aging periods have marginal effects on overall alkalinity.

Treatment methods that included bitumen-coating, bathing in Al(III) solutions and addition of an alum-based drinking water treatment residual (WTR) were evaluated based on reduction in pH levels and leachate alkalinity. 10% (wt./wt.) alum-based drinking water treatment residual (WTR) addition to slag was determined to be the most successful mitigation method, providing 65−70% reduction in alkalinity both in batch-type and column leach tests, but final leachate pH was only 0.5−1 units lower and leachates were contaminated by dissolved Al(+III) (≥3−4 mM). Based on the interpretation of calculated saturation indices and SEM and EDX analyses, formation of calcium sulfoaluminate

phases (i.e., ettringite and monosulfate) was suggested as the mechanism behind alkalinity mitigation upon WTR-modification.

The residual alkalinity in WTR-amended slag leachates was able to be completely eliminated utilizing a biosolids compost with high base neutralization capacity. In column leach tests, effluent pH levels below 7 were maintained for 58−74 pore volumes worth of WTR-amended slag leachate using 0.13 kg compost (dry wt.) per 1 kg WTR-amended slag on average; also, dissolved Al(+III) was strongly retained on the compost.

MITIGATION OF HIGH ALKALINITY IN LEACHATES OF AGED STEEL SLAG

by

ENES ÖZKÖK

Dissertation submitted to the Faculty of the Graduate School of the
University of Maryland, College Park, in partial fulfillment
of the requirements for the degree of
Doctor of Philosophy
2015

Advisory Committee:

Professor Allen P. Davis, Chair
Professor Ahmet H. Aydilek, Co-advisor
Professor Alba Torrents
Professor Birthe V. Kjellerup
Professor Mohamad I. Al-Sheikhly

ACKNOWLEDGEMENTS

First and foremost, I would like to thank my advisors, Professor Allen P. Davis and Professor Ahmet H. Aydilek for their guidance and patience throughout my graduate studies at the University of Maryland, College Park. I am very grateful to all of the faculty and staff members of the Department of Civil and Environmental Engineering for their resourcefulness and my fellow labmates for their companionship in the laboratory.

Lastly, thanks to my beloved family for their support and also a special thanks is owed to Diane Ye for her help on reviewing the manuscript.

TABLE OF CONTENTS

LIST OF TABLES

TABLE OF FIGURES

CHAPTER 1: INTRODUCTION

Steel slag is a by-product of the steelmaking industry that is rich in calcium and iron oxides. It is generated during both the refinement of crude iron and recycling of scrap steel in basic-oxygen and electric-arc furnaces and hence, its generation rate is a function of steel production. On average, 100−150 kg of steel slag is produced per metric ton of crude steel output (USGS, 2015a). The world crude steel production was doubled between the years of 2000 and 2014, becoming 1.7 billion metric tons (WSA, 2015), and the amount of steel slag produced worldwide in 2014 was estimated at 170−250 million metric tons (USGS, 2015b). The generation of steel slag in such large quantities makes the management of this industrial by-product an increasingly crucial environmental challenge. In addition to increasing annual generation rate, there are large amounts of steel slag stockpiled near the operational and closed steel mills that are still waiting to be handled for final disposal (Yildirim and Prezzi, 2009; Piatak et al., 2015).

Unless utilized, industrial solid by-products (e.g., steel slag, iron slag and coal combustion by-products) are usually landfilled occupying valuable storage space; thus, increasing beneficial use of steel slag in various applications instead of landfilling is an important issue in the context of sustainable waste management practices and industrial development. 35% of steel slag produced in Europe (Motz and Geiseler, 2001) and 15−40% in the U.S. (Yildirim and Prezzi, 2011) are dumped in landfill sites. Steel slag is a dense and durable material with favorable physical properties (e.g., good frictional properties, durability, hardness and skid resistance) either comparable to, or better than, natural aggregates (Motz and Geiseler, 2001; GHP, 2010). Conventionally, the primary method of beneficial use for it is utilization in civil engineering applications as an aggregate. In 2013, 82% of 7.8 million

metric tons of sold/used steel slag was utilized as aggregate, replacing natural aggregates in road construction, fills, and asphaltic concrete production (USGS, 2015a). However, pristine steel slag has a tendency to swell (volumetrically expand) in the presence of air moisture and/or water due to its rich hydratable mineral content (Juckes, 2003; Yildirim and Prezzi, 2011). The common practice to alleviate swelling, often called "aging", is allowing steel slag piles to weather through exposure to atmospheric conditions over a period of months, in order to hydrate and expand the steel slag prior to utilization in construction. In the United States, nineteen companies process and market steel slag using this method in 109 different locations (USGS, 2015a). Utilization of steel slag in other types of applications is usually not feasible. For example, unlike iron slag (blast-furnace slag), steel slag exhibits weak cementitious properties due to its low silica content and it is not suitable to use as a cement additive in concrete production or as a cement clinker feed (Alizadeh et al., 2003; Wang et al., 2013).

Aged steel slag has a huge potential to substitute natural aggregates in road bases/subbases, embankments and subgrades, where swelling at low rates after application is tolerable (Motz and Geiseler, 2001; Yildirim and Prezzi, 2009; Wang et al., 2010). With the current technology, using aged steel slag in road construction appears to be the most viable option to increase beneficial use of steel slag. Initiatives, such as the Green Highway Partnership in the U.S., also try to foster use of industrial solid by-products in road construction, in order to reduce consumption of natural materials as aggregates and energy used and emissions produced during the excavation and processing of natural materials (Edil, 2006; GHP, 2010). However, the growing number of studies elucidating the potential environmental impacts of steel slag increases the concerns over steel slag globally (Piatak

et al., 2015). As more encompassing and restricted environmental regulations are implemented, utilization of steel slag in large quantities may be impeded in the future despite the increase in slag generation rates.

The literature review demonstrates that the major environmental risk seems to be the high pH of steel slag leachates which is mainly attributed to weathering of CaO-containing constituents of steel slag. Calcium oxides in steel slags (30−65% based on dry weight) are found in the form of different mineral phases (Shi, 2004), such as lime, calcium silicates and calcium aluminates. Gradual weathering of all these CaO-containing compounds forms $Ca(OH)_2$, which disassociates and releases Ca^{2+} and hydroxide alkalinity (Yan et al., 2000). Consequently, rich CaO content of steel slags enables production of highly alkaline leachates (pH>12) over long periods of time and uncontrolled seepage from steel slag fills was reported to impair the quality of receiving surface waters and aquifers for decades (Koryak et al., 2002; Roadcap et al., 2005; Mayes et al., 2006; Riley and Mayes, 2015). Environmental regulations in the State of Maryland impose that a discharge cannot raise the pH in receiving waters over pH 8.5 (Hunter et al., 2014; COMAR, COMAR 26.08.02.033 A(4)). Additionally, extreme alkaline conditions can stimulate toxic trace element leaching from steel slag, especially Cr and V in the form of oxyanions, which are more mobilized under alkaline conditions (Proctor et al., 2000; Chaurand et al., 2007; De Windt et al., 2011).

Beneficial use of steel slags in lieu of natural aggregates can be cost-effective, especially in locations where local natural aggregate sources are limited; however, it is evident that steel slag causes a long-term alkalinity problem when left unchecked. At old steel slag dump sites, in situ remediation methods can include aeration to induce precipitation of

calcite and acid addition for neutralization (Roadcap et al., 2005; Mayes et al., 2006). However, these kinds of remediation methods require long-term investment and monitoring. In the case of steel slag use in road construction, where slag would be applied over a long stretch of land, such remediation methods are not feasible. In this context, it was hypothesized that a feasible treatment method should directly aim to hinder the formation of hydroxide alkalinity caused by hydration/dissolution of calcium oxides, instead of the more challenging task of neutralization of alkalinity after it is released. Additionally, favorable engineering properties of steel slag should be maintained after the treatment. Development of a feasible treatment method that alleviates alkalinity production capacity of aged steel slags can promote steel slag utilization in road construction in meaningful quantities and minimize the amount of landfilled and stockpiled steel slags.

Although there are numerous studies focusing on topics such as steel slag's mechanical properties (Shen et al., 2009; Wang et al., 2010; Sorlini et al., 2012), leaching behavior (Proctor et al., 2000; Chaurand et al., 2007; De Windt et al., 2011), hydration activity (Wang and Yan, 2010; Belhadj et al., 2014), and geochemistry (Roadcap et al., 2005; Mayes et al., 2008), no documented study exists on mitigation of alkalinity formation in aged steel slag leachates. By conducting this study, we aimed to fill the knowledge gap in alkalinity of aged steel slag samples and design a treatment method that allows for the utilization of steel slag in road construction without creating environmental risks, while maintaining favorable engineering properties of this industrial by-product.

Firstly, aged basic-oxygen furnace (BOF) steel slag samples that were weathered for ~6 months, ~1 year and 2+ years by a contractor were characterized for their alkalinity producing capacity. Next, three different types of treatment methods were devised to

decrease hydration reactions on the surface of slag particles. The effectiveness of each treatment procedure was evaluated through batch-type tests by comparing the reduction in leachate pH, alkalinity and dissolved Ca concentrations from the leachates of treated steel slags to the values obtained from the leachates of untreated steel slag. After the most promising treatment option was selected among different methods, the effectiveness of the alkalinity mitigation effect was tested in column tests simulating the field conditions in order to evaluate and validate the performance of the treatment method. Additionally, the predominant mechanism of alkalinity mitigation was investigated using various methods wet chemistry techniques and energy-dispersive X-ray spectroscopy in order to understand the limits and possible ways of improving the performance of the mitigation.

1.1. Literature Review

1.1.1. Chemical Composition and Physical Properties of Steel Slags

Steel is a crucial material for construction of infrastructure, urbanization and industrial development and steel slag generation increases in parallel to the increasing annual output of crude steel. World steel production increases every year and is driven by the economic growth of developing countries, especially India and China (WSA, 2013). From the year of 2000 to 2014, annual world crude steel production was doubled and became 1.67 billion metric tons; 49% of this was produced in China (WSA, 2015). Within the same time period (2000−2014), annual steel production in USA decreased from 102 million metric tons to 88 million metric tons (WSA, 2015).

Steel slag is generated as result of the interaction of fluxing agents (i.e., lime, limestone and dolomite) and impurities (e.g., Al, Si and P) in pig iron and scrap steel that are refined to produce steel (Lewis, 1992; Wintenborn and Green, 1998). Thus, steel slag has a

complex matrix structure that is mainly composed of fused oxides of calcium, iron, silicon, aluminum, magnesium, and manganese (Wintenborn and Green, 1998; Shi, 2004; Yildirim and Prezzi, 2011). Inside the hot ladle, lighter molten steel slag floats on top of the molten liquid steel and is tapped from the furnace separately. After steel slag is cooled and crushed, magnetic separators are used to recover entrained metals in steel slag, and the separated part of steel slag is returned to furnaces (USGS, 2013). Depending on the efficiency of the furnace, a certain amount of the iron can not be recovered during the conversion of the molten iron into steel and instead is trapped in the slag (USGS, 2013). Even after metal recovery, there is still a large quantity of slag available to be disposed of and/or to be re-used in various applications (Emery, 1984). The amount of marketable steel slag remaining after metal recovery processes is roughly equivalent to 10–15% of the crude steel output by weight (USGS, 2013). Accurate data on steel slag production in the United States is unavailable because the amount of generated steel slag is not routinely measured, but it was estimated to be in the range of 9 to 13 million metric tons in 2013 using the ratio of 100−150 kg of steel slag per metric ton of crude steel output and the data for U.S. steel production (USGS, 2015a).

There are two main types of steel-making slags that can be used as synthetic aggregates, each one named for the process from which they are generated; the basic-oxygen-furnace (BOF) process by which a mixture of molten pig iron and a low amount of steel scrap is converted to steel, and the electric-arc-furnace (EAF) process which is mostly used to recycle steel scraps (Fruehan, 1998). Although chemical composition of steel slag slightly varies for each type of metallurgical process and from plant to plant, the steel slags from different sources are generally comparable (Proctor et al., 2000; Motz and Geiseler, 2001).

Differences arise from the use of dolomite rather than lime, with the effect of a higher MgO-content in steel slag (Motz and Geiseler, 2001).

The main chemical constituents of BOF slag are silica, iron oxides and lime. The percentage of Ca, Fe and Si oxide contents in BOF slag by weight are 36−52%, 14−34% and 7−18%, respectively (Yildirim and Prezzi, 2009). BOF slag has a low silica content and is not self-cementitious. The lack of silicate in the chemical composition results in limited dicalciumsilicate formation and a higher uncomplexed free lime content (Motz and Geiseler, 2001).

The electric-arc furnace (EAF) steelmaking process involves mainly recycling steel scraps. EAFs use high-power electric arcs to produce heat and melt the recycled steel scrap, in order to produce refined high quality steel. Oxygen is injected to the furnace through an oxygen lance; fluxing agents are fed to the furnace either together with scrap steel or during melting (USGS, 2013). EAF slag contains high amounts of CaO and has low silica content, similar to BOF slag. The main difference between EAF slag compared to BOF slag is the higher Fe and Al oxide contents; the percentage of Ca, Fe, Si and Al oxide contents in EAF by weight are 22−60%, 18−42%, 6−18% and 3−14%, respectively (Yildirim and Prezzi, 2011).

There are other metallurgical processes that generate different types of slags. Another type of steel slag is ladle slag (or failing slag). Ladle slag has a very high percentage of fine powder, which makes materials handling more difficult and makes it unsuitable for use as aggregates (Yildirim and Prezzi, 2009). There is also iron-making slag, or blast-furnace (BF) slag, and it is also largely used as an aggregate –more commonly as compared to steel

slag– but it should not be confused with steel slag. The blast furnace is a type of metallurgical furnace where the iron ore is smelted and crude iron is produced. A blast furnace can be integrated with a steel mill and hence both iron-making slag and steel slag can be produced within the same facility. Blast-furnace (BF) slag has different chemical compositions and pozzolanic properties. The rich silica content of iron ore is retained in BF slag during iron production; thus, calcium in the fluxing agents are mostly reacted with silica from ore at high temperatures and CaO in BF slag is in the form of calcium silicates; free lime content is low due to the high silica content (Yildirim and Prezzi, 2009). BF slag is commonly utilized as an additive in cement and concrete production and utilization of BF slag in highway construction is not impeded because it is volumetrically more stable.

Steel slag bears physical features that are comparable or even more favorable compared to natural aggregates and hence, it is usually used in various engineering applications (Wintenborn and Green, 1998; Motz and Geiseler, 2001). Steel slag is a durable and dense material due to its significant iron content (Ahmedzade and Sengoz, 2009). The bulk density of steel slags is within the range of 3.1−3.7 g/cm^3 and higher than basalt (2.8−3.1 g/cm^3) and granite (2.6−2.8 g/cm^3) (Juckes, 2003). The density of steel slag increases with increasing iron oxide content (Yildirim and Prezzi, 2011) and the maximum dry unit weight is in ranges from 20−26 kN/m^3 and optimum moisture content changes between 3% and 12% (Yildirim and Prezzi, 2011). Steel slag has a high bearing capacity and excellent frictional properties, and is also resistant to abrasion and polishing (Motz and Geiseler, 2001; GHP, 2010). Steel slags show a variable gradation with a wide range of particle sizes. Typically, the percentage of silt-size particles is in the range of 10−15% (Barra et al., 2001).

1.1.2. Swelling Phenomenon

Although steel slag is considered to have favorable engineering properties, its high hydratable content impedes its use immediately after its generation (Motz and Geiseler, 2001; Juckes, 2003). The intentional addition of Ca-based compounds as fluxing agents in order to purify final product (crude steel) generates a porous by-product (steel slag), which is rich in free (unhydrated) calcium oxide and other hydratable oxides. Once steel slag contacts air moisture and/or porewater, it exhibits a tendency to volumetrically expand which is predominantly attributed to free (unhydrated) lime (CaO) and free magnesium oxide (MgO) (Juckes, 2003; Yildirim and Prezzi, 2009). In the presence of water, CaO in steel slag is rapidly react and transforms to $Ca(OH)_2$ (Eq. 1.1). Since $Ca(OH)_2$ has a lower bulk density compared to CaO, the transformation as a result of hydration causes steel slag to volumetrically expand, also referred as "swelling" (Yildirim and Prezzi, 2011). Weathering of MgO in steel slag composition also contributes to swelling, analogous to CaO (Eq. 1.2).

$$CaO + H_2O \leftrightarrow Ca(OH)_2 \quad (1.1)$$

$$MgO + H_2O \leftrightarrow Mg(OH)_2 \quad (1.2)$$

To effectively utilize steel slag in both bound and unbound sections of the road, it is important to assess its swelling potential. Volumetric instability due to swelling can result in unevenness and cracks in the superstructure, such as pavement surfaces. The common practice for alleviating swelling effects prior to employing steel slag in engineering applications is open-air stockpiling of the steel slag to provide adequate exposure to atmospheric conditions for an extended period of time, often called "aging" (Juckes, 2003). During the aging period, piles of steel slag are gradually weathered and labile CaO and

MgO in steel slag are reacted through hydration, carbonation and oxidation reactions (Juckes, 2003). While carbonation and oxidation of steel slag are also expansive reactions, compared to hydration reactions, their contribution to swelling are considered to be insignificant (Yildirim and Prezzi, 2009). If aging is properly conducted, most of the hydration reactions can complete prior to utilization of steel slag. It is recommended that steel slag is aged/cured for at least 6 months before it is used (Yildirim and Prezzi, 2009). Sorlini et al. (2012) claimed that EAF should be aged for 2-3 months to decrease swelling below ASTM limit of 0.5% (ASTM, 2009). Many state departments of transportation in the United States that use slag publish their own standards on how to conduct aging and evaluate the suitability of aged slag (SCDOT, 2007; KYTC, 2012; ODOT, 2013).

Although aging is a common practice, it appears that the chemical changes occurred during aging are not carefully considered in most cases, whereas mitigation of swelling is always considered as the priority. However, weathering over long periods of time can create conditions causing more leaching for toxic elements. Suer et al. (2009) performed accelerated aging of a steel slag sample and reported decreased Ca, Cu, Ba, Fe, Mn, Pb leaching but increased V, Si, and Al leaching.

Another challenge that arises with steel slag utilization in highway construction is tufa formation due to saturation of carbonated calcium compounds in slag leachate that is exposed to atmospheric CO_2, resulting in precipitation of calcium carbonates (Yildirim and Prezzi, 2009). Tufa formation can plug the drainage systems of highways.

1.1.3. Alkalinity of Steel Slag

As mentioned above, steel slag is rich in free calcium oxide (Eq. 1.1), magnesium oxides (Eq. 1.2), calcium silicates (Eq. 1.3 and 1.4) and calcium aluminoferrites (Eq. 1.5) (Shi, 2004). All these Ca- and Mg-based compounds have the potential to hydrate and eventually generate Ca and Mg hydroxides in the presence of water, although rates of reactions may vary largely (Yan et al., 2000). Dissolution of Ca and Mg hydroxides (Eq. 1.6 and 1.7) load permeating porewater with high alkalinity and create leachates that are highly alkaline and slightly reducing (van Zomeren et al., 2011).

$$2\ (CaO)_2{\cdot}SiO_2 + 4\ H_2O \leftrightarrow (CaO)_3{\cdot}(SiO_4)_2{\cdot}3\ H_2O + Ca(OH)_2 \quad (1.3)$$

$$2\ (CaO)_3{\cdot}SiO_2 + 6\ H_2O \leftrightarrow (CaO)_3{\cdot}(SiO_4)_2{\cdot}3\ H_2O + 3\ Ca(OH)_2 \quad (1.4)$$

$$(CaO)_4{\cdot}Al_2O_3{\cdot}Fe_2O_3 + 10\ H_2O \leftrightarrow (CaO)_3{\cdot}Al_2O_3{\cdot}6\ H_2O + 2\ Fe(OH)_3 + Ca(OH)_2 \quad (1.5)$$

$$Ca(OH)_{2\,(s)} \leftrightarrow Ca^{2+}{}_{(aq)} + 2\ OH^-{}_{(aq)} \quad (1.6)$$

$$Mg(OH)_{2\,(s)} \leftrightarrow Mg^{2+}{}_{(aq)} + 2\ OH^-{}_{(aq)} \quad (1.7)$$

C-S-H (calcium silicate hydrate) gel and $Ca(OH)_2$ are the main hydration products of steel slag, and the hydration rate of steel slag is stimulated at high pH (Wang and Yan, 2010). Chemical composition is an important parameter to determine the hydration activity of steel slag. The alkalinity of leachates from steel slag results mainly due to dissolution of $Ca(OH)_2$; hence, the major dissolved ion in slag leachates is Ca^{2+} (Xu et al., 2012). In order to define and model the acid-base characteristic of the steel slags, natural pH of the leachate, total concentration of dissolved acidic or alkaline substances, and the acid or base neutralizing capacity should be known.

This high alkalinity does not only produce an apparent high pH ~12.5, but also gives steel slag suspensions a high capacity to neutralize strongly acidic media (Navarro et al., 2010). The high acid neutralizing capacity (ANC) of steel slag makes it an attractive and economic material for neutralizing acid mine drainage (AMD). Simmons et al. (2001) conducted batch-type sequenced leaching tests using steel slags from four different sources. 100-g steel slag was agitated in 2-L AMD in cycles (contact time=18 h) and at the end of each cycle, the pH of the filtered effluent was measured. After 16-30 cycles, the effluent pH decreased to pH ~7 from initial pH of 10−12. Mayes et al. (2006) investigated the remediation of high-pH (>12) steel slag (CaO content= 42% wt.) leachate by letting the leachate flow through a wetland covering an area of around 1500 m^2. The alkaline leachate was supersaturated with respect to calcite upstream of the wetland (SI calcite values +2.3) and became less saturated as it travelled across the wetland, to SI calcite values of +0.27 at the wetland outlet; the pH of the wetland outlet became ~8.

The results mentioned above shows that acid-neutralization capacity due to hydration of high lime, MgO and other basic compounds is able to provide very high alkalinity over a long term (Yildirim and Prezzi, 2009). However, acid-base properties of solid wastes are usually analyzed using short-term titration tests without considering the long-term reactivity of the solid waste. In order to evaluate long-term acid neutralizing capacity (ANC) of an EAF steel slag (22% Ca on dry wt. basis), Yan et al. (2000) conducted acid titration tests using HNO_3 for 4000 h. Their findings suggested that only 60% of long-term ANC could be counted in 24-h titration tests and the experiments should be run for at least 500 hours to obtain 95% of the long-term ANC of the steel slag. Short-term ANC was mainly produced by rapid hydration of free CaO and MgO, whereas long-term ANC

depended on slow dissolution of Ca-aluminosilicates. Yan et al. (2000) also observed that the acid neutralizing capacities of the steel slag are different for different pH levels. Most of the capacities were consumed in a relatively high pH range (above pH 8.5), indicating that carbonation of steel slag does not significantly decrease leachate pH (Yan et al., 2000).

Limited effect of carbonation of hydrated calcium and magnesium compounds were confirmed in studies investigating carbonation of steel slags for atmospheric CO_2 sequestration (Huijgen and Comans, 2006; Baciocchi et al., 2009; Xu et al., 2012). Huijgen and Comans (2006) conducted accelerated carbonation of steel slag (CaO content= 32% wt., pH 12.4) under high CO_2 pressure (19 bar); however, even 74% carbonated (relative to total Ca content) samples had a pH 9.4 that was significantly higher than the pH of a solution saturated with calcite (pH 8.3).

Suer et al. (2009) investigated the chemical composition of a 10-year-old road base containing steel slag. The chemical composition of the samples from the 10-year-old road base showed no significant difference compared to fresh steel slag; hydration and carbonation effects were minimal and the leachate pH of the aged slag was 11.6 (initial pH value was 12.2 that was measured prior to application) (Suer et al., 2009). On the other hand, the study by Fällman (2000) reported steel slag leachates pH values ranging from 8.5 to 9.5 in lysimeter tests, compared to leachate pH ~12 for the same material in batch-type tests. Even under atmospheric conditions, it appears to be very hard to neutralize alkalinity of steel slag leachates.

1.1.4. Elemental Leaching from Steel Slag

The major constituents of steel slags are environmentally benign oxides of calcium, iron, and silicon. Additionally, steel slags contain heavy metals (antimony, arsenic, barium, beryllium, cadmium, chromium, cobalt, copper, lead, mercury, nickel, selenium, thallium, vanadium, etc.) at concentrations higher than those in background soils (Proctor et al., 2000). The potential environmental impact that may be caused by the release of pollutants in the slag at alkaline conditions can also impede the use of steel slag as an aggregate in highway bases.

The most extensive investigation on leaching behavior of steel slags in the literature was conducted by Proctor et al. (2000), who studied the leaching potential of 73 composite iron- and steel-making slag samples from 58 steel mills throughout the United States and Canada and analyzed the results using statistical methods. The mobility of heavy metals (i.e., As, Ba, Cd, total Cr, Cr^{VI}, Hg, Se and Ag) under acidic conditions was analyzed using Toxicity Characteristic Leaching Procedure (TCLP) tests described in the U.S. Environmental Protection Agency Method 1311. Despite having much higher metal concentrations compared to background soils, the results from TCLP tests demonstrated that none of the steel slag samples exceeded the EPA standards for hazardous materials. Also, ASTM water leach tests, WLT, (ASTM, 2006a) were performed on a representative number of samples for each slag type (BF, BOF, and EAF slag samples) in order to assess the mobility of 27 elements (plus hexavalent chromium). According to the WLT results, metal leaching was low relative to total metal content (<1%) and metals mostly remained bonded to the slag matrix even under harsh weathering conditions simulated in WLTs (solid-to-liquid ratio=1:20 g/mL, tumbled for 18 hours). It was concluded that the potential

for metals to leach from slag and migrate through environmental media is lower than from soil. Although the leachate pH from the WLT samples were 11−12 and the solubility of Se and Cr increased with increasing pH unlike other metals analyzed in that study, the relative mobility of these two metals in steel slags were still lower compared to Se and Cr in soils.

The most abundant heavy metal present in steel slags is chromium and the second element with the highest concentration in steel slags is another toxic metal, vanadium (Proctor et al., 2000). Accordingly, studies investigating heavy metal leaching from steel slags are usually focused on these two elements. Chaurand et al. (2007) showed that BOF slag leached almost up to 0.5% of its total vanadium content at pH 5 throughout the duration of batch-type water leach tests (L:S =1:30 g/mL, 47 days). On the other hand, highest Cr leaching was always below 0.02% of the total Cr content. The oxidation states of Cr and V in BOF slag was determined as +III and +IV, respectively, using X-ray absorption spectroscopy (XAS) (Chaurand et al., 2007). De Windt et al. (2011) reported that the redox conditions in steel slag leachates were slightly reducing, ranging from −0.3 to +0.3 mV and that Cr in steel slag was completely in the form of Cr(III) due to the reducing nature of the slag. Cr release was less than 0.05% of total Cr content; V leached up to 1.7% of its total content (De Windt et al., 2011).

The literature shows that inorganic pollutant leaching from steel slags is usually very low, because the high calcium and iron levels create an environment that is generally conducive for sequestration of these pollutants. The retention capacity of alkaline steel slag was reported in numerous studies. In the study by Simmons et al. (2001), Fe, Al, Mn, Ca, Mg, Ag, As, Ba, Be, Cd, Cr, Cu, Hg, Pb, Ni, Sb, Se, Tl, V, and Zn were analyzed. Their

findings showed that at least 83% of metals in acid mine drainage were sequestrated by steel slag.

There are many studies which focused on removing P using steel slags as a sorbent surface (Drizo et al., 2006; Pratt et al., 2007; Claveau-Mallet et al., 2013). Results from these studies demonstrated the highly efficient P removal capacity of slag due to adsorption onto ferric iron oxides and precipitation of hydroxyapatite ($Ca_5(PO_4)_3OH$). Grubb et al. (2011) investigated the possibility of arsenate removal using steel slag as a sorbent, and demonstrated that steel slag from Sparrow Points, MD was able to retain a significant amount of arsenate, which has a similar configuration to phosphate. Zhou and Haynes (2011) found that steel slag and BF slag exhibited high adsorption affinity for spiked heavy metal cations, especially for Cu, Pb and Cr, at pH 4, 6 and 8. Ortiz et al. (2001) reported significant nickel removal from the solution using slag and demonstrated that the adsorption process followed the Freundlich isotherm model.

1.1.5. Steel Slag as an Aggregate in Construction

Despite its swelling potential and high alkalinity producing capacity, steel slag is a durable and dense synthetic material due to its significant iron content and is being used to replace natural aggregates in construction of surface layers of the pavement and unbound sections of the road such as bases and subbases (Ahmedzade and Sengoz, 2009). The USGS (2013) reported that in total, 7.3 million metric tons of steel slag were utilized in 2011; 46.5% was used in construction of road bases and surfaces; 12.1% was used in asphaltic concrete production.

The primary concern about using steel slag in road bases and subbases is its volumetric expansion capacity mainly due to hydration of its free lime content (Motz and Geiseler, 2001). On the other hand, Suer et al. (2009) reported no apparent chemical change due to carbonation or hydration on EAF slag samples from the subbase of a 10-year old asphalt road. Wang et al. (2010) simulated volumetric expansion of steel slag using a semi-empirical model and calculated that steel slag containing a free lime content up to 3.7–3.9% under the weight of a 10-cm thick upper layer of asphalt pavement might be used in road base construction. Shen et al. (2009) proposed a recipe for preparing a solidified material composed of a mixture of steel slag, fly ash and phosphogypsum to be used in road bases, in order to reduce the risk of reflective cracking of pavement above the base.

Reuse of steel slag as an aggregate to produce asphaltic concrete has been studied since 1970s (Sorlini et al., 2012). There are a large number of studies investigating the swelling properties and durability of steel slag aggregates in bituminous pavement construction and all studies agreed that replacing steel slag with natural aggregates in asphaltic concretes relatively improved mechanical properties (Wu et al., 2007; Ahmedzade and Sengoz, 2009; Pasetto and Baldo, 2011; Arabani and Azarhoosh, 2012; Behnood and Ameri, 2012; Sorlini et al., 2012; Xie et al., 2013). Steel slag utilization in asphaltic concrete production resulted in a final product that was more resistant to low temperature cracking, permanent deformation at high temperature, and abrasion and friction (Wu et al., 2007; Ahmedzade and Sengoz, 2009; Behnood and Ameri, 2012). Wu et al. (2007) found out that the volume properties of stone mastic asphalt (SMA) mixture prepared with steel slag satisfied the related specifications and expansion rate below 1% after seven days and reported that test roads showed excellent performance after two years of service. Moreover, steel slag retains

heat longer than conventional natural aggregates, which can be beneficial during cold weather applications (Ahmedzade and Sengoz, 2009). High alkalinity of steel slag also causes better bonding between bitumen binder and slag particles (Xie et al., 2013). Furthermore, asphaltic concrete containing steel slag has higher electrical conductivity and hence, it can be utilized to produce conductive thermo-electrical asphalt pavements of roads and airfield runways where de-icing is necessary (Ahmedzade and Sengoz, 2009).

While there were overwhelming results of improvements on performance of asphaltic concrete containing steel slag, some of the studies reported concerns about slag utilization in this way. Sorlini et al. (2012) investigated metal leaching from bitumen/aged steel slag mixtures and found that releases of all measured pollutants were generally lower than that of steel slag alone, but dissolved organic carbon (DOC) concentrations were very close to limit values and V leaching seemed not to be affected by the presence of bitumen binder around slag particles. Steel slag has porous surfaces and hence it can absorb more bitumen relative to natural aggregates (Ahmedzade and Sengoz, 2009). A slag aging period of minimum two to three months must be allowed before use, in order to reduce swelling rate to an acceptable level (Sorlini et al., 2012).

1.1.6. Other Possible Uses of Steel Slag

According to USGS (2013), 4.7% of the sold steel slag in 2011 was utilized as a cement clinker raw material. However, it must be used in a fine powder form to ensure a higher cementitious activity (Wang et al., 2011). Even in this case, steel slag replacement with conventional raw materials produced a weaker cement, which required a longer setting period and exhibited lower compressive strength, higher porosity, and higher permeability in the long-term (Kourounis et al., 2007; Wang et al., 2013). Besides, steel slag is a durable

and hard material. Thus, it is not feasible to grind steel slag by mechanical means (Wang et al., 2013). Steel slag's lack of silica and high ferric oxide content renders it unsuitable to be utilized in concrete production (Alizadeh et al., 2003).

A relatively more recent research topic is investigation of carbon sequestration methods using steel slag. Steel slag has a high calcium and magnesium content; hence, it is considered as a Ca and Mg source and can act as a CO_2 sink (Huijgen and Comans, 2006; Baciocchi et al., 2009; van Zomeren et al., 2011; Chang et al., 2013; Said et al., 2013). Said et al. (2013) suggested a carbonation process involving selective Ca extraction using an aqueous solution of ammonium salt to obtain a Ca-rich slurry. Another approach is to use steel slag particles and directly react it with CO_2 (Huijgen and Comans, 2006; Baciocchi et al., 2009; van Zomeren et al., 2011; Chang et al., 2013). Huijgen and Comans (2006) described the carbonation mechanism as: first, free lime in steel slag rapidly hydrates, dissolves and then forms calcite; once free lime is consumed, further carbonation requires leaching of Ca in Ca-silicates and this can be hindered by calcite precipitation on the surface and formation of a Ca-depleted silicate layer around particles.

Although carbon sequestration has been achieved in the laboratory, this technique is still in its infancy and there is no existing commercial application (Yi et al., 2012). The ultimate degree of carbonation and overall efficiency of the process for all types of processes were reported to greatly depend on particle size; reducing the particle size of steel slag improved the carbonation efficiency (Huijgen and Comans, 2006; Baciocchi et al., 2009; van Zomeren et al., 2011; Chang et al., 2013; Said et al., 2013). However, it should be considered that grinding steel slag will result in more CO_2 emissions (Chang et al., 2013). Besides, most of these carbon sequestration processes are required to be carried out under

high pressure and high temperature for high carbonation efficiency (Huijgen and Comans, 2006; Baciocchi et al., 2009; Chang et al., 2013). Furthermore, an increase in V leaching upon carbonation was reported by Huijgen and Comans (2006) and van Zomeren et al. (2011), suggesting V association primarily to Ca-phases in steel slag.

Another beneficial reuse of steel slag is its utilization as an agricultural soil amendment, since steel slag contains significant amounts of elements that are beneficial for plant growth such as Ca, Fe, Mg, Mn and P (Yi et al., 2012). It is reported that steel slag application can remedy Fe-deficiency in calcareous soils (Wang and Cai, 2006). Besides, steel slag's alkalinity-producing capacity along with its rich nutrient content may be used to remediate acidic soils. However, any land application involving steel slag demands careful testing and handling due to potentially hazardous impurities in steel slag. Mäkelä et al. (2012) demonstrated the promising potential of steel slag mixed with wastes from the paper-making industry as a soil conditioner for acidic soils, but elevated Cr and V leaching were noted as the result of steel slag use, compared to other tested mixtures. Therefore, improperly handled land applications can result in overloading soil in terms of toxic contaminants. A study from Sweden positively correlated improper land application of steel slag (containing ~3% vanadium by weight) and vanadium-poisoning in grazing animals (Frank et al., 1996).

Other possible uses of steel slag reported in literature are: stabilization of fine grained soils, where slag acts as a binder (Poh et al., 2006); neutralization of acid mine drainage (Simmons et al., 2001); utilization in landfill cover construction (Diener et al., 2010; Andreas et al., 2014); treatment of dredged sediments (Miraoui et al., 2012); and immobilization of heavy metals (Ortiz et al., 2001; Jagupilla et al., 2012) and phosphorous

(Drizo et al., 2002; Drizo et al., 2006; Bowden et al., 2009; Barca et al., 2012a; Barca et al., 2012b) in wastewater or stormwater.

CHAPTER 2: TREATMENT METHODS FOR MITIGATION OF HIGH ALKALINITY IN LEACHATES OF AGED STEEL SLAG

2.1. Introduction

The objective of the experimental studies presented in this chapter was to develop new treatment procedures with the aim of reducing the alkalinity of aged steel slag leachates by hindering $Ca(OH)_2$ dissolution and to investigate the extent of resulting alkalinity mitigation levels to a feasible treatment procedure. For this purpose, different types of batch tests were conducted on basic-oxygen furnace slag samples, which were aged for different periods of time, to characterize the alkalinity producing capacities of aged slag samples and to investigate the relationship between Ca(+II) release and hydroxide alkalinity in order to confirm the source of the alkalinity from steel slag as $Ca(OH)_2$. Next, three treatment methods were devised and evaluated based on dissolved the reduction in Ca(+II) concentrations and leachate pH values to determine the metrics for each procedure, where the performance was of the procedure was optimum. Alkalinity measurements were conducted on filtered effluents to quantify the changes in alkalinity of the leachates from various treated steel slags.

The first treatment that was tested was “bitumen coating”. It was assumed that mixing hot bitumen with steel slag can provide a physical barrier over the steel slag particles and reduce water contact during WLTs. The second treatment method involved bathing steel slag in Fe(III), Al and phosphate salts and was referred as “passivation”. Here it was hypothesized that precipitation of metal hydroxides or Ca-P complexes as a layer on steel slag particles might alter the properties of the steel slag surface and hinder hydration reactions. Preliminary results from passivation treatment showed that aluminum sulfate

had a significant effect on Ca release; thus, the third treatment method was simply mixing steel slag and an alum-based drinking water treatment residual (WTR) under dry conditions.

2.2. Materials and Methods

2.2.1. BOF Steel Slag Samples and Other Materials

Aged BOF steel slags originated from a steel mill in Maryland, USA were collected from 6-month-old (6M), 1-year-old (1YR) and more than 2-year-old (2YRS) steel slag piles. Basic oxygen furnace (BOF) slag is a by-product of the conversion of pig iron to steel; it is formed through fusion of Ca-based fluxing agent and impurities in the pig iron at high temperature in basic-oxygen furnace, along with large amounts of inseparable iron trapped in its complex structure. Steel slags have a swelling tendency due to their rich hydratable constituents and the residual unreacted fluxing agent in their content. It is imperative that steel slags are aged to minimize its tendency for volumetric expansion. Aging process involves allowing steel slag piles to weather through exposure to atmospheric conditions over extended periods of time, in order to hydrate steel slag. Since aging of steel slag is standard practice before utilization in road construction, only aged steel slag samples were used in this study. Aged steel slag samples were oven-drying for 24 hours at 105°C and then they were sieved through a U.S. #10 sieve (opening size=2.00 mm) and #16 (1.18 mm) sieves. Only the particles steel slag retained on the U.S. #16 sieve (1.18 mm–2.00 mm) was used in further tests (Figure 2.1a). The two reasons for using the portion of slag with small diameter and within a very narrow size range were: (1) to account for the smaller size of the testing equipment used in water leach tests, and (2) to minimize variation between independent test runs due to possible changes in particle size distribution.

Performance-Graded 64-22, per AASHTO M 320-10, asphalt binder bitumen was used to coat steel slag samples (AASHTO, 2010). Water treatment residual (WTR) was obtained from the Rockville drinking water treatment plant in Potomac, Maryland. WTR, an aluminum-based sludge, is a by-product of the drinking water treatment process that uses alum [$Al_2(SO_4)_3 \cdot xH_2O$] as a coagulant in the primary clarification tank. WTR was in cake form (21% dry solids) when brought to the laboratory. Prior to the tests, WTR was oven-dried (24 hours at 105 °C), and then crushed and sieved through a U.S. #40 (<0.42 mm) sieve. For passivation methods, $Fe_2(SO_4)_3 \cdot nH_2O$ (Amresco, ≥73%), $Al_2(SO_4)_3 \cdot nH_2O$ (Alfa Aesar, ≥97%) and $NaH_2PO_4 \cdot H_2O$ (Sigma-Aldrich, ≥98%) were used to prepare the bathing solutions. The amount of Fe and Al per unit weight of $Fe_2(SO_4)_3 \cdot nH_2O$ and $Al_2(SO_4)_3 \cdot nH_2O$ were measured using a Model 5100 ZL (Perkin Elmer, Waltham, MA) flame atomic adsorption spectrophotometer, in order to correctly determine the amount of Al and Fe used in the bathing solutions.

2.2.2. Water Leach Tests

Two types of batch water leach tests (WLT) were conducted using untreated and treated slag samples: 4-hour water leach tests (4hWLT) and 18-hour water leach tests (18hLT). 18hWLTs followed ASTM D3987 with modifications (ASTM, 2006a). The first modification was use of 50-mL of total liquid volume instead of 2-L to account for the available laboratory equipment. The second modification was the use of 0.02 M NaCl in deionized (DI) water as the extraction liquid instead of type-IV DI water to simulate the ionic strength of water percolating through soil. Leach test samples were continuously end-to-end tumbled on a rotator at ambient temperature (18−21 ºC). 18hWLTs were conducted according to the specifications on tumbling speed and contact time that are prescribed in

ASTM D3987; tumbling duration was 18 hours and the tumbling speed was 29 rpm (revolutions per minute). A liquid-to-solid ratio (LS) of 20 mL/g (vol./wt.) was used in most leach tests matching the ASTM standard; solid mass was 2.50 g. In addition to these standard 18hWLTs, a separate series of 18hWLTs were conducted using 6M samples by utilizing 0.25, 0.50, 1.00 and 1.50 g of steel slag.

The second type of leach test, 4hWLT, was similar to 18hWLT except the tumbling duration was 4 hours and the tumbling speed was set to 10 rpm. The tumbling speed and duration were decreased to complete more tests in shorter time periods and to decrease abrasion. Steel slag particles are not agitated under field conditions; thus, it was presumed that less agitation in leach tests would provide a more conservative approximation of leaching behavior. However, the results from 18hWLTs were used for final evaluation of the performance of treatment methods in the end, since they were conducted per the ASTM standard.

At the end of the tumbling period, the samples were centrifuged at 3000 rpm for 5 minutes and immediately analyzed for leachate pH. Then, samples were filtered through 0.2-µm pore-sized membrane filters (PALL, Supor© 200) using 60-mL syringes and 25-mm filter holders. Finally, 0.25 mL trace metal grade concentrated HNO_3 (J.T. Baker, ~15.8 M) were added to filtered samples and samples were preserved at 4ºC until further analysis were conducted. All WLTs were replicated twice or more. The average of the measurements from replicated tests were plotted on the graphs and error bars delineate the standard deviation between the measurements. In tables, values given after "±" sign represent the standard deviation.

2.2.3. Steel Slag Treatment Procedures

2.2.3.1. Bitumen Coating

The “bitumen coating” treatment method assumed that mixing hot bitumen with steel slag can provide a physical barrier over the steel slag particles reducing water contact.

10.0 grams of steel slag and various amounts of bitumen were placed into 60-mL aluminum dishes and heated to 180°C in a muffle furnace. After 10 minutes of heating, samples were removed from the furnace and thoroughly mixed for approximately 1 minute. This heating-mixing procedure was repeated three times for each sample; the total heating period was 30 minutes. Next, 2.50 grams of bitumen-covered slag samples were sampled from each batch (Figure 2.1b); special attention was paid not to damage the coating. Finally, duplicate WLTs were conducted for all bitumen-coated samples and the controls (6M with 0% bitumen content). The bitumen contents are reported based on dry weight of the total mass of the mixture (wt./wt.).

2.2.3.2. Passivation

It is hypothesized that precipitation of metal hydroxides or Ca-PO_4 complexes as a layer on steel slag particles may alter the properties of the steel slag surface and hinder hydration reactions. Many studies have successfully formed layers of Al and Fe hydroxides on the surface of sand by bathing the aggregates in a metal solution while increasing the pH of the solution (Lo et al., 1997; Kuan et al., 1998; Lai et al., 2000; Chang et al., 2008; Ding et al., 2010). In this study, similar coating procedures were applied to steel slag particles. The surface modifications made here using metal salts are assumed to provide a thin coating layer via precipitation over the particles and are simply referred to as “passivation”, since the purpose was to minimize hydration reactions.

Reagent grade chemicals [$NaH_2PO_4 \cdot H_2O$, $Fe_2(SO_4)_3 \cdot nH_2O$, and $Al_2(SO_4)_3 \cdot nH_2O$] were dissolved in deionized water at different concentrations (~0.03 M to ~0.4 M). 10.0 grams of steel slag samples were placed into a 60-mL aluminum dish. The dishes were placed on plastic stands in glass beakers and beakers were filled with 200-mL passivating solutions of different kinds (L:S= 20 mL/g) (Figure 2.2). The passivating solution was constantly-stirred using magnetic stirrers. The pH values of resulting solutions varied broadly –initial pH of $Al_2(SO_4)_3$ solutions were ranging within pH 3.4-3.8; $Fe_2(SO_4)_3$ solutions were pH <2.3; NaH_2PO_4 solutions were pH 4.2-4.5. It was assumed that the greatly varying pH levels in different solutions could significantly affect Ca(+II) release from steel slag and the chemistry between passivation runs. Thus, for consistency, the pH of all the solutions was manually adjusted to 4.0 via 4 M NaOH or 4 M HCl additions before they were used for passivating samples.

After 30 minutes of contact, bathed steel slags in the dishes were removed from the solution and dried at 105°C for 24 hours (Figure 2.1c-d). Finally, dried passivated steel slag samples and the controls (slags bathed in HCl solution at pH 4) were subjected to 4hWLTs and 18hWLTs. 6M samples passivated using $NaH_2PO_4.H_2O$, $Fe_2(SO_4)_3 \cdot nH_2O$ and $Al_2(SO_4)_3 \cdot nH_2O$ solutions are denoted as PO_4/6M, Fe/6M and Al/6M, respectively. The remaining passivating solutions were analyzed for pH and then preserved for dissolved Ca(+II) measurement. All samples were acidified and stored at 4ºC prior to metal analysis.

In addition to WLTs conducted using passivated steel slags, modified WLTs were also conducted using different concentrations of the passivating salts (0.005 M to 0.05 M) mixed with 0.02 M NaCl as the extraction solution, along with 2.50 g 6M steel slag. In these tests, no pH adjustments were made to the extraction solutions.

2.2.3.3. Admixture Addition

Preliminary results from passivation treatment showed that aluminum sulfate had a significant effect on Ca(+II) release; thus, the third treatment method was devised involving simply mixing steel slag and an alum-based drinking WTR under dry conditions at different percentages (based on dry weight). WTR is a waste product known to be composed of precipitated aluminum hydroxide and other settled pollutants during drinking water treatment. Al is the most abundant constituent of WTR (16%, wt./wt.), along with a sulfur content of 4,750 mg/L (Table 2.1). Thus, WTR/steel slag mixtures were prepared and water leach tests were conducted to observe changes in Ca(+II) release and pH.

2.2.4. Acid Neutralizing Capacity Tests

For acid neutralizing capacity (ANC) measurements of the solids, samples were prepared similar to leach test samples, but 50-mL acid solutions at different concentrations were added to the tubes as extraction solution. Acid solutions were prepared by adding different volumes of 1 N HCl into DI water. 1 N HCl was prepared by diluting concentrated HCl (~15.8 M) in DI water. Then, tubes were tumbled for 18 hours at 29 rpm as done for water leach tests (18hWLTs). At the end of the tumbling period, the pH of the samples were measured and values were plotted against the amount of H^+ added per kg solid material. The consumed acid concentration at specific pH values was estimated by interpolating the available data.

Additionally, another type of ANC test was conducted over 49 days using 25-g 6M steel slag in 500-mL bottle (L:S=20 mL/g). Small volumes of concentrated HCl was daily added to the solution and the sample was let tumbled. Then pH was measured 24 hours later. Acid

addition was contained daily for 49 days. The solution pH was not let to drop less than pH 6 during acid additions.

2.2.5. Leachate Alkalinity Measurements

ASTM Standard D1067 was followed to analyze alkalinity of 18hWLT leachates (ASTM, 2011). 0.05 N and/or 1 N HCl solutions in small volumes were incrementally added to 100-mL filtered leachates while the leachates were being constantly stirred and the pH of the leachates were being monitored using a pH probe. Acid addition was continued until the pH of the leachate decreased to ~4.0. The amount of acid consumption and the pH reading for each addition step were noted. The alkalinity results are reported as the amount of H^+ that was consumed to reach at pH 7 in units of milliequivalents (mEq) per liter of the leachate. Total volume change due to acid addition was kept below 5% in all titrations.

2.2.6. Analytical Techniques

Total elemental analyses (TEA) for all steel slags and WTR were performed by the University of Wisconsin Soil Testing and Plant Analysis Laboratories using inductively coupled plasma optical emission spectrometry (ICP-OES) and employing a laboratory-developed standard operating procedure (UW, 2005) (Table 2.1). X-ray fluorescence (XRF) spectrometry analysis on steel slags and WTR were carried out by ALS Minerals Laboratory (ALS Code ME-XRF06) (Table 2.2).

Steel slag leachate pH was analyzed using a Model 520A meter (Orion, Boston, MA) equipped with a Sure-Flow Model pH probe (Thermo Scientific, Beverly, MA), per ASTM E70 (ASTM, 2007). Because of the high pH values encountered in the leachates (pH>12), pH meter were calibrated using commercially available reference buffer solutions at pH

7.00, 10.01 and 13.00 at 25°C (Ricca Chemical, Arlington, TX). If the pH of the samples were found to be below pH 10, pH meter was calibrated using buffer solutions at pH 4.01, 7.00 and 10.01 at 25°C. The pH of replicated samples were reported as the geometric mean of the readings from replicated discrete samples.

Leachate conductance was measured with a YSI Model 35 conductance meter and the readings were converted to electric conductivity (EC) in $\mu S\ cm^{-1}$ units at 25°C. The ionic strengths of leachates from WLTs conducted using different masses of 6M (0.25-2.50 g) were roughly estimated based on comparing electric conductivity measured in 0.02 M NaCl and 6M leachate from 18hWLTs. Leachate pH values were converted to OH^- concentrations using calculated activity coefficients and the Extended Debye-Hückel Equation (Stumm and Morgan, 1996).

Dissolved Ca and Mg concentrations in the leachates were determined using a Model 5100 ZL (Perkin Elmer, Waltham, MA) flame atomic adsorption spectrophotometer (FAAS). The amount of Fe and Al per unit weight of $Fe_2(SO_4)_3 \cdot nH_2O$ and $Al_2(SO_4)_3 \cdot nH_2O$ were also measured using FAAS. All analyses were conducted following "standard methods" (APHA, 2005).

Visual MINTEQ v3.0 (Gustafsson, 2012) was utilized for simulating acid-titration curves for solutions containing different $Ca(OH)_2$ concentrations. Input Ca(+II) concentrations were determined based on the measured dissolved Ca(+II) concentrations in the leachates from WLTs. 0.02 M Na^+ and Cl^- (background electrolytes) were entered for all estimations (no atmospheric CO_2 exposure, T=20ºC). pH was calculated based on "mass and charge balance" and the default database was used.

2.3. Results and Discussion

2.3.1. Alkalinity Producing Capacity of Aged Steel Slag Samples

TEA and XRF analyses results for the three types of aged BOF slags demonstrates that Fe and Ca were the major constituents in all samples, along with significant amounts of Al, Mn and Mg (Tables 2.1 and 2.2). Calcium was the most abundant extractable element (~17%, wt./wt.) in all steel slag samples.

Table 2.3 shows that all steel slag samples produced leachates with pH values above 12. Leachate pH values were significantly higher in 18hWLTs (pH>12.4) compared to 4hWLTs. For both 4hWLTs and 18hWLTs, the highest dissolved Ca(+II) concentration was detected in leachates of steel slag aged for 6 months (6M): 670 mg/L for 4hWLT, corresponding to 7.7% of the total extractable Ca content, and 806 mg/L for 18hWLT (9.3%). The difference in dissolved Ca(+II) concentrations between 4hWLT and 18hWLT for 6M shows that Ca(+II) release potential for 6M was higher when the contact time was longer and the abrasion due to longer tumbling period. 1YR slag leached statistically similar amounts of Ca(+II) both in 4hWLTs and 18hWLTs (567±32 mg/L vis-à-vis 588 ±71 mg/L of total Ca(+II) content, p=0.65). Interestingly, 2YRS slag released more Ca(+II) than 1YR; 598 ±42 mg/L dissolved Ca(+II) (6.9%) according to the results from 4hWLTs and 702±86 mg/L dissolved Ca(+II) (8.1%) for 18hWLTs, suggesting that prolonged aging may have negative effects on the solubility of Ca-containing minerals in steel slags.

While results from the TEA imply that the overall chemical compositions and total Ca content of all 3 samples are similar, varying amounts of Ca(+II) release from the 3 types of steel slag during 18hWLTs indicate a significant difference in Ca solubility for each

kind of slag. This suggests that dissolution rates of Ca-containing mineral phases were different in different kinds of aged steel slag samples. Nonetheless, the aged slags are still capable of producing extremely alkaline leachates with high concentrations of dissolved Ca(+II).

The final pH values for steel slags obtained from acid neutralizing capacity (ANC) tests are plotted in

Figure 2.3, as a function of added H^+ equivalent per kg steel slag. Results showed that different steel slag samples had different ANC values within the alkaline pH range. 6M had the highest ANC above pH 11, followed by 2YRS. All three types of aged steel slag produced leachate pH values below pH 8.5 when 1.5−2 equivalent H^+ was added per kg steel slag. The ANC at pH 7 for 6M, 1YR and 2YRS were estimated at 2.05 Eq/kg, 1.82 Eq/kg and 1.90 Eq/kg, demonstrating that prolonged periods of aging had marginal effect on overall alkalinity producing capacity. The results from 49-day ANC tests, where daily acid addition were made, demonstrate that time was also another important parameter affecting ANC. ANC of 6M within 49 days was estimated at 4.3 Eq/kg at pH 8.5, whereas ANC of 6M was 1.4 Eq/kg at pH 8.5 according to the results from 18-h tests. It appears that hydration and dissolution reactions on steel slag particles continued over extended periods of time and that 18-h ANC tests represented only a fraction of the total ANC of steel slags (Yan et al., 2000).

Figure 2.4 shows laboratory-measured alkalinity of filtered leachates from 18hWLTs, along with Visual MINTEQ simulations based on the dissolved Ca(+II) concentrations reported in Table 2.3. Since the alkalinity of aged steel slag leachates was considered to be

predominantly due to $Ca(OH)_2$ dissolution, this type of alkalinity gives the 6M titration curve a characteristic shape; high buffering capacity at pH >11. Agreement between measured data and simulations strongly suggests that the hydroxide alkalinity originated predominantly from dissolved $Ca(OH)_2$. $Ca(OH)_2$ and C-S-H gel are reported to be the main products of steel slag hydration (Wang and Yan, 2010).

Figure 2.5 demonstrates the linear correlation between dissolved Ca(+II) concentration and estimated hydroxide concentration in the leachates from 18hWLTs that were conducted using different amounts of 6M (from 0.25 to 2.5 g), indicating that both $[OH^-]$ and $[Ca^{2+}]$ were released proportionally. The average $[OH^-]$:$[Ca^{2+}]$ ratio was 4.3. However; if all of the dissolved Ca(+II) originated from disassociated $Ca(OH)_2$, the excepted value of $[OH^-]$:$[Ca^{2+}]$ ratio should be 2. Also note that the $[OH^-]$:$[Ca^{2+}]$ ratios listed in Table 2.3 range from 1.0 to 2.5 (with a standard deviation as high as 1.5). This high deviation is believed to be caused by the inaccuracy in pH measurements in the highly alkaline steel slag leachate, which were used to estimate hydroxide concentrations. Extremely low H^+ activities at high pH values are difficult to detect accurately by probes. The dissolved Ca(+II) concentrations measured using AAS and pH measurements at circumneutral and acidic ranges used to construct alkalinity curves are considered to be more accurate compared to leachate pH values. Thus, results given in Figure 2.4 were considered more dependable and hence, the predominant source of alkalinity in the leachates was considered to be $Ca(OH)_2$ disassociation. Similarly, Roadcap et al. (2005) also showed a direct correlation between dissolved Ca(+II) and OH^- in steel slag seepage. MgO in steel slag can also produce OH^- alkalinity similar to $Ca(OH)_2$. Dissolved Mg concentrations in all three

kinds of steel slag leachates were below the detection limit (1 mg/L), in spite of that slags contained 4.7-5.1% Mg (wt./wt.) according to TEA results (Table 2.1).

Based on these observations, measured changes in dissolved Ca(+II) concentrations in treated slag leachates were employed as the primary indicator of the extent of slag hydration and dissolution reactions and are used to evaluate performance of the treatment methods. Designed treatment procedures were applied on 6M, since the highest leachate alkalinity, leachate pH, and dissolved Ca(+II) concentrations were detected in 6M.

2.3.2. Bitumen Coating

According to the results presented in Figure 2.6, 6M without bitumen coating (control) released 602±75 mg/L Ca(+II) and pH was 12.10 in 4hWLTs. For 4hWLTs, addition of as little as 2.1% bitumen (dry wt.) decreased the Ca(+II) concentration to 366±17 mg/L – corresponding to a 39% decrease relative to Ca(+II) release from untreated 6M. Between 3.9 and 6.1% bitumen content, Ca(+II) release decreased 75% on average and the pH was within the range of 11.4–11.9. When the bitumen content was increased to 10-12.3%, Ca(+II) release decreased by 94% on average and the geometric mean of the pH was ~11.1 in 4hWLTs.

The results obtained from 18hWLTs showed a higher variation and, overall, dissolved Ca(+II) concentrations were greater due to the higher tumbling speed and the longer contact time (Figure 2.6). For 18hWLTs, 6M without bitumen (control) released 804±60 mg/L and mean pH was 12.39. Within the range of 4–6% bitumen content, average reduction in dissolved Ca(+II) concentrations was 76% (196±75 mg/L), which was approximately the same level of reduction observed for 4hWLTs despite the higher Ca(+II) release potential

over 18 hours, and the mean pH was ~11.6 (-0.8 pH units). Between 10.0 and 12.3% bitumen content, average Ca(+II) release was 88% lower (99±16 mg/L) and pH was ~11.3.

As the bitumen-to-slag ratio was increased, a thicker and more complete physical sealing layer was formed on the steel slag particles. WLT results confirmed this observation. Results from both 4-h and 18-h WLTs indicate that the trend of reduction in Ca(+II) release was similar. Ca(+II) release decreased exponentially with increasing bitumen content up to 4–6% and bitumen contents greater than 6% provided only marginal continued reductions in Ca(+II) release. Comparison of the 4hWLT and 18hWLT results suggests that the bitumen-coating was durable despite the increased agitation speed and duration.

A large number of studies have investigated the swelling properties and durability of steel slag used in bituminous pavement construction and all agree that using steel slag instead of natural aggregates improves mechanical properties of pavements (Wu et al., 2007; Ahmedzade and Sengoz, 2009; Sorlini et al., 2012; Xie et al., 2013). Nonetheless, steel slags have highly porous surfaces and can absorb more bitumen relative to natural aggregates (Ahmedzade and Sengoz, 2009). It was observed that addition of as high as 4% bitumen produced a granular material without significant binding between the particles. Considering the cost of bitumen and that strong binding is not required for steel slag use in road bases and embankments, 4% bitumen content appears to be the optimal value for coating steel slag.

Figure 2.7 shows the impact of bitumen coating on alkalinity titration curves obtained for 18hWLT leachates. Alkalinity tests were duplicated for each type of treatment procedure and the two curves obtained for each replicate were plotted in Figure 2.7. The alkalinity of

6M was 31.3±2.7 mEq/L at pH 7. A similar shape was also observed for the leachates from 6M samples with 4% bitumen content (4% bitumen/6M); the average alkalinity was 15.7±0.7 mEq/L at pH 7, corresponding to 50% of 6M alkalinity. Similarly, the dissolved Ca(+II) concentration in these 4% bitumen/6M leachate samples was 369±9 mg/L, corresponding to 46% of the Ca(+II) concentration found in 6M leachates. The proportional dissolved Ca(+II) concentrations and alkalinity, and the similar shape of the curves relative to 6M indicate that the alkalinity in bitumen-coated 6M leachates also resulted from dissolved $Ca(OH)_2$ and that the bitumen coating caused no observable chemical change in the leachate, except the reduction in leachate alkalinity. It should be noted that bitumen can release dissolved organic carbon (Sorlini et al., 2012).

2.3.3. Passivation

Calcium release measured in the passivating solution after 30-minute bathing of 6M steel slag samples, and dissolved Ca(+II) concentrations and pH values in the leachates from corresponding 4hWLTs, are plotted in Figure 2.8. In this graph, the zero point on x-axis corresponds to 4hWLTs conducted using 6M bathed in DI water at pH 4 (pH adjusted via HCl addition) and applied Al/Fe/PO_4 concentration corresponds to concentration of Al(+III) in $Al_2(SO_4)_3$ solution, Fe in $Fe_2(SO_4)_3$ solution and PO_4 in NaH_2PO_4 solution used during bathing. This passivation procedure comprised of 2 steps –passivating and drying. The rationale behind employing this procedure involving 2-steps was to produce a treated aggregate which can be directly applied in the field. The Ca(+II) release in acidic DI water within 30 minutes of bathing was 77 mg/L Ca(+II), corresponding to 0.9% of the total extractable Ca(+II) content detected in TEA. After the control samples were dried and tested, they leached another 440 mg/L Ca(+II) during 4hWLT (Leachate pH=11.8),

corresponding to an additional 5.0% of the total Ca content. This 5.9% total is less than 7.7% leached from untreated 6M during 4hWLT (670±14 mg Ca/L at pH 12.15); however, a layer of white residue formed and remained in the drying dish, indicating possible additional leached Ca(+II) that was not counted in this mass balance.

During the 30-minute reaction of steel slag samples in various passivating solutions, it was observed that a thin precipitate layer formed only on steel slag particles as expected. However, upon drying passivated samples, precipitate layers were observed to form not only on the steel slag particles, but also on the drying dish containing the samples: white residuals for Al/6M and PO_4/6M, and a red residual for Fe/6M. Thus, it was considered that the two-step test procedure did not to allow for a complete Ca(+II) mass balance. Also, actual amounts of Al(+III), Fe or PO_4 reacted with steel slag were unknown. To investigate the efficiency of two-step passivation procedure, additional WLTs were conducted where the same chemicals were added to the extraction solution directly and leachate pH and Ca(+II) concentrations were measured and the results are plotted in Figure 2.9; the zero on the x-axis corresponds to results from WLTs conducted with untreated 6M.

For 6M steel slag passivated using NaH_2PO_4, Ca(+II) release during bathing was within the range of 4.2–8.3 mg/L, considerably lower compared to control samples (Figure 2.8). After 30-min bathing, the pH of passivating solutions increased to 6.2 for 0.05 M PO_4/6M and 4.9 for 0.4 M PO_4/6M, suggesting significant changes in solution composition. In subsequent 4hWLTs, dissolved Ca(+II) declined with increasing applied PO_4 concentration. 0.05 M NaH_2PO_4 treatment resulted in 342±29 mg/L dissolved Ca(+II) concentration at pH 11.84, corresponding to a 49% reduction. Dissolved Ca(+II) concentration in 0.4 M PO_4/6M leachate was 119±16 mg/L at pH 11.55 (82% reduction).

The reduction in Ca(+II) release for phosphate treatment is assumed to be due to formation of insoluble Ca-P mineral phases that accumulated on slag particles. For instance, reaction of Ca(+II) released from steel slag and phosphate in passivating solution can form stable hydroxyapatite precipitates as a secondary mineral phase (Eq. 2.1). Hydroxyapatite [$Ca_5(PO_4)_3OH$] is a Ca-P mineral with a low solubility product; $K_{sp} \leq 10^{-57}$ (Kaufman and Kleinberg, 1979). In recent studies, formation of hydroxyapatite on steel slag particles was observed when steel slag was used to retain phosphorous in polluted waters (Barca et al., 2012a; Claveau-Mallet et al., 2013; Hussain et al., 2014).

$$5\ Ca(OH)_2 + 3\ NaH_2PO_4 \leftrightarrow Ca_5(PO_4)_3OH \downarrow + 3\ NaOH \quad (2.1)$$

Direct addition of NaH_2PO_4 to the extraction solution of 4hWLTs also had significant impact on Ca(+II) release at one order of magnitude smaller PO_4 concentrations compared to the 2-step passivation procedure (Figure 2.9). The presence of PO_4 as low as 0.010 M decreased the dissolved Ca(+II) concentration to 1.1±0.1 mg/L, pH was 12.25. These results demonstrate the low efficiency of 2-step procedure in terms of employing phosphate on slag particles. According to the stoichiometry of Equation 2.5, precipitation occurs at a $[PO_4^{3-}]$:$[Ca^{2+}]$ ratio of 3/5. 0.010 M NaH_2PO_4 stoichiometrically precipitates 0.0167 M $Ca(OH)_2$ (corresponding to 667 mg/L Ca^{2+}), explaining the significant reduction in dissolved Ca(+II) concentrations. However, if the $Ca(OH)_2$ dissolution occurs first, this reaction does not eliminate OH^- alkalinity release; the pH was not significantly affected when the PO_4 concentration was below 0.015 M (pH≥11.89). When PO_4 concentration exceeded 0.020 M, it appears that excess NaH_2PO_4 addition neutralized some of the alkalinity and dropped the pH to ≤7.2, dissolved Ca(+II) concentration was ≤5.1 mg Ca/L.

Significantly decreased dissolved Ca(+II) concentrations over a broad pH range (pH 6.3-12.3) also indicate formation of a stable secondary mineral phase, most likely hydroxyapatite.

Exposure to $Fe_2(SO_4)_3$ during bathing resulted in even higher Ca(+II) release relative to the results obtained for 6M bathed in DI water at pH 4 (Figure 2.8). When 0.03 M and 0.06 M $Fe_2(SO_4)_3$ was applied during the bathing, 248±103 and 298±78 mg/L Ca(+II) leached into the passivating solution, respectively. The pH of the passivating solutions increased to 7.5–7.7 after bathing and a red-colored precipitate formed on the steel slag particles, which is assumed to be $Fe(OH)_3$ (Eq. 2.2).

$$Fe^{3+} + 3\ OH^{-} \leftrightarrow Fe(OH)_3 \downarrow \quad (2.2)$$

0.03 M and 0.06 M Fe/6M released 343±29 and 331±32 mg/L additional Ca(+II) during 4hWLTs, respectively, leachate pH values were ~11.8). The combined Ca(+II) release during bathing and 4hWLT summed up to 6.9–7.3% of 6M's total Ca content. Apparently, presence of ferric sulfate caused higher Ca(+II) release compared to bathing in water at pH 4.0. Even if a $Fe(OH)_3$ coating formed at the end of passivation, this layer was likely to be dissolved under alkaline conditions (pH ~11.8) during the water leach testing and/or abraded off. Overall, passivation by slag bathing in ferric sulfate solution did not provide any beneficial results.

The lowest Ca(+II) leaching was obtained by application of 0.05 M and 0.10 M Al(+III) as $Al_2(SO_4)_3$ (Figure 2.8). For Al/6M samples, only 0.3–1.0 mg/L Ca(+II) was released during 30-min bathing and after bathing, the pH values of passivating solutions were 4.0-4.2 compared to initial value of pH 4, indicating that Ca^{2+}, which is highly soluble under acidic

conditions, did not diffuse into the solution and that the composition of the solution did not change significantly. A thin white layer (slightly brighter white compared to slag bathed in DI) was formed on dried steel slag particles. This layer assumed to be aluminum hydroxide precipitated onto the particles during passivation (Eq. 2.3). As in the case of ferric sulfate passivation, the coating formed after passivation was likely to be removed due to abrasion and highly alkaline conditions (pH >10.8) attained during WLTs.

$$Al^{3+} + 3\ OH^{-} \leftrightarrow Al(OH)_3 \downarrow \quad (2.3)$$

Ca(+II) concentrations from 4hWLTs of 0.05 M and 0.10 M Al/6M corresponded to 74% (111±3 mg/L Ca at pH 11.69) and 77% (100±1 mg/L Ca at pH 11.78) reductions in Ca(+II) release compared to 4hWLT of 6M passivated in DI waster at pH 4, respectively (Figure 2.8); 83% and 85% reductions in Ca(+II) release compared to 4hWLT of untreated 6M. 18hWLTs using 0.1 M Al resulted in 69% reduction in Ca(+II) release (249±43 mg Ca/L at pH 12.25) compared to leachate from 18hWLT of untreated 6M; reduction in leachate pH was ~0.26 units. The alkalinity of the leachate from 18hWLTs using 0.1 M Al/6M was 10.5±3.9 mEq/L at pH 7, corresponding to a 66% reduction in alkalinity compared to untreated 6M leachate (Figure 2.7) and proportional to the reduction in dissolved Ca(+II) concentration.

Similar to NaH_2PO_4 passivation, the reduction in Ca(+II) release for aluminum sulfate treated steel slag is thought to be due to formation of less soluble secondary mineral phase/s as a result of excess aluminum in the solution. But unlike NaH_2PO_4, increasing the concentration of $Al_2(SO_4)_3$ during bathing did not result in higher reduction in Ca(+II)

release; in 4hWLTs, 0.2 M Al/6M released 196±3 mg/L Ca(+II) at pH 11.76. It appears that this type of treatment requires precision control for dosage.

Variations in the Ca(+II) release were also observed in 4hWLTs and 18hWLTs where $Al_2(SO_4)_3$ was added directly to extraction solution (Figure 2.9). For 4hWLTs, 0.010 M Al addition caused a minor change in Ca(+II) release (-9%) compared to control samples and pH was 10.4. 0.015 M Al(+III) addition resulted in an increase of 9% in Ca(+II) release and the pH decreased to 9.7 apparently due to presence of higher $Al_2(SO_4)_3$ concentration. However, when Al(+III) exceeded 0.020 M, pH was below 4.2 and Ca(+II) release was reduced 42–91%. Direct addition of 0.005–0.010 M Al(+III) in 18hWLTs performed better in terms of Ca(+II) reduction but final leachate pH values were higher compared to the results from 4hWLTs. Results from 18hWLTs showed that 0.005 M Al/6M released 169±29 mg/L at pH 12.05 and that 0.010 M Al/6M released 265±23 mg/L at pH 10.76. When 0.020 M Al(+III) was introduced to 6M, pH decreased to 9.56 and Ca(+II) release was 764±56 mg/L which was as high as the release from untreated 6M. The changes in Ca(+II) release from Al(+III) treated slags were sensitive to the pH and the final leachate pH was a function of applied $Al_2(SO_4)_3$ concentration and contact time. Significant reduction in Ca(+II) release was achieved above pH 10.4 and within the pH range of 3.9–4.2, suggesting formation of different types of secondary minerals that removed Ca(+II).

C-S-H (calcium silicate hydrate) and $Ca(OH)_2$ are the main hydration products in BOF slag (Wang and Yan, 2010). Addition of Al^{3+} and SO_4^{2-} in a system rich in $Ca(OH)_2$ can cause precipitation of calcium aluminates and calcium sulfoaluminates, such as ettringite (Thomas et al., 2003; Barbarulo et al., 2007; Myers et al., 2015). Formation of ettringite ($Ca_6Al_2(SO_4)_3(OH)_{12}\cdot 26\ H_2O$) is favored at high alkalinity and it is stable above pH 10.7

(Baur et al., 2004). Therefore, ettringite precipitation/dissolution might significantly decrease in Ca(+II) concentration in $Al_2(SO_4)_3$-passivated 6M leachates followed by an increase as added $Al_2(SO_4)_3$ concentrations got higher and pH values approached circumneutral pH range (Figure 2.9). For the decrease in Ca(+II) concentrations at acidic range (pH 3.9−4.2), ettringite precipitation could not be responsible. Myneni et al. (1998) reported decreased Ca^{2+} activity below pH 5 in a $Ca(OH)_2$–$Al_2(SO_4)_3$–H_2O system and observed precipitation of poorly crystalline Ca-Al-hydroxyl sulfate phases.

2.3.4. WTR Admixtures

Results of dissolved Ca(+II) concentration and leachate pH measurements from 4hWLT and 18hWLT conducted using WTR/steel slag mixtures are presented in Figure 2.10 as a function of WTR content (% of total mixture mass, wt./wt.). For 100% WTR (no slag), the dissolved Ca(+II) concentration was 19 mg/L for 4hWLT and 51 mg/L for 18hWLT and leachate pH was ~7 in both tests. Although WTR did not produce acidic leachates on its own, WTR addition to 6M steel slag resulted in significant decrease in leachate pH and dissolved Ca(+II) concentration. Despite the alkalinity-producing capacity of 6M at longer contact time and greater agitation, reductions in Ca(+II) concentrations and leachate pH were greater for 18hWLTs compared to 4hWLTs. Leachate pH and dissolved Ca(+II) concentration detected in the 18hWLT control (6M without WTR addition) was 12.42 and 798±41 mg/L, respectively. For 18hWLTs, addition of as low as 5% WTR decreased Ca(+II) release by 75% (203±13 mg/L Ca) and resulted in a leachate pH of 12.16. Upon addition of 10% WTR, dissolved Ca(+II) concentration was 84% lower (128±2.5 mg/L Ca) and leachate pH decreased by 0.96 units (pH 11.46) compared to 6M. 30% WTR addition resulted in 88% (97±1 mg/L Ca) lower dissolved Ca(+II) release and decrease of 2 units in

leachate pH from 12.42 to 10.42. For both 4hWLT and 18hWLT, adding more than 20% WTR did not result in further reduction in Ca(+II) release, significantly.

The reduction in dissolved Ca(+II) and leachate pH was also reflected in reduced leachate alkalinity of WTR-steel slag mixtures. Figure 2.11 demonstrates that WTR addition to 6M significantly reduces the leachate alkalinity. But WTR addition also changed the shape of the titration curves significantly compared to alkalinity curve of pristine, bitumen-coated and Al-passivated 6M leachates (Figure 2.7). The alkalinity of 6M leachate was estimated at 31.3±2.7 mEq/L at pH 7. The leachate of 5%WTR/6M has alkalinity of 12.0±0.1 mEq/L at pH 7; 10%WTR/6M leachate alkalinity was estimated at 9.1±0.7 mEq/L at pH 7. Therefore, 5% WTR addition decreased the alkalinity at pH 7 by 50% and 10% WTR decreased it by 70%. The alkalinity values of 10%, 20% and 30% were statistically similar (p>0.40, according to t-test results). Addition of more WTR did not change alkalinity reduction significantly, suggesting that 10% WTR addition was sufficient to reduce an optimum amount of alkalinity. The presence of WTR removed most of the alkalinity above pH 7, possibly due to greatly reduced Ca solubility, which was considered to be linked to $Ca(OH)_2$ dissolution and OH^- alkalinity release from steel slag. Undetermined soluble constituents released from WTR appeared to contribute to alkalinity, especially at pH 8−10 and pH ≤4.5. As mentioned before, WTR has a large Al content (Table 2.1) and Al(+III) can dissolve in form of aluminate, $Al(OH)_4^-$, under alkaline conditions (Stumm and Morgan, 1996). Thus, the buffering capacity between 10 and 8 is suspected to be caused by $Al(OH)_{4\,(aq)}^-$ to $Al(OH)_{3(s)}$ transformation (Hendricks, 2010). Visual inspection of the samples during acid titration also provided evidence for a precipitation process; the clear filtered leachates became cloudy with a white hue when the pH was decreased below ~10.

This also explains the increased buffering capacity at pH 4.3–4.5. Buffering capacity at pH ≤4.5 was most likely due to $Al(OH)_3$ dissolution (Hendricks, 2010; Huang et al., 2011). Nevertheless, the overall reduction in alkalinity and Ca(+II) release was considerable compared to other more complex treatment methods. The mechanism of this impact is unclear and under further investigation but formation of Ca-aluminates as secondary mineral phases are suggested, as discussed above for the aluminum sulfate passivation.

2.4. Conclusions

Steel slag samples that were aged for different periods of time (6 months, ~1 year and over 2+ years) had a high leachate pH (≥12) and a great capacity to release alkalinity over extended periods of time. Comparison of ANC values at pH 7 for aged steel slag samples demonstrates that prolonged aging periods (1 year and 2+ years) had marginal effects on reducing the overall alkalinity producing capacity. Leachate alkalinity values, OH^- and dissolved Ca(+II) concentrations in the leachates were all found to be strongly correlated for all aged steel slag samples, regardless of their age and furthermore, release rate of dissolved Ca(+II) was also proportional to steel slag mass within 18 hours of hydration. These observations indicates that the source of alkalinity in leachates from aged steel slag samples was predominantly OH^- alkalinity originated from $Ca(OH)_2$ dissolution reactions.

Next, three types of treatment methods devised for reducing the alkalinity formation in aged steel slag leachates were investigated. Performances of the treatment methods were evaluated solely based on reduction in three parameters; Ca(+II) release, leachate pH and alkalinity in the leachate of treated steel slag samples. Based on 18hWLT results, bitumen coating (4% of dry weight) and $Al_2(SO_4)_3$ passivation (0.05−0.10 M) were able to reduce Ca(+II) release 46% and 69%, respectively, and the degree of alkalinity mitigation was

proportional to the reductions in Ca(+II) release (-50 and -66%). Decrease in final leachate pH for these two methods was 0.3−0.6 units. WTR admixtures demonstrated the most successful based on the reduction in all three parameters through an undefined mitigation mechanism. 84% of the Ca(+II) release and 71% of the original slag alkalinity was reduced upon WTR addition of 10% by dry weight; leachate pH decreased approximately 1 unit in 18hWLTs.

Although amending slag with WTR results in less slag use in construction, WTR addition to steel slag still appears to be the most promising and straightforward treatment method from an engineering perspective among the three treatment methods discussed here. In order to reach similar reduction in Ca(+II) release, 6−8% or higher bitumen addition is required compared to 10% WTR addition. $Al_2(SO_4)_3$ passivation was not as effective and direct $Al_2(SO_4)_3$ introduction method requires careful dosage, which is less of an issue in WTR admixtures. In addition to mitigation effect on leachate alkalinity, physical properties of WTR-amended steel slag also seems promising. It was reported in another study that WTR addition to aged BOF steel slag alleviated the overall volumetric expansion rate compared to the original material (Dayioglu et al., 2014). Nonetheless, the final leachate pH values were still high in the alkaline pH range (>10.5−11.5) despite the relatively high rate of reduction in leachate alkalinity and dissolved Ca(+II) concentrations were high upon WTR addition. Besides, the indirect evidence for a possibly very high dissolved Al(+III) release should be investigated further.

TABLES

Table 2.1. Chemical composition of steel slag and WTR according to total elemental analyses (TEA).

Element (mg/kg) [a]	6M	1YR	2YRS	WTR
Ag	< 0.6	< 0.6	< 0.6	274
Al	9990	11900	10600	160000
As	< 3	< 3	< 3	13
B	63.4	72.4	41.6	10.4
Ba	82.5	118	68.5	n/a
Ca	173000	171000	173000	5120
Cd	<0.4	<0.4	<0.4	< 0.4
Co	2.59	2.8	1.88	12.2
Cr	1320	1160	1250	< 0.1
Cu	32.3	28.2	19.7	56.4
Fe	129000	122000	114000	22600
K	41	109	19.5	2650
Li	16.7	17.1	16.7	24.2
Mg	47300	47300	50900	2990
Mn	18300	16700	18100	4350
Mo	2.786	2.33	1.567	2.41
Na	336	420	299	284
Ni	< 0.3	< 0.3	< 0.3	6.18
P	2500	2250	2130	2070
Pb	12.1	13.1	16	< 2
S	489	770	617	4750
Sb	< 0.81	< 0.81	< 0.81	1.79
Se	< 3	< 3	< 3	< 3
Si	322	301	457	516
V	555	528	521	41.5
Zn	99.6	185	189	98.1

[a] **:** All values are based on dry weight (wt./wt.).

Table 2.2. Chemical composition of steel slag and WTR according to XRF analyses.

XRF (%) [a]	6M	1YR	2YRS	WTR
Fe_2O_3	36.5	35.9	37.1	3.68
CaO	32.8	32.4	32.4	1.07
SiO_2	11.5	12.2	11.7	28.1
MgO	10.0	10.1	9.29	0.78
Al_2O_3	4.1	3.68	3.60	29.7
MnO	3.57	3.22	3.27	0.54
P_2O_5	0.72	0.6	0.65	0.39
TiO_2	0.44	0.43	0.47	0.48
Cr_2O_3	0.25	0.21	0.22	< 0.01
Na_2O	0.12	0.06	0.06	0.28
K_2O	0.04	0.02	0.02	1.12

[a] **:** All values are based on dry weight (wt./wt.).

Table 2.3. Results from 4hWLT and 18hWLT for three types of steel slag.

	0.02 M NaCl	6M	1YR	2YRS	6M	1YR	2YRS
Duration of WLTs		4 h	4 h	4 h	18 h	18 h	18 h
# of Replicates	3	3	3	3	8	6	6
Leachate pH	6.09	12.15	12.09	12.09	12.51	12.44	12.48
Dissolved Ca (mg/L)		670±14	567±32	598±42	806±42	588±71	702±86
Leached Ca Content (%) [a]		7.7	6.6	6.9	9.3	6.9	8.1
EC (mS/cm at 25ºC)	2.62	8.65	7.46	8.17	11.01	8.7	10.17
$[OH^-]$ (mM)		22±1	15±1	16±1	41±19	34±24	43±22
$[Ca^{2+}]$:$[OH^-]$		1.3±0.1	1.1±0.1	1.0±0.1	2.1±1.2	2.2±1.2	2.5±1.5

[a] **:** Leached Ca(+II) content was estimated based on dissolved Ca(+II) mass per kg slag normalized by total Ca concentration (mg/kg) obtained from TEA.

FIGURES

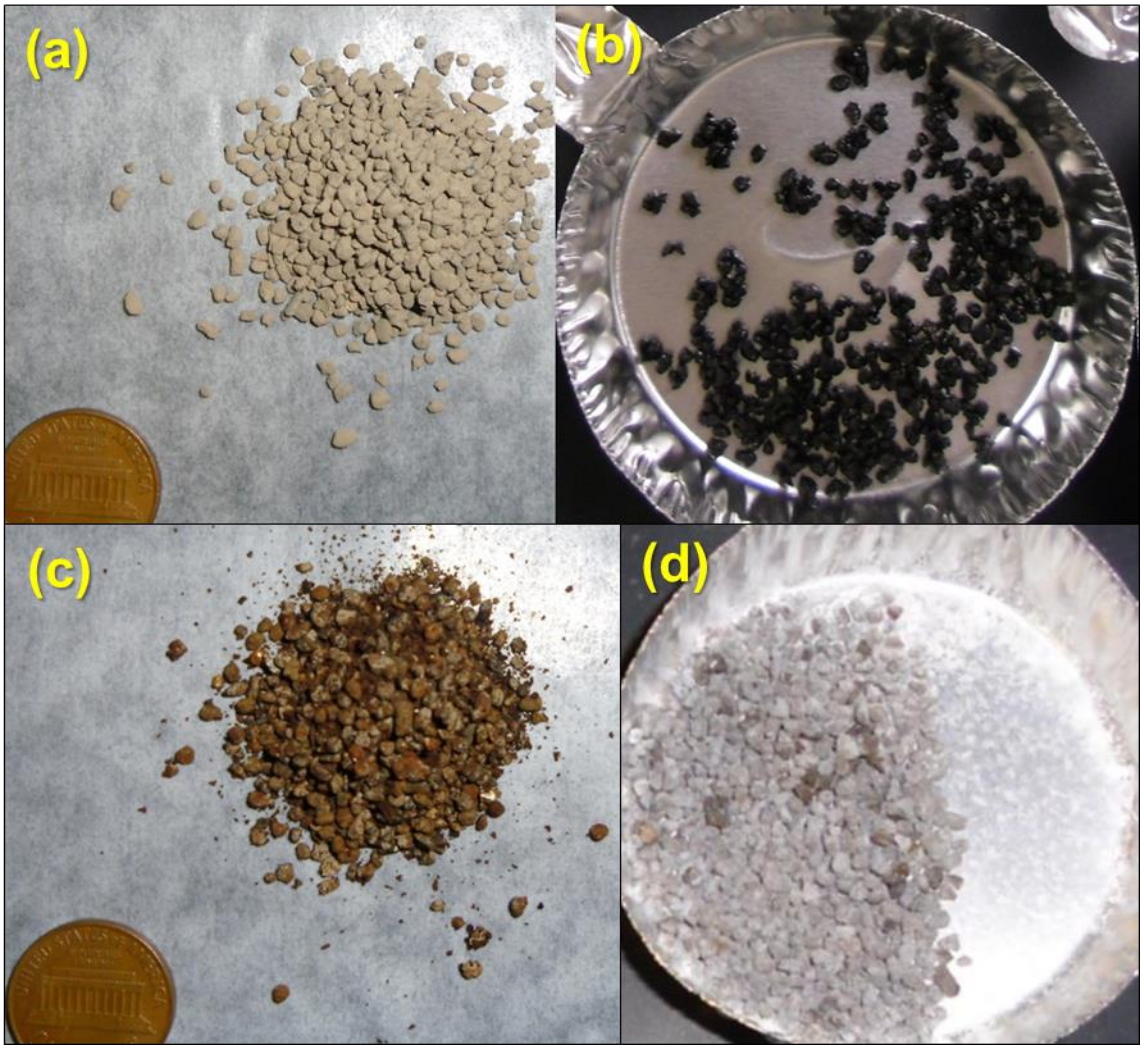

Figure 2.1. (a) Sieved 6M particles (1.18−2.00 mm); **(b)** bitumen-coated 6M particles; **(c)** 6M passivated in $Fe_2(SO_4)_3$ solution; **(d)** 6M passivated in $Al_2(SO_4)_3$ solution.

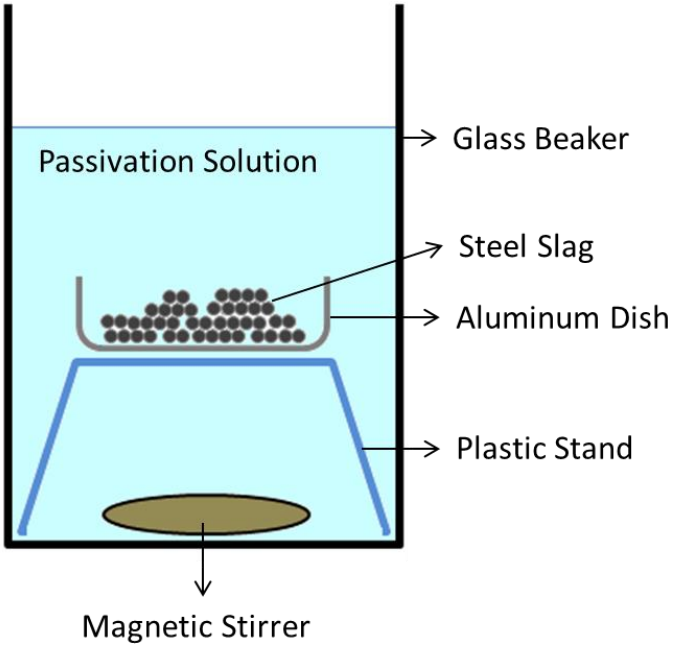

Figure 2.2. Diagram of the set-up used for coating processes.

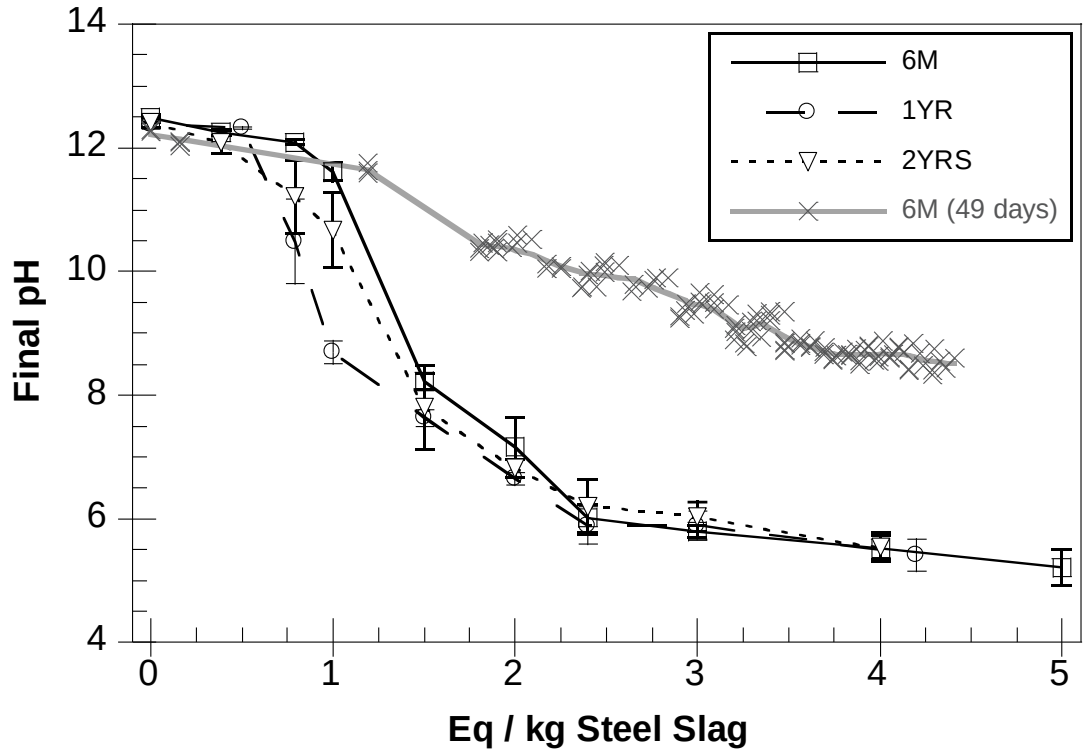

Figure 2.3. Acid neutralization capacity (ANC) of steel slag samples that were aged for 6 months (6M), ~1 year (1YR) and >2 years (2YRS) from 18-h ANC tests, along with the results from 49-day ANC test of 6-month-old steel slag.

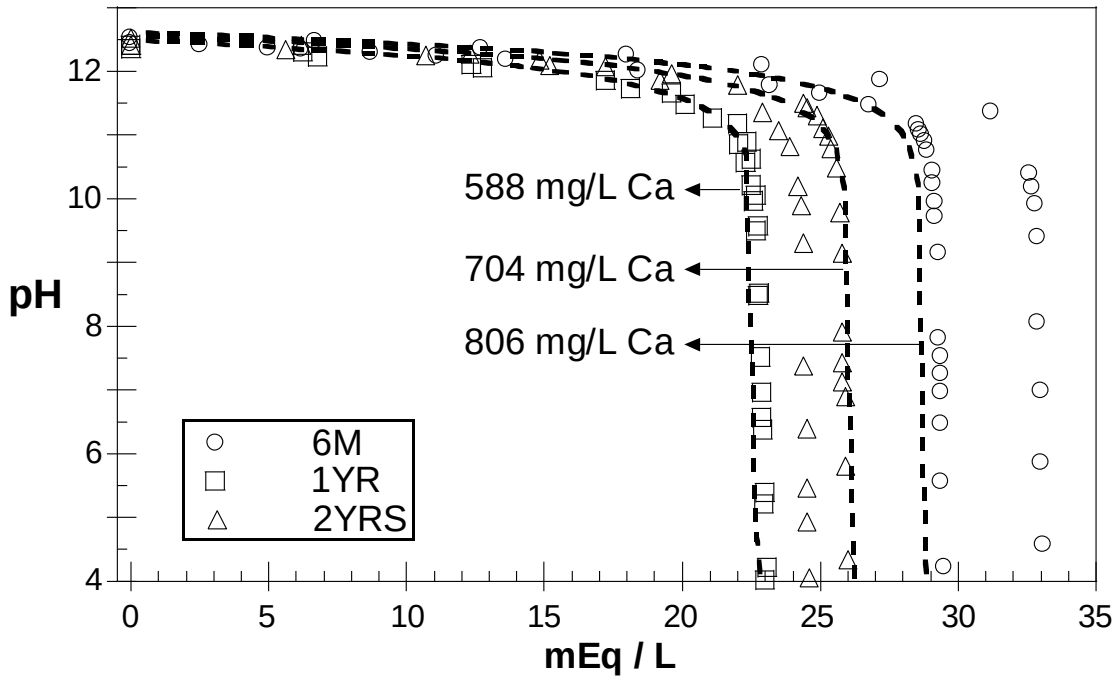

Figure 2.4. Leachate alkalinity curves for three types of steel slags and the results from titration simulations containing 588 mg/L, 704 mg/L and 806 mg/L Ca(+II).

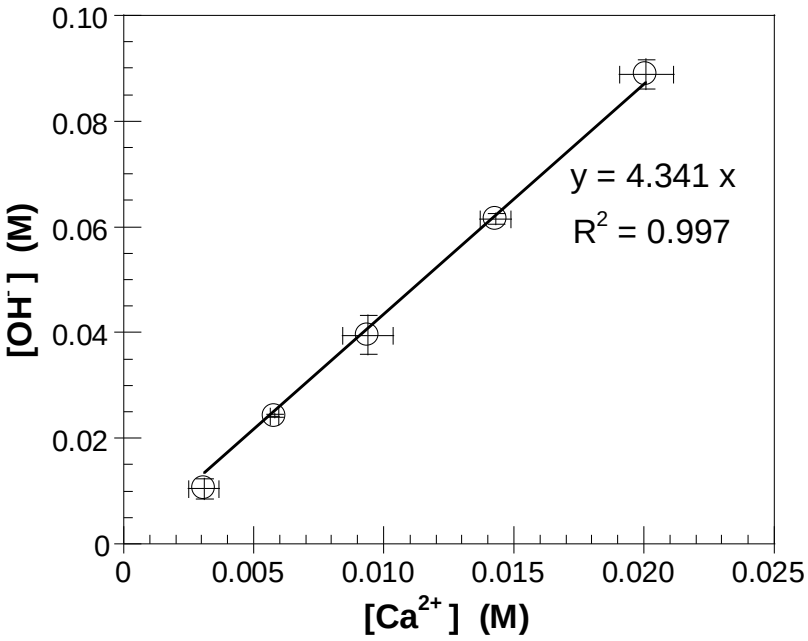

Figure 2.5. Correlation between estimated [OH^-] and measured [Ca^{2+}] in 6M leachates from 18hWLTs.

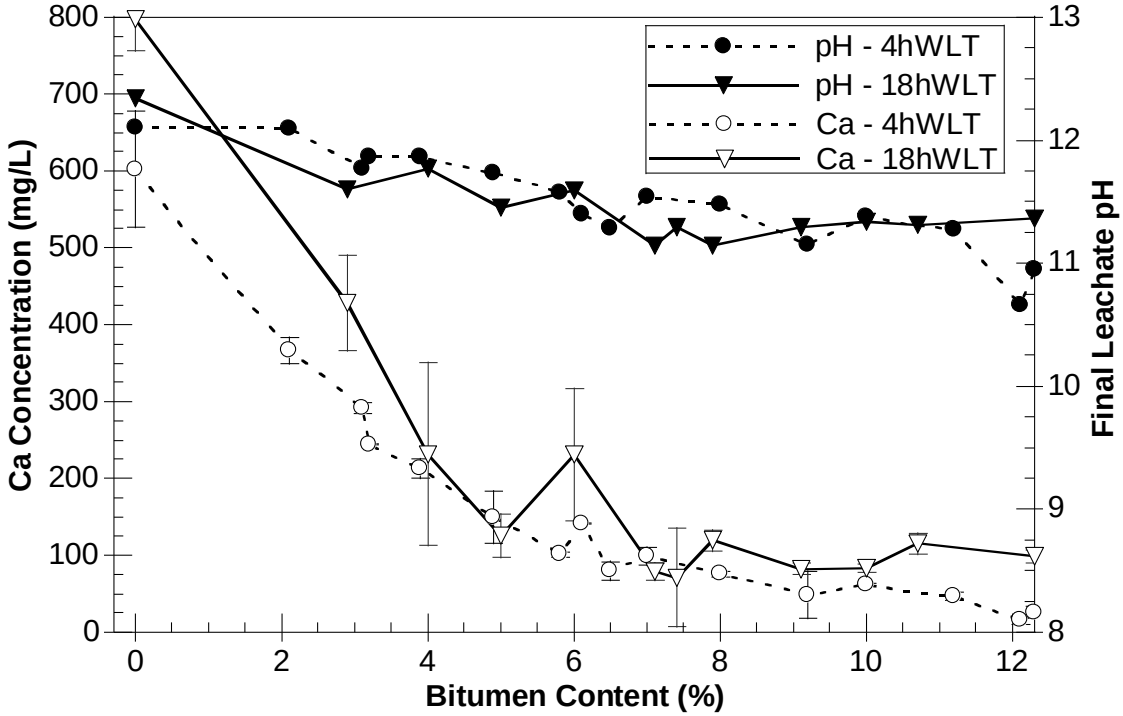

Figure 2.6. Leachate pH and calcium concentrations in bitumen-coated 6M leachates.

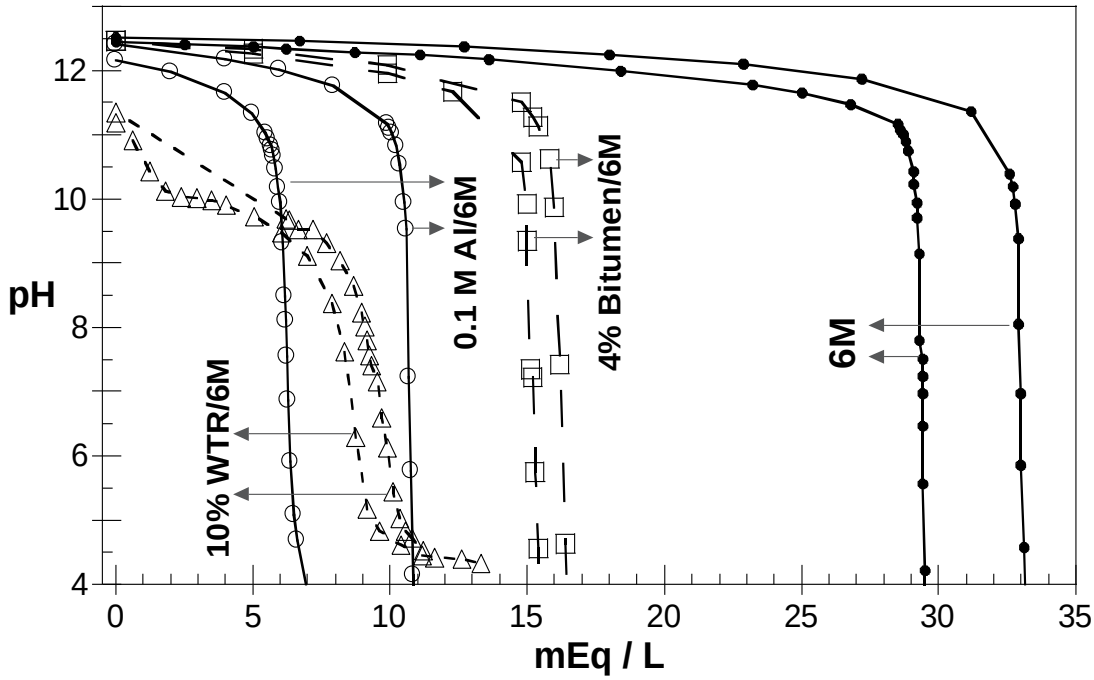

Figure 2.7. Replicated alkalinity curves of 6M and treated 6M leachates.

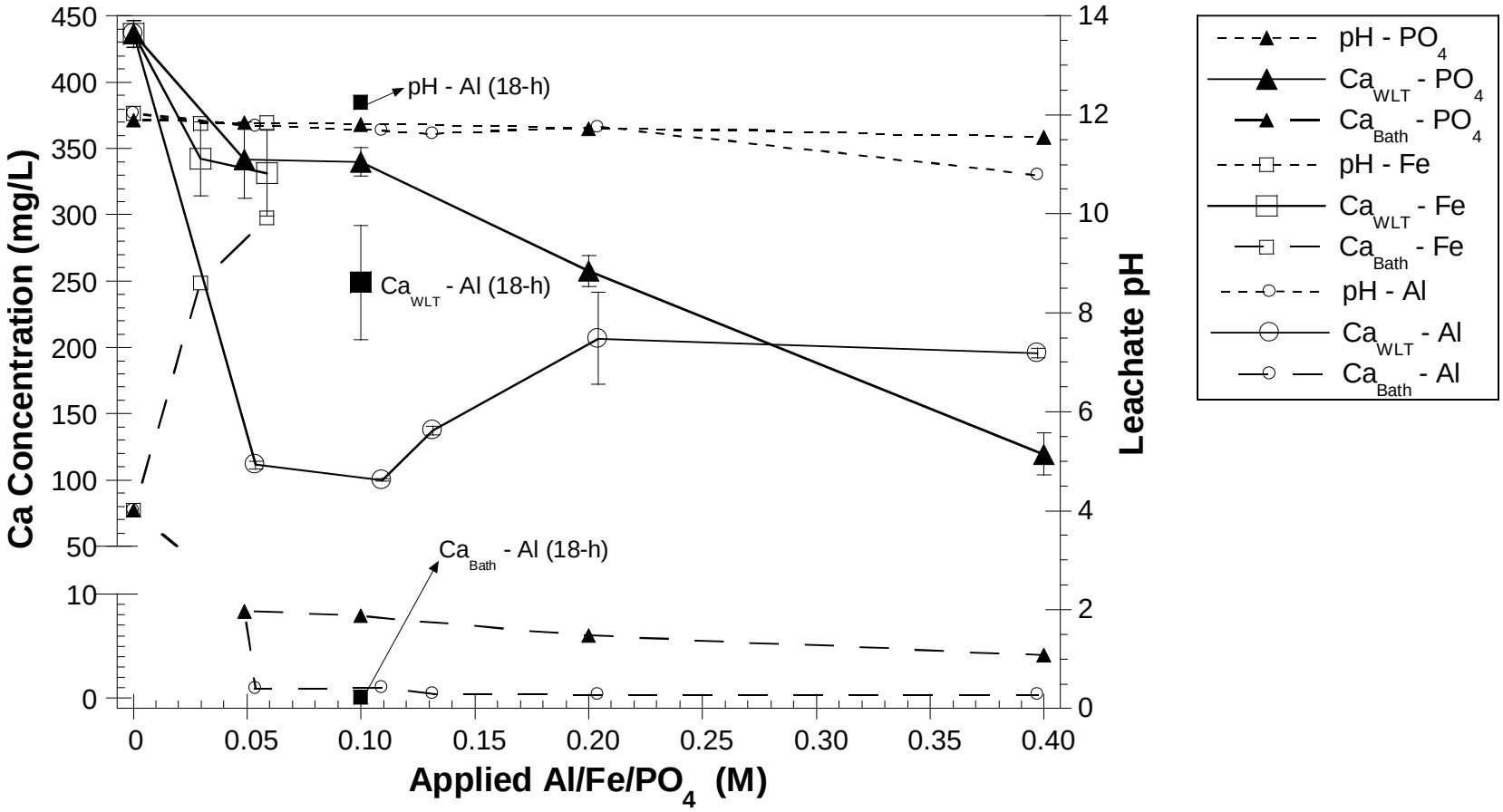

Figure 2.8. Ca concentration (Ca_{WLT}) and pH from 4-h and 18-h WLTs of passivated 6M, along with Ca release during bathing (Ca_{Bath}).

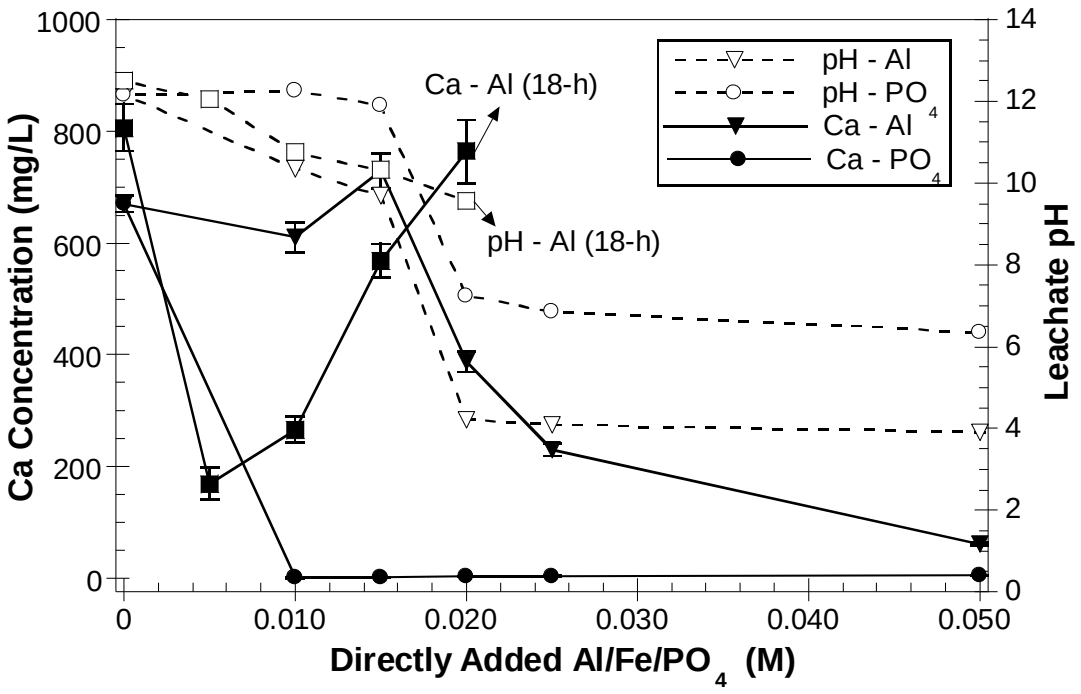

Figure 2.9. Dissolved Ca concentration and pH from 4hWLTs where passivation chemicals were added into extraction solutions, along with 18hLTs using Al(+III) passivated slag.

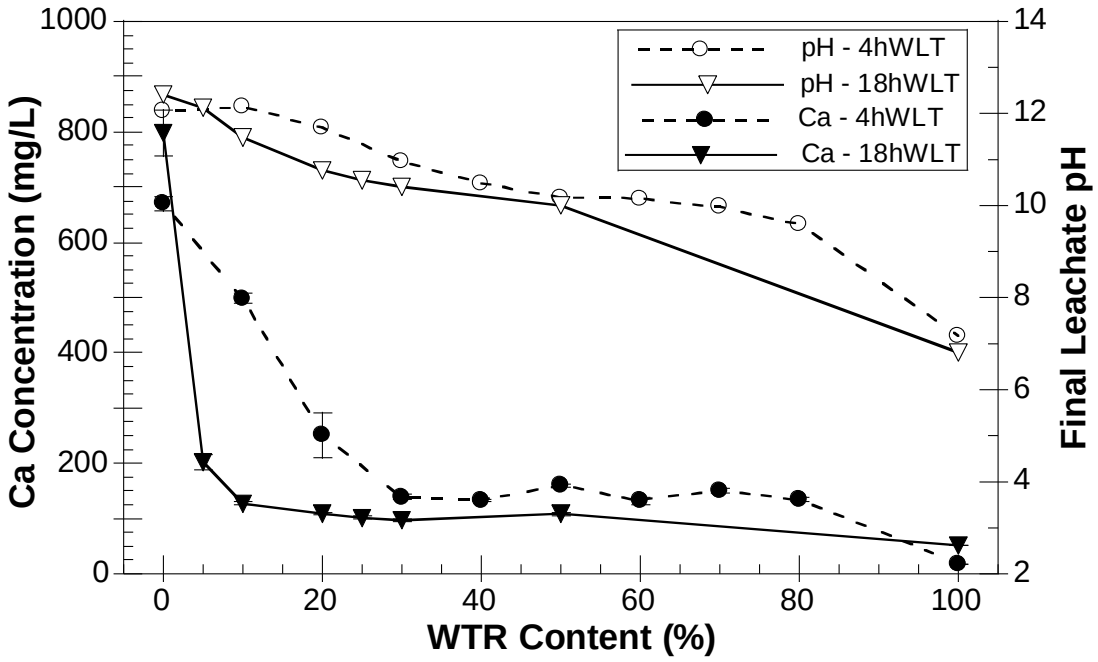

Figure 2.10. Ca concentrations and leachate pH in WTR-6M mixtures.

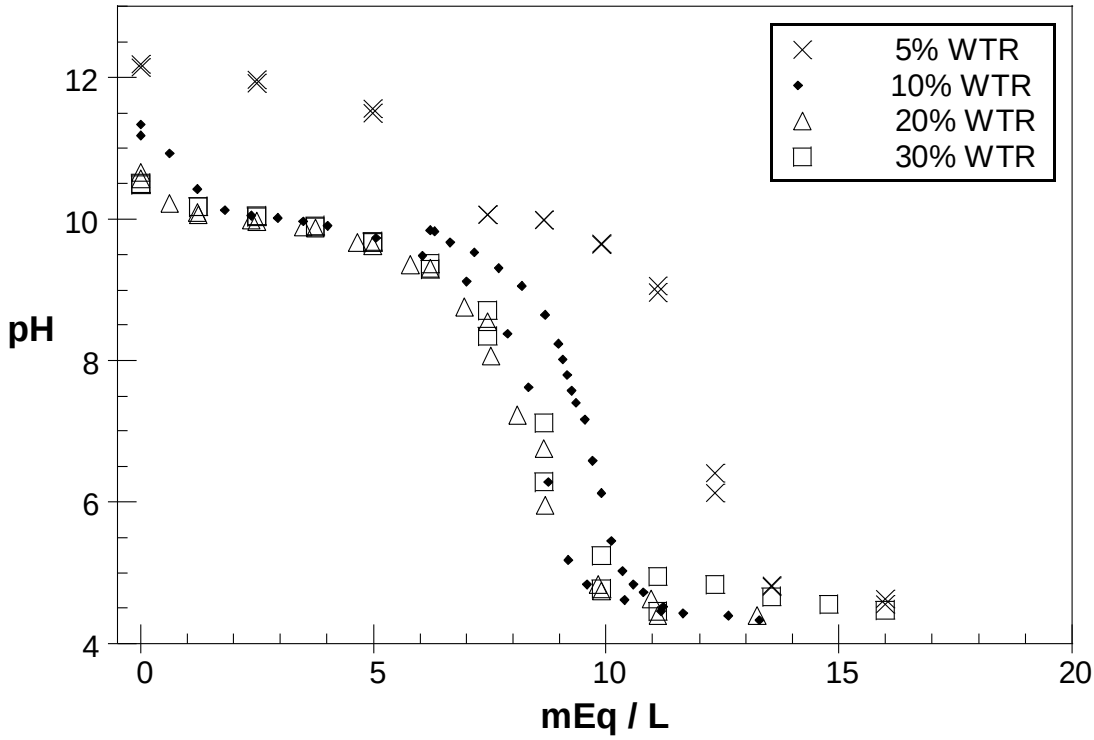

Figure 2.11. Leachate alkalinity curves for 5% WTR, 10% WTR, 20% WTR and 30% WTR leachates.

CHAPTER 3: ALKALINITY MITIGATION MECHANISM IN WATER TREATMENT RESIDUAL−MODIFIED AGED STEEL SLAG

3.1. Introduction

In the previous part of the study, alkalinity production in steel slags was shown to be correlated to Ca(+II) and OH releases that was most likely controlled by $Ca(OH)_2$ solubility, and preliminary evidence was presented about the success of WTR addition as a way of mitigating the alkalinity producing capacity of aged steel slag. Mixing WTR into steel slag caused significant reductions in pH (1-2 units), leachate alkalinity, and Ca(+II) release from the aged steel slag in batch-type leach tests. The mechanism behind this mitigation effect was speculated to be formation of ettringite [$Ca_6Al_2(SO_4)_3(OH)_{12}•26H_2O$; AFt] and monosulfate [$Ca_6Al_2SO_4(OH)_{12}•6H_2O$; AFm] as secondary mineral phases.

Ca(+II) and OH release from aged steel slags were high; Alum-based WTR is rich in am-$Al(OH)_3$ which can be dissolved at high pH and contains small amounts of sulfur. In an $Al_2O_3−CaO−SO_4−H_2O$ system at ambient temperatures, ettringite is the most stable solid phase under highly alkaline conditions (pH 10.7−12.5) (Hampsoim and Bailey, 1982; Warren and Reardon, 1994; Thomas et al., 2003; Baur et al., 2004). At above pH 11.6, ettringite can transform to metastable monosulfate (Hampsoim and Bailey, 1982; Gabrisová et al., 1991; Damidot and Glasser, 1993; Myneni et al., 1998). Therefore, $Ca(OH)_2$ solubility-governed alkalinity production in hydrated steel slags could have been altered, shifting the control of Ca(+II) and OH release to calcium sulfoaluminate phases by WTR-modification.

The objective of this second part of the study was to investigate and explain the mechanism of alkalinity mitigation upon WTR addition. Batch-type leach tests were conducted to further study the alkalinity mitigation effects of WTR addition and determine the Al and S release from WTR/slag mixtures. Acid/base additions were made to adjust the final pH of the leachates from batch-type leach tests, in order to study the chemistry of the leachates within a wider range. Also ways of improving the success of mitigation were explored by extra sulfate addition to WTR-amended slag. Saturation indices of ettringite and monosulfate were calculated for the filtered leachates from these batch-type tests, in order to investigate the likelihood of ettringite or monosulfate formation and saturation levels of other possible solids. Furthermore, scanning electron microscopy (SEM) and energy-dispersive x-ray spectrum (EDX) analyses were also conducted on the surfaces of hydrated steel slag particles in slag alone and WTR/slag mixtures to observe the differences occurred upon WTR addition. Finally two types of column leach tests using different particle size ranges and flow rates were employed on slag alone and WTR/slag mixtures to investigate the stability of the mitigation effect under dynamic conditions.

3.2. Materials and Methods

3.2.1. Aged Steel Slag and Other Materials

The same 6-month-old basic-oxygen furnace (BOF) steel slag and water treatment residual (WTR) described in Chapter 2 were used in the following studies. 6-month-old steel slag was designated as “6M”. Water treatment residual (WTR) was added to 6M at different proportions based on dry weight and batch-type leach tests were conducted using these mixtures. WTR/6M mixtures were labeled as according to their WTR content; for example, 10WTR for 10% WTR plus 90% 6M mixtures. The specific gravity of the steel slag and

water treatment residual was 3.45 and 1.8, respectively (ASTM, 2010a; Dayioglu et al., 2014).

Alum precipitate was prepared by precipitating hydrated $Al_2(SO_4)_3 \cdot xH_2O$ (Alfa Aesar, Ward Hill, MA, >97%) in a NaOH solution. Aluminum sulfate was dissolved in DI water and the pH was raised to 7.0 by adding NaOH. After the supernatant was discarded and replaced by DI water, the precipitate was allowed to settle again and the supernatant was discarded again. Removal of the supernatant and DI water addition was repeated three times to purge the alum slurry from more soluble impurities, i.e., Na and SO_4. Then, the settled solids were separated and washed one last time with methanol to remove moisture. Next, the precipitate was dried at 105°C over 24 hours. Finally, alum precipitate was grounded and rendered into a white power. All reagents used in this research study are ACS Grade.

3.2.2. Batch-type Leach Tests

Batch-type leach tests (LT) were conducted to investigate water-soluble constituents from 6M steel slag and WTR/6M mixtures. 2.50 g of solid specimens were placed into a 50-mL high density polyethylene centrifuge tube and 50-mL DI (extraction liquid) was added. The liquid-to-solid ratio of 20 mL/g (volume/weight) was used in all leach tests. The type of extraction liquid was sometimes different depending on the variant of the leach test. After the addition of extraction liquid, the tubes were capped and were end-to-end tumbled continuously on a rotator at 29 rpm (rotations per minute) at the ambient temperature of the laboratory (20±1 ºC). For most of the leach tests, the duration of the tumbling period was set to 18 hours and these 18-h leach tests were designated as “18hLT”. In other leach

tests, tubes were tumbled for 48 hours and 168 hours. 168-hour leach tests were designated as “168hLT”.

At the end of the tumbling period, all sample tubes were centrifuged at 4000 rpm for 5 minutes to separate the supernatants, which are referred as “leachates” in this study, and the pH of the leachates were measured. After pH measurements, leachates were decanted and filtered through 0.2-µm pore-sized membrane filters (PALL, Port Washington, NY, Supor 200) into other 50-mL high density polyethylene centrifuge tubes, and were acidified to pH<2 using trace metal grade concentrated HNO_3 (J.T. Baker, Center Valley, PA, ~15.8 N) for preservation. All samples were stored at 4ºC in a refrigerator until further analyses. Each leach test was replicated twice.

For the leach tests that were conducted to investigate the elemental leaching from 6M and WTR/6M mixtures, the extraction liquid was 0.02 M NaCl in deionized (DI) water. 0.02 M NaCl was used as extraction liquid for these LTs to simulate the ionic strength of stormwater percolating through soil.

3.2.3. Leach Tests with Modified Final Leachate pH

In order to investigate the pH dependency of Al, Ca and S leaching from 6M and 6M/WTR mixtures, leach tests were designed and conducted to obtain leachates with final pHs that were different than the original pH. These tests were a variant of the 18-h leach tests where DI water was used as extraction solution. First, 6M and 6M/WTR mixtures were subjected to 18hLTs as described above. At the end of the 18-h tumbling period, the caps of the tubes were removed and the samples were spiked with different amounts of trace metal grade concentrated 15.8 M HCl or 5 M NaOH to modify the final leachate pH value. Added acid

or base volume was ≤0.4 mL and it was presumed that solid-to-liquid ratio of the samples were not affected. After acid spiking, the tubes were sealed and were tumbled for an additional 4 hours. Finally, after the second tumbling period, the samples were processed and preserved similar to other leach test samples.

3.2.4. Sodium Sulfate Additions

Ettringite formation was assumed to be the reason of decreased Ca release in 6M/WTR. It was assumed that presence of additional sulfate in the leachate might improve ettringite formation. To test this hypothesis, sulfate solutions with different concentrations were used as extraction liquid in 18hLTs that were employed using WTR/6M mixtures. Sulfate solutions were prepared by dissolving different amounts of sodium sulfate [$Na_2(SO_4)$, ≥99%, Ricca Chemical, Arlington, TX] in DI water.

3.2.5. Determination of Neutralizing Capacity of Solids

For acid neutralizing capacity (ANC) and base neutralizing capacity (BNC) measurements, samples were prepared similar to 18-h leach test samples, but 50-mL acid or base solutions at different concentrations were added to the tubes as extraction solution. Acid solutions were prepared by adding different volumes of 1 N HCl into DI water. 1 N HCl was prepared by diluting concentrated HCl (~15.8 M) in DI water. Base solutions were prepared by mixing 1 N NaOH solution with DI water. The 1 N NaOH solution was prepared by dissolving NaOH pellets in DI water. Then, tubes were tumbled for 18 hours at 29 rpm as done for leach tests. At the end of the tumbling period, the pH of the samples were measured and values were plotted against the amount of H or OH added per kg solid material. The consumed acid concentration at specific pH values was estimated by

interpolating the available data. These type of buffering tests were referred as “18hLTs with acid/base addition”.

In addition to the neutralizing capacity tests where acid or base was added at the start of the test, some neutralizing capacity tests were initially run as 18hLTs using DI water as extraction liquid and after the 18-h tumbling period, acid or base was added. Finally, samples were tumbled an additional 4 hours and then the pH of the leachates were measured. These tests were referred as “18h+4hLTs with acid/base addition”.

3.2.6. Acid Ammonium Oxalate Extraction

To estimate the amounts of amorphous aluminum oxides, ammonium oxalate extraction (AOE) method was utilized as described in Özkök et al. (2013). 0.275 M AOE solution was prepared by dissolving 0.175 M ammonium oxalate and 0.1 M oxalic acid in DI water. The pH of the solution was adjusted to pH 3.0±0.1 with 1 M HCl addition. 1.0-g WTR samples were combined with 100 mL ammonium oxalate solution and other kind of samples were combined with 50 mL solution. Samples were mixed continuously, end-to-end tumbled for 2 h in the dark at 75 rpm, and then centrifuged for 5 min at 4000 rpm. Finally, supernatants were filtered through 0.2-μm membrane filters. These filtrates were then collected and stored at 4°C until they were analyzed. The oxalate-extractable Al concentration was presumed to be a surrogate of amorphous Al (hydr)oxide content.

3.2.7. WTR in CaO and $Ca(OH)_2$ Solutions

$Ca(OH)_2$ (Fisher Scientific, Fair Lawn, NJ) was dissolved in water to prepare alkaline solutions with different Ca concentrations. Then, these solutions were used as extraction liquid in 18hLTs that were employed on 2.50 grams of WTR. The results were used to

observe the reaction of WTR with pure $Ca(OH)_2$ and residual Ca, Al and S concentrations were compared to the tests that were using WTR/6M mixtures. In some tests, CaO (J.T.Baker, Phillipsburg, NJ) was used instead of $Ca(OH)_2$ to determine if the WTR was also able to reduce Ca release from pure CaO.

3.2.8. Extraction in NaOH Solution at pH 12.5

2.5 g of WTR was placed into a HDPE container that was containing 500-mL NaOH solution at pH 12.5 and the samples were tumbled for 18 hours. At the end of 18 hours, the supernantant (extract) was filtered. Next, 50-mL of this WTR extract was used as extraction liquid in 18hLTs that were conducted using 2.0 g 6M. As a control, some 18hLTs were conducted using the NaOH (≥97%, Sigma-Aldrich, St. Louis, MO) solution at pH 12.5 as extraction liquid. In addition to WTR, 1.25-g alum-precipitate was extracted in 500-mL NaOH solution at pH 12.5 and the resulting alum-precipitate extract was also used in 18hLTs that were conducted using 2.0 g 6M.

3.2.9. SEM and EDX Analyses

Scanning electron microscopy (SEM) and energy-dispersive X-ray spectroscopy (EDX) analyses were employed on hydrated 6M and WTR/6M mixtures. 18-h leach tests (using DI water as extraction liquid) were conducted using 6M and 10WTR employing the specifications given for these tests. At the end of the tumbling period, supernatant was removed and remaining solids inside the tubes were drained as much as possible. Drained samples were placed into plastic containers with a separate compartment containing KOH pellets (87.8%, J.T.Baker, Phillipsburg, NJ). KOH pellets were used to remove CO_2 in the environment. Samples were air-dried inside small desiccators for a 5 days before analyses.

The morphology of the surfaces of steel slag particles from hydrated mixtures were qualitatively examined using scanning electron microscope (Hitachi Model SU3500, Tokyo, Japan) without applying any coating on the samples and micrographs of the surfaces were produced. Qualitative chemistries of the surfaces were obtained separately with an EDX spectrometer (Amray, Model 1820D, Bedford, MA) using a 12 mm working distance with an accelerating voltage of 15−20 kV and at 20 degrees tilt.

3.2.10. Calculation of Ion Activity Products and Saturation Indices

Elemental Al, Ca, Na, Mg, P and S concentrations in the filtered samples were measured using ICPE spectrophotometry and pH of the leachates were measured using the pH meter. Concentrations below the detection limit were assumed to be at the half of the detection limit value in IAP calculations, unless otherwise mentioned. The measured dissolved S concentrations were assumed to be all found in SO_4(-II) form in the leachates. Dissolved P concentrations in the samples were under the detection limit (0.34 mg/L for P).

The measured dissolved Ca, Al, Na, Mg and S elemental concentrations and the pH values for each leachate were used as input values in *Visual MINTEQ v3.1* (Gustafsson, 2015), a geochemical modeling program. The software was used to estimate activity of SO_4^{2-}, $Al(OH)_4^-$, OH^- and Ca^{2+} using the default thermodynamic databases supplied with the program (Table 3.1) and the Davies' Equation (Eq. 3.1). Temperature was set to 20ºC. The samples from the leach tests with adjusted pH values, molar concentrations Cl were estimated based on the added HCl concentrations; Cl(-I) in leachates from column tests was assumed to be 0.02 M where influent was 0.02 M NaCl; for all other samples without HCl, Cl(-I) concentrations were measured using an ion chromatographer (Dionex Model

ICS-1100, Sunnyvale, CA). Any set of calculations, where charge balance error calculated in *Visual MINTEQ* was >30%, was excluded and not reported.

$$\log \gamma_i = -A\, z_i^2 \left(\frac{\sqrt{I}}{1+\sqrt{I}} - 0.3\, I\right) \quad (3.1)$$

where y_i is the activity coefficient for ion *i*; *A* is a constant dependent on the dielectric constant of water and temperature (~0.5 at 20 °C); *z* is the charge of ion; and *I* is the ionic strength of the solution (Stumm and Morgan, 1996; Gustafsson, 2015).

The estimated activities were used to calculate *IAP* values at 20 °C for ettringite, monosulfate, gypsum, portlandite and amorphous Al-hydroxide using the equations and values that were given in Table 3.2. ΔH_r values that were reported in Table 3.2 and the van Hoff equation (Eq. 3.2) were used to convert *IAP* values calculated for 20ºC to *IAP* values at 25ºC values.

$$\ln\left(IAP_{(25°C)}\right) = \ln\left(IAP_{(20°C)}\right) - \frac{\Delta H_r}{R}\left(\frac{1}{298} + \frac{1}{293}\right) \quad (3.2)$$

where $IAP_{(20°C)}$ and $IAP_{(25°C)}$ was ion activity product of the chemical at 20C and 25C, ΔH_r is the standard enthalpy change reported for the compound, and *R* was the ideal gas constant. By comparing the K_{sp} values and *IAP*s calculated for different mineral phases, the saturation indices at 25ºC for solids compounds were estimated (Eq. 3.3).

$$\text{Saturation Index (SI)} = \log IAP - \log K_{sp} \quad (3.3)$$

3.2.11. Column Leach Tests (CLT)

Two types of column leach tests (CLT) using different particle size ranges and flow rates were employed on 6M alone and WTR/slag mixtures to investigate the stability of the

mitigation effect under dynamic conditions. The specification of the CLTs were given in Table 3.3.

The first type CLTs were referred as “small columns tests” or simply as “column tests”. Glass tubes having a 25-mm inside diameter and 200-mm height were used as columns. The columns were filled with 6M or 10WTR without any compaction other than tapping the column while it was being filled. Particle size of WTR was <0.42 mm and particle size 6M was 0.25 mm−2.00 mm. 0.02 M NaCl dissolved in deionized (DI) water was used as the influent to simulate the ionic strength of water percolating through soil (Morar et al., 2012). Influent solution was provided in an upflow direction through a peristaltic pump (Masterflex) and plastic tubing. The average flow rate in these small columns tests was 0.195±0.008 mL/minute. The volume of water passed through the columns were normalized by the pore volume (PV) of the column and reported in units of PV.

The second type of CLT was label as “big column tests”. These column tests were conducted to more realistically simulate field conditions following ASTM Standard D4874 (ASTM, 2006b). All specimens (i.e., 6M and 10WTR) were compacted at 2% dry of optimum moisture content (OMC) in a polyvinyl chloride (PVC) tube having a 102-mm inside diameter and 305-mm height, in order to obtain higher hydraulic conductivities for collecting enough column effluent in a reasonable time as recommended in Bin-Shafique et al. (2006). Standard Proctor compaction tests (ASTM, 2012) were conducted to determine the dry unit weight of steel slag and 10WTR samples at its optimum moisture content. 600 kN-m/m^3 compaction energy was applied to the fill material during compaction. ASTM Standard D4874 demands that solid material used to fill columns must have a particle size less than 1/10 of the diameter of the column. Thus, the columns were

filled with steel slag sieved through US sieve Size #3/8 (<9.5 mm); Particle size of WTR was <0.42 mm. After compaction, the column reactors were fabricated by placing porous stones at each end of the sample, and then capping the column with latex end plates, which were held in place through threaded rods and sealed with silicone sealant. The end caps included ports for influent and effluent tubing attached to plastic connectors. Again, 0.02 M NaCl dissolved in deionized (DI) water was used as the influent. Influent solution was provided in an upflow direction and flow rate for the influent was set at around 1 mL/min (0.990±0.128 mL/min), which is selected to simulate typical velocities (3×10^{-3} to 2×10^{-2} m⁄d) expected under field conditions (Morar et al., 2012).

3.2.12. Other Analytical Techniques

Leachate pH was analyzed using a Model 520A meter (Orion, Boston, MA) equipped with a Thermo Scientific Model Sure-Flow pH probe (Beverly, MA), per ASTM E70. Because of the high pH values (>pH 12) encountered in the leachates, care was taken to calibrate pH probes using standard buffer solutions at pH 4.01, 7.0, 10.01 and 13.0. The leachate pH of replicated samples were reported as the geometric mean of measured pH values. Leachate conductance was measured with YSI Model 35 Conductance Meter (Yellow Springs, OH), immediately after sample collection. The conductance readings were converted to electrical conductivity (EC) in $\mu S\ cm^{-1}$ units at 25°C.

An inductively coupled plasma emission spectrophotometer (Shimadzu Model ICPE 9000, Tokyo, Japan) was used to measure dissolved elemental concentration of Al, Ca, Na, Mg, P, Fe, Si and S. All standards prepared for metal analysis were be prepared in a matrix similar to the samples and all analyses were be conducted following the standards given in APHA (2005). Only calibration curves with a coefficient of determination (R^2) of 0.9975

or higher were accepted. Detection limits were; 1 mg/L for Mg, Al, Na and K; 0.25 mg/L for Fe; and 0.34 mg/L for P; 0.33 mg/L for S; and 0.2 mg/L for Si. Concentrations below the detection limit are plotted as ½ of the detection limit. The average of the measurements from replicated tests were plotted on the graphs and error bars delineate the standard deviation between the measurements. In tables, values given after "±" sign represent the standard deviation.

SO_4(-II) and Cl(-I) ions were measured using an ion chromatographer (Dionex Model ICS-1100, Sunnyvale, CA). SO_4 concentrations measured in IC and S concentrations from ICPE were compared to determine whether all measured elemental S concentrations were matching the SO_4 measurements. Concentrations from 19 samples were compared in this way and differences were found to be statistically insignificant (p<0.05). Dissolved phosphate in leachates were analyzed colorimetrically at 880 nm as described by Pote and Daniel (2009) using a spectrophotometer (Agilent Technologies Model Cary 60 UV-Vis, Santa Clara, CA) and compared to elemental P concentrations measured in ICPE. Concentrations in 28 samples were compared in this way and differences were found to be statistically significant (p>0.05).

3.3. Results and Discussion

3.3.1. Aluminum Leaching from 6M/WTR Mixtures

Elemental leaching from for aged steel slag (6M) and water treatment residual (WTR) in 18hLTs using DI water as extraction liquid and ammonium oxalate extractions are given in Table 3.4. WTR was an alum-based sludge and had a high ammonium oxalate extractable Al content of 113,000 mg/kg, corresponding to 66% of the total Al content measured in TEA (Table 2.1), indicating that Al in WTR was mainly in amorphous form.

In 18hLTs, Al in WTR was sparingly soluble (30 mg/kg) at pH 6.9. By comparison with WTR, the amount of ammonium oxalate extractable Al content in 6M was very small (940 mg/kg), corresponding to 0.09% of its total Al content. Al content of 6M appeared to be insoluble (<10 mg/kg) in its leachate at pH 12.5.

Iron was the second most abundant element in the 6M but it was not soluble under alkaline and acidic conditions, similar to Al content of 6M. Of 129,000 mg/kg total Fe content in 6M, only 0.28% was ammonium oxalate extractable. Dissolved Fe concentrations in 6M leachates were below detection limit (<0.004 mM) despite the highly alkaline conditions.

Dissolved Al(+III) and Ca(+II) concentrations, along with final leachate pH values, measured in the leachates of WTR/6M mixtures from 18-hour (18hLT) and 168-h leach tests (168hLT) using 0.02 M NaCl as extraction liquid are presented in Figure 3.1a as a function of WTR content (% of total mixture mass, wt./wt.). The data from 18hLTs using 0.02 M NaCl as extraction liquid for WTR/6M mixtures was previously discussed in Chapter 2 but solely based on dissolved Ca(+II) concentrations that were measured using atomic absorption spectrophotometry. Here, same type of 18hLTs were repeated for WTR/6M mixtures to examine Ca(+II) and Al(+III) leaching together; dissolved Ca(+II) and Al(+III) concentration were measured using ICPE spectrophotometry.

According to results from 18hLTs (extraction liquid was 0.02 M NaCl), adding as low as 5% WTR to 6M decreased the amount of Ca(+II) release from 18.4 mM to 6.1 mM and increasing the WTR content to 10% resulted in 5.3 mM Ca(+II) release. Adding more than 10% WTR resulted in only marginal reduction in Ca(+II) release; 50% WTR/6M leached 4.2 mM Ca(+II). The pH decreased steadily with increasing WTR content and dropped to

pH 11.5 and pH 10.0 at 10% and 50% WTR, respectively. In conjunction with the decline in Ca(+II) leaching, dissolved Al(+III) concentrations in the leachates markedly increased with the addition of WTR. In 18hLTs, 6M released only 0.06 mM Al(+III) despite the highly alkaline conditions of its leachate at pH 12.5. Dissolved Al(+III) concentration increased to 8.4 mM with 10% WTR addition and peaked at 9.0 mM at 20% WTR (pH 10.8) before decreasing at WTR percentages above 20%. Al(+III) release from 50% WTR mixtures was 2.9 mM. For the 100% WTR leachate, the dissolved Al(+III) concentration was below detection limit (<0.02 mM Al) at pH 6.8. It appears that amorphous Al(+III) in WTR was very soluble at high pH (>pH 10.8) and became less mobile as the pH approached circumneutral range due to increasing WTR fraction.

Both the results from 18hLT and 168hLT (extraction liquid was 0.02 M NaCl) were not very different in terms of Ca(+II) and Al(+III) release and leachate pH, suggesting that the WTR/6M mixtures were stable despite longer contact time and greater agitation in the week-long tests (Figure 3.1a). Calcium leaching capacity of 6M appeared to be greater in 168hLTs likely due to increased abrasion of steel slag particles (22.6 mM Ca vis-à-vis 18.4 mM Ca); nevertheless, the relative reduction levels in Ca(+II) release were very similar; 67−75% reduction within the range of 5%−30% WTR addition. Notice that dissolved Al(+III) and leachate pH was slightly higher in 168hLTs compared to 18hLTs.

As seen in Figure 3.1b, electric conductivity (EC) decreased in accordance with the reduction in Ca(+II) concentrations (e.g., 11 m*S*/cm for 6M and 3.9 m*S*/cm for 10% WTR). Note that these EC measurements are from 18hLTs using 0.02 M NaCl solution as extraction liquid and that the EC of 0.02 M NaCl was 2.6 m*S*/cm. Therefore, the total amount of the dissolved species in the leachates was significantly reduced upon WTR

addition. This suggests that the removal of OH^- alkalinity and Ca(+II) from the solution was due to a precipitation or sorption mechanism instead of an ion exchange mechanism.

In Table 3.5, the concentrations of the major elements measured in the leachates from 18hLTs (using WTR/6M mixtures and DI water as extraction liquid) and the activities of species of these elements that were calculated in *Visual MINTEQ* are listed, along with calculated ionic strength (*I*) and relative charge difference values. In addition to the elements reported in Table 3.5, dissolved Mg, K, Fe, Si and P concentrations in the filtered samples were measured in the samples, but they were all found to be below detection limit (0.021 mM for Mg; 0.026 mM for K; 0.004 mM for Fe; 0.011 mM for P; and 0.007 mM for Si). In 6M, 85% of the dissolved elemental Ca(+II) concentration in the leachates was in form of Ca^{2+} and 15% in form of $Ca(OH)^+$. In WTR-amended samples, dissolved Al(+III) was almost completely in form of $Al(OH)_4^-$ (>96%). According to the electro-neutrality calculations (Eq. 3.4), there was a significant charge imbalance in 10WTR and 20WTR, indicating an error either in the analytical techniques or the simplifications made to calculate the activities in these 5 leachates.

$$\{H^+\}+2\{Ca^{2+}\}+\{CaOH^+\}+\{Na^+\}=\{OH^-\}+\{Al(OH)_4^-\}+\{Cl^-\}+2\{SO_4^{2-}\} \quad (3.4)$$

At the end of the previous chapter, the alkalinity in the leachates of WTR added 6M samples were not only shown to be lower compared to the 6M leachates but also the pH ranges where the leachates buffered most were also significantly changed. Alkalinity in aged steel slag leachates were shown to be correlated to OH^- alkalinity originated from $Ca(OH)_2$ dissolution (Eq. 3.5 and 3.6). It was speculated that dissolved Al(+III) in the

WTR-amended steel slag leachates were also contributing to the alkalinity. Al(+III) in form of $Al(OH)_4^-$ could consume H^+ that was added in alkalinity measurements (Eq. 3.7).

$$Ca(OH)_2 \leftrightarrow Ca^{2+} + 2\ OH^- \quad (3.5)$$

$$Ca(OH)_2 \leftrightarrow CaOH^+ + OH^- \quad (3.6)$$

$$Al(OH)_4^- + H^+ \leftrightarrow H_2O + Al(OH)_{3\,(s)} \qquad \log K_{Al(OH)4^-} = 12.35 \quad (3.7)$$

In Table 3.6, the concentrations of $Al(OH)_4^-$, $CaOH^+$, OH^- in the leachates from 18hLTs using 0.02 M NaCl as extraction liquid were estimated and compared to the H^+ concentrations that were consumed to reach pH 7 during leachate alkalinity measurements, assuming that Al(+III) completely precipitated at pH 7 and Ca(OH)+ dissociated completely. The calculation indicate that a significant portion of the leachate alkalinity for WTR-amended samples could be associated to dissolved Al(+III) concentrations (38−103%), whereas 91% of alkalinity in 6M leachates was correlated to [$CaOH^+$] and [OH^-].

In order to provide further evidence for the contribution of Al(+III) species on alkalinity, the middle points for reactions presented in Eq. 3.7 and Eq. 3.8 were calculated for acid-titrated 10WTR leachates (Figure 3.2). Dissolved Al(+III) concentration in 10WTR was 8.4 mM. According to the calculations carried out using *Visual MINTEQ*, the ionic strength was 0.0361 M, Al(+III) in 10WTR leachate was completely in form of $Al(OH)_4^-$ and activity of $Al(OH)_4^-$ was 7.1 mM ($10^{-2.15}$ M). The log K values for the reactions presented in Eq. 3.7 and 3.8 were 12.35 and -10.4, respectively (Hendricks, 2010). Based on these values, the middle point, where half of the Al(+III) was in form of $Al(OH)_4^-$ and the other half precipitated in form of $Al(OH)_{3\,(s)}$, was calculated at pH 9.9 (Eq. 3.9); pK_{a1} = 9.90.

The point where $\{Al(OH)_3\}$:$\{Al^{3+}\}$ ratio was 50:50 was estimated to be pH 4.28 (Eq. 3.10); pK_{a2} = 4.28. Therefore, isoelectric point was pH 7.09 [(pK$_{a1}$ + pK$_{a2}$)/2]. As seen in Figure 3.2, these calculated pK_a points and the titration data were in good agreement, clearly delineating how transformations among Al(+III) species affected the buffering capacity of the leachate at different pH ranges (pH 9−10 and pH 4−4.5).

$$Al(OH)_{3\,(s)} + 3\,H^+ \leftrightarrow Al^{3+} + 3\,H_2O \qquad \log K_{Al(OH)3} = -10.4 \tag{3.8}$$

$$\{Al(OH)_4^-\} = \frac{10^{-2.15}}{2},\ K_{Al(OH)4^-} = \frac{1}{\{Al(OH)_4^-\}\ \{H^+\}} = 10^{12.35} \ \rightarrow\ \{H^+\} = 10^{-9.90} \tag{3.9}$$

$$\{Al^{3+}\} = \frac{10^{-2.15}}{2},\ K_{Al(OH)3} = \frac{\{Al^{3+}\}}{\{H^+\}^3} = 10^{-10.4} \ \rightarrow\ \{H^+\} = 10^{-4.28} \tag{3.10}$$

3.3.2. Neutralizing Capacity of WTR and Aged Steel Slag

Figure 3.3 shows the acid neutralizing capacity (ANC) or base neutralizing capacity (BNC) of 100% 6M (6M), 100% WTR (100WTR) and 10% WTR added mixtures (10WTR) obtained in 18h and 18h+4h neutralization capacity tests. The amount of the acid or base that was consumed to obtain final pH values at pH 7 and pH 8.5 was estimated by interpolating the measured data (Table 3.7). Aged steel slags had a high ANC, especially above pH 11.6. Within 18 hours, 6M(18h) consumed approximately 2080 mEq/kg acid to reach pH 7. In comparison, 100WTR(18h) had initial pH ~7 and buffered the acidic solutions below pH 4 and the basic solutions above pH 11.4. According to these results from 18-h tests, it is clear that WTR lacked the potential of neutralizing alkalinity produced by 6M based on its BNC. For example; ANC of 6M(18h) was 1450 mEq/kg at pH 10 and BNC of WTR was 550 mEq/kg at pH 10, but the pH of the leachate produced by 50%WTR+50%6M mixtures at the end of 18 hours was 10. Thus, the reduction in leachate

pH values should have occurred through a mechanism other than or alongside simple neutralization.

10WTR(18h) exhibited significantly different neutralizing capacity at final pH values above 10.6 compared to 6M(18h), but its ANC values approached to 6M(18h) below pH 10.6. ANC of 10WTR(18h) was 1600 mEq/kg at pH 7, suggesting that acid buffering capacity of 10WTR(18h) was only 23% lower than 6M(18h). However, in the previous experiments, it was shown that the alkalinity in the leachates from 10WTR (pH 11.5) was 71% less compared to 6M leachates. The discrepancy between ANC of 10WTR and leachate alkalinity of 10WTR along with the disappearance of great difference between the ANC profiles of 6M(18h) and 10WTR(18) below pH 10.6 imply that excessive acid addition at the beginning of the test reduced the pH of the contacting solution to the levels, where the conditions causing the alkalinity mitigation effect did not occur during 18 hours.

Therefore, the neutralizing tests were repeated but this time 10WTR mixtures were tumbled contacting with DI water for 18 hours to let the mitigation effect take place and then different amounts of concentrated HNO_3 was added to the samples. Acid-added samples were tumbled for an additional 4 hours and pH measurements were made afterwards.

Results from 6M(18h+4h) was very similar to 6M(18h), indicating that this modified version of the test was as capable to reflect the neutralizing capacity of highly alkaline samples. On the other hand the ANC profile of 10WTR(18h+4h) was very different below pH 10.3 compared to 10WTR(18h). ANC of 10WTR(18h+4h) at pH 7 were estimated to be 72% less than ANC of 6M(18h+4h) at pH 7 (780 mEq/kg vis-à-vis 2050 mEq/kg). These

results demonstrate that alkaline pH levels (≥10.6) were required for the occurrence of the mitigation effect.

3.3.3. WTR/6M Mixtures with Adjusted Final pH

Figure 3.4a shows the dissolved Ca(+II) concentrations in the leachates from the 18h+4hLTs with either HCl or NaOH addition. Dissolved Ca(+II) concentration in 6M leachates from 18hLTs was 18 mM at the leachate's original pH of 12.4. In comparison, dissolved Ca(+II) concentrations decreased to 14.3 mM at pH 12.7 and increased to 53.7 mM at pH 5.2. In Chapter 2, it was discussed that Ca(+II) leaching from steel slags should be predominantly controlled by $Ca(OH)_2$ solubility. $Ca(OH)_2$ becomes less soluble as the pH increases and hence, NaOH addition decreases the $Ca(OH)_2$ solubility (Duchesne and Reardon, 1995). Accordingly, dissolved Ca(+II) concentrations in 6M leachates decreased when pH increased and increased when pH decreased [Eq. 3.11, (Stumm and Morgan, 1996)].

$$Ca(OH)_2 + 2\,H^+ \leftrightarrow Ca^{2+} + 2\,H_2O \qquad \log\{Ca^{2+}\} = 22.8 - 2\,pH \qquad (3.11)$$

Dissolved Ca(+II) concentrations in 10WTR leachates at pH 11.5 and pH 12.2 were 3.8 mM, corresponding to a 12% decrease in Ca(+II) solubility relative to its original leachate at pH 11.1. At pH ≤10.3, dissolved Ca(+II) concentrations in 10WTR significantly increased (11.8 mM at pH 10.3 and 24.8 mM at pH 5.8) and becomes very similar to dissolved Ca(+II) concentrations in 5WTR. Although 5WTR and 10 WTR were containing 95% and 90% 6M, Ca(+II) release from these samples was less than half of the Ca(+II) release from 6M leachates under both acidic and alkaline conditions.

In Figures 3.4b and 3.4c, dissolved Al(+III) and S concentrations measured in the leachates are given. Within the pH range of 5.2–12.2, Al(+III) in 5% and 10% WTR/6M leachates were always markedly higher compared to Al(+III) release from 6M (≤0.51 mM). WTR/6M mixtures leached 0.14−0.15 mM Al(+III) at pH 7.8−8.0. Dissolved S concentrations in all leachates were very low (≤0.42 mM) compared to Ca(+II) and Al(+III) concentrations. S leaching from 6M was increased when the pH was increased or decreased relative to original leachate pH of 12.4. S releases from 5WTR and 10WTR were very similar below pH 10.3 (~0.3 mM) as in the case of Ca(+II) releases.

3.3.1. Sodium Sulfate Addition to WTR/6M Mixtures

Sodium sulfate [$Na_2(SO_4)$] solutions at concentrations varying from 2.6 to 15 mM were introduced as extraction liquid in the 18hLTs that were conducted utilizing 2.5-g 5WTR and 10WTR. Due to presence of additional SO_4(-II), leachate pH of the samples were changed only 0.1−0.2 pH units; leachate pH of 5WTR decreased from 11.7 to 11.5−11.6 within the range of 2.6−15 mM added SO_4(-II), whereas leachate pH of 10WTR decreased from 11.1 to 10.9-11.0 (Figure 3.5a). Dissolved S concentrations in the leachates were linearly increased with increasing SO_4(-II) addition; the average ratio between measured residual S concentrations and additional SO_4(-II) concentrations was approximately 0.8 to 1. Generally, Al(+III) concentrations were increased in both 5WTR and 10WTR leachates upon SO_4(-II) addition (Figure 3.5b). Dissolved Al(+III) in 5WTR was initially 5.3 mM and increased to 5.9−6.1 mM within the range of 2.6−15 mM SO_4(-II) addition. Although dissolved Al(+III) concentration in 10WTR dropped from its initial value of 7.3 mM to 6.4 mM at 2.6 mM SO_4(-II) addition, it increased to 8 mM at 15 mM SO_4(-II) addition. The most noteworthy results from the sodium sulfate added samples were that Ca(+II)

concentrations in 5WTR leachates were decreased to levels similar to Ca(+II) concentrations in 10WTR leachates. Initial dissolved Ca(+II) concentrations of 7.1 mM in 5WTR and 4.3 mM in 10WTR were decreased to 3.1 mM and 2.7 mM, respectively, with the addition of 2.6 mM sodium sulfate. At 5−15 mM SO_4(-II) addition, dissolved Ca(+II) concentrations in 5WTR and 10WTR were 2.7±0.2 mM.

Although additional SO_4(-II) in 5 WTR and 10WTR caused dissolved Ca(+II) concentrations to decrease to 2.4−3.0 mM from 4.3−7.0 mM, it generally resulted in elevated Al(+III) and S concentrations in the leachate without a significant effect on leachate pH. It was decided that sodium sulfate addition did not produce any significant beneficial results that can justify its application.

3.3.2. NaOH-extractable Al in WTR and Alum Precipitate

In Table 3.8, Al(+III) and Ca(+II) concentrations and final pH values for WTR and alum-precipitate extracts that were extracted in NaOH solution at pH 12.5 and the 18hLTs that were using these extracts as the extraction liquid.

The leachate from 2.0-g of 6M, which was extracted in NaOH solution at pH 12.50, contained 7.2 mM Ca(+II) and the final leachate pH of this leachate was 12.61; dissolved Al(+III) concentration was below detection limit (<0.02 mM). The Ca(+II) release from 2.0 g 6M in NaOH solution was lower compared to 2.5 g 6M in DI water (7.2 mM vis-à-vis 18 mM) possibly due to lower mass of the steel slag and lower Ca solubility at higher pH (pH 12.61 vis-à-vis pH 12.38).

The ammonium oxalate extraction results shows that WTR contained approximately half the amount of oxalate-extractable Al compared to alum-precipitate and accordingly, 1.25-

g alum-precipitate and 2.50-g WTR was used in the NaOH extractions to obtain extracts with similar Al(+III) concentrations (Table 3.4). The Al concentrations in alum-precipitate and WTR extract were 31.4 mM and 32.8 mM, respectively. It appears that the amorphous Al in WTR could be easily extracted at high pH. These extracts were used as the extraction liquid to conduct 18hLT that was using 2.0 g 6M steel slag. The final leachate pH values were 0.05−0.08 log units lower than pH 12.61, thus the Ca(+II) release potential from 6M should be >7.2 mM in these tests. Nonetheless, the Ca(+II) release was 0.67 mM for WTR-extract and 0.25 mM for alum-precipitate-extract; significantly lower compared to 7.2 mM. There was also a decrease by 1.4–1.6 mM in dissolved Al(+III) concentrations in the final leachate compared to the Al(+III) concentrations in the WTR and alum precipitate extracts.

These results demonstrates the alkaline soluble constituents of alum-based WTR had an effect on steel slag's Ca(+II) release rate similar to NaOH-extracted alum-precipitate's leachate, which was containing similar amounts of Al(+III). Therefore, dissolved Al(+III) from WTR should be the main constituent reacting with Ca(+II) from 6M, and reducing $Ca(OH)_2$ solubility and consequently OH^- alkalinity release. It should be noted that alum-precipitate had 12 times more oxalate-extractable S content compared to WTR (Table 3.4). However, it was shown that increasing sulfate concentrations alone had a limited effect on decreasing Ca mobility in WTR/6M systems.

To provide further evidence for the reaction of Al(+III) from WTR and Ca oxides from steel slag, 2.5-g WTR was mixed with pure $Ca(OH)_2$ and CaO powders. Mixtures of WTR and $Ca(OH)_2$ or CaO in DI 50-mL water were used to conduct 18hLTs and the resulted leachate was analyzed for residual dissolved Ca(+II) and Al(+III) concentrations (Table 3.9). In 50-mL DI water, 0.065 g $Ca(OH)_2$ and 0.05 g CaO had the potential to release

Ca(+II) concentrations at levels similar to ones in 2.5-g 6M in 18hLTs (16.8−18.5 mM). When 2.5-g WTR and these pure Ca^{2+} sources were reacted for 18 hours, the final Ca(+II) concentration in both cases was ~3.9 mM Ca(+II) at pH 9.4–9.5. Even when liable Ca(+II) concentration was doubled by adding 0.1 g CaO (35.7 mM), the final pH and the dissolved Al(+III) concentrations increased but Ca(+II) release ascended only 13%. These results suggests that the source of Ca(+II) was also did not matter and that presence Al(+III) and other soluble constituents from WTR helped decrease the Ca mobility by controlling the Ca solubility by a phase different than $Ca(OH)_2$.

3.3.3. Mitigation Mechanism

Figure 3.6 shows the IAP values calculated for ettringite ($Ca_6Al_2(SO_4)_3(OH)_{12}\cdot 26\ H_2O$) and monosulfate ($Ca_4Al_2SO_4(OH)_{12}\cdot 6\ H_2O$) using the dissolved elemental concentrations in 5WTR and 10WTR mixtures from 18hLTs using only DI water and 18h+4hLTs with acid/ base addition. The $IAP_{\text{ettringite}}$ values for 10WTR (at its original pH of 11.1) were above the K_{sp} of ettringite and $IAP_{\text{monosulfate}}$ was less than K_{sp} of monosulfate, suggesting that ettringite formation in 10WTR samples was more likely compared to monosulfate formation. In acid-added 10WTR (pH 10.3), the leachate was slightly under-saturated in terms of ettringite and Ca mobility was three folded in this sample compared to its original state (Figure 3.4). On the other hand, for base-added 10WTR samples (pH 11.5 and 12.2), monosulfate formation in addition to ettringite appears to be possible and in these samples Ca mobility was 13% lower. The same argument can be made for 5WTR leachates at pH 10.3 and 11.7. For these samples, the changes in Ca mobility in WTR/6M mixtures seem to be explainable by precipitation/dissolution of ettringite and monosulfate. Ettringite and monosulfate can be both present in the same system and they can transform into one and

other depending on pH and sulfate levels (Gabrisová et al., 1991; Damidot and Glasser, 1993; Warren and Reardon, 1994; Myneni et al., 1998).The relatively higher $IAP_{ettringite}$ compared its K_{sp} values implies that ettringite was the more stable state in 5WTR and 10WTR (Thomas et al., 2003; Baur et al., 2004).

Figure 3.7 shows the saturation indices (SI) of ettringite and monosulfate calculated for the leachates from 6M and WTR/6M leachates from 18hLTs using only DI water; 18h+4h leach tests with acid/ base addition; and 18hLTs with sulfate additions within the pH range of 7.8−12.7, along with SI of four other compounds that can be present in association with ettringite and monosulfate in alkaline $CaO-Al_2O_3-SO_4-H_2O$ systems; gypsum [$CaSO_4 \bullet 2H_2O$], portlandite [$Ca(OH)_2$], amorphous Al-hydroxide [$Al(OH)_3$] and hydrogarnet [$Ca_3Al_2(OH)_{12}$] (Hampsoim and Bailey, 1982; Damidot and Glasser, 1993; Myneni et al., 1998). The SI of ettringite and monosulfate were increasingly undersaturated as the pH decreased. SI of monosulfate became negative at pH ~11.5 and ettringite started to be under-saturated at pH ≥10.5. Gabrisová et al. (1991) reported that ettringite phase starts to disappear below pH 10.7 and monosulfate starts to disappear below pH 11.6. It appears that Al, Ca, SO_4 and OH releases were controlled by ettringite and monosulfate phases only above pH 10.5 in WTR/6M mixtures.

In addition to evaluating SI values based on their sign, it is also helpful to compare the saturation levels of different phases. SI of am-$Al(OH)_3$ and gypsum intersected and surpassed SI of ettringite at pH <10.5. Below 10.5, Al(+III) and Ca(+II) release should be governed by solubility of am-$Al(OH)_3$ and gypsum, respectively, since SI of these minerals were higher. Below pH 10.7, ettringite was reported to incongruently dissolve into gypsum and am-$Al(OH)_3$ (Myneni et al., 1998).

In an alkaline, Al- and Ca-rich environment at 20°C, hydrogarnet can form as a stable solid mineral phase (Lothenbach et al., 2012). SI of hydrogarnet approached 0 only in 6M or base-added 10WTR leachates and was very low compared to monosulfate below pH 12.4, demonstrating that control of Al(+III) and Ca(+II) release by this phase was not possible.

Fe-ettringite and Fe-monosulfate formation at alkaline pH was also possible, but Ca(+II) removal due to dissolution/precipitation of these phases was considered to be unlikely. Formation of these phases were much slower compared their Al-containing counterparts (Möschner et al., 2008) and Fe concentrations were always below the detection limit (<0.004 mM).

Based on these findings, the alkalinity mitigation mechanism for WTR-addition can be elucidated as follows (Figure 3.8): (1) upon it is wetted, rich CaO content of aged steel slag hydrated to $Ca(OH)_2$; (2) $Ca(OH)_2$ was dissolved releasing Ca^{2+} and OH alkalinity; (3) pH levels in the environment increased; (4) amorphous $Al(OH)_3$ content of WTR started to dissolve and $Al(OH)_4^-$ concentrations rose; (5) dissolved Ca(+II) and Al(+III) in the solution started to react with SO_4 which can originate both from WTR and 6M; (6) ettringite and monosulfate start to form controlling the Al, Ca, S and OH concentrations in the solution.

Quantitative inspection of the surface of the hydrated 6M and 10WTR elucidate the pronounced changes upon WTR-addition. The surface of the steel slag particles were mostly covered by apparent fine bundles of C-S-H and hexagonal plates that were typical for $Ca(OH)_2$ (Stutzman, 2001; Baur et al., 2004) (Figures 3.9a and 3.9b). In some locations, hexagonal formation were prevailing at higher abundance, supporting the assumption of

that $Ca(OH)_2$ was predominantly controlling the Ca(+II) and OH^- release from aged steel slag particles (Figures 3.9c and 3.9d). The surface of hydrated 10WTR appeared to be smoother without any hexagonal plates (Figure 3.10). The small brighter clusters that were littering the surface was possibly ettringite but they did not look like a typical neat needle-like formations of ettringite in pure solutions (Baur et al., 2004; Möschner et al., 2009). Impurities in the leachates might resulted in distorted crystal formation. According to EDX spectrum of 6M, Ca and O were the most abundant elements on the surface of steel slag particles in hydrated 6M sample, followed by Fe, Si and Mg (Figure 3.11a). For surfaces in 10WTR sample, relative Ca fraction was smaller and the Al peak became more prominent (Figure 3.11b). On both surfaces, S fraction was very low. It was calculated that the ratio of number of O atoms to Ca atoms to Al atoms was 60:26:1, confirming $Ca(OH)_2$ formation on 6M. The same ratio for 10WTR was 18:3:1 (O:Ca:Al). This result does not contradict the assumption of that calcium sulfoaluminate formation occurred on 10WTR surfaces. Same ratio (O:Ca:Al) for a molecule of monosulfate and ettringite is 11:2:1 and 25:3:1, respectively.

3.3.4. Column Leach Tests

In order to examine the effect of WTR addition in a dynamic system, column leach tests were conducted using columns filled with only 6M or 10WTR mixtures (particle size was 0.25 mm−2.00 mm for slag and <0.42 mm for WTR). In Figure 3.12, the effluent pH, effluent alkalinity and dissolved Al(+III) and Ca(+II) concentrations measured in the effluents were plotted as a function of pore volume (PV). Effluent pH of 10WTR columns were initially within the range of 11.2–11.5 and stabilized at pH ~12 beyond 30 PV, whereas effluent pH of 6M columns was stayed at 12.4–12.5 throughout the duration of

the test (Figure 3.12a). The decrease by 0.5 pH units corresponds to a 60% reduction in H^+ activity. It was estimated that the total amount of H^+ activity released from 10WTR columns was ~77% more within the range of 1.2–65 PV compared to 6M columns.

Figure 3.12b shows that the alkalinity of 10WTR effluent was decreased compared to 6M effluent. Alkalinity release from 6M did not fluctuate significantly; the mean value of the alkalinity values measured in 6M column's effluent within the range of 4.4−51.5 PV was 44.8±0.7 mEq/L. Alkalinity in 10WTR effluent decreased from 26.1 mEq/L at 4.4 PV to 14.2 mEq/L at 19.9 PV, and alkalinity slowly increased and reached to 17.1 mEq/L at 54.9 PV. It was estimated that the total amount of alkalinity (mEq) released from 10WTR columns was ~64% less within the range of 4.4−51.5 PV compared to 6M columns. The total mass of the released alkalinity was calculating based on the area under interpolated data points in Figure 3.12b (mEq/L * L).

WTR addition also caused significant changes in Al(+III) and Ca(+II) leaching from the columns similar to the observations in batch-type tests (Figure 3.12c). 6M column released 21.5±0.5 mM Ca(+II) at 0−2 PV and above 2 PV, Ca(+II) release stabilized at the level of 24.7±0.5 mM; Al(+III) release was below detection limit (<0.02 mM) throughout the test. For the 10WTR columns, at the first 5 PV, dissolved Al^{III} concentration was rapidly increased peaking at ~19 mM which was matched by the lowest measured dissolved Ca(+II) concentrations averaged at ~7 mM. After the peak, Al^{III} release was decreased from ~19 mM to ~7 mM within the range of 5–20 PV. Al(+III) leaching from 10WTR stabilized at 2.3±1.0 mM beyond ~30 PV. After the lowest points at around 5 PV, Ca(+II) release from 10WTR stabilized at 8.5±0.7 mM beyond ~12 PV.

Relative to Al(+III) and Ca(+II) concentrations detected in the leachates, the S leaching was much smaller and often below detection limit (Figure 3.13). 6M released 0.03 mM S at 2.3 PV and S concentrations were below detection limit (<0.01 mM) for the rest of the test (33 out of 34 measurements). In 10WTR columns, S was detected to be released over 0.01 mM in 15 out 32 measurements; average S release for the samples above detection limit was 0.09±0.04 mM. Depletion of SO_4 and increased OH activity in the environment can stimulate ettringite-to-monosulfate transformation (Hampsoim and Bailey, 1982; Gabrisová et al., 1991; Damidot and Glasser, 1993). Therefore, the monosulfate formation could be favored over ettringite in 10WTR columns where pH was ~11.5−12.

Based on the elemental concentrations detected in the effluents from the columns, saturation indices for ettringite, monosulfate, portlandite, gypsum and am-$Al(OH)_3$ were calculated (Figure 3.14). In 6M effluents, portlandite was the phase with SI values that were closest to its solubility product, overall (-0.4±0.1). In 10WTR effluents, the highest saturation levels on average were of ettringite (0.9±1.9) and monosulfate (0.3±0.6) and considerably higher than SI of portlandite, gypsum and am-$Al(OH)_3$. Therefore, it can be concluded that Ca(+II) release and pH was controlled by portlandite solubility in 6M columns and that ettringite and monosulfate was controlling the Ca(+II) and Al(+III) dissolution in 10WTR columns, similar to batch-type tests.

In addition to column leach tests that were conducted using glass cylinder columns with 2.5-cm diameter and 20-cm height, another kind of column leach tests were conducted in larger cylinders using different steel slag particles sizes (<9.5 mm, including slag fines). In these other type of column leach tests, 30-cm-long PVC cylinders with a diameter of 10.4

cm were used. The average contact time was 15.0 h, compared to 4.2 hours in small columns (Table 3.3).

In Figure 3.15, Ca(+II) and Al(+III) release from the big and small column leach tests were compared. Effluent pH values for both type of big columns, 6M(Big) and 10WTR(Big), were higher compared to their small counterparts. Effluent pH of 6M(Big) columns was 12.5–13 throughout the test. Effluent pH of WTR10(Big) column was initially ~11.8 and reached 12.3–12.4 above 30 PV. Effluent pH values for the big columns were approximately 0.5 pH unit greater compared to effluents from small columns.

Despite the great differences between small and big CLTs (e.g., flow speed, dimensions, total mass, particle size), the results from these tests were in good agreement, except increased pH levels. Ca(+II) release except Ca(+II) concentrations in 6M(Big) leachates appeared to decrease relative to small columns at >45 PV, but this can be due to experimental error. Al(+III) release from 6M(Big) was below detection limit as in small columns throughout the tests. Above PV 12, Ca(+II) release from 10WTR(Big) columns was 6.0±1.5 mM, whereas small columns released 8.5±0.7 mM (no statistically significant difference; n_{Big}=27, n_{Small}= 20, $p<0.05$). Above 30 PV, Al(+III) release from 10WTR(Big) was slightly higher at 3.6±0.9 mM compared to 2.3±1.0 mM Al(+III) release from small columns (No statistically significant difference; n_{Big}=20, n_{Small}= 12, $p<0.05$). Contact times between big and small columns hugely varied, too, but effluent quality did not change significantly. These observations suggests that significant changes in flow rate, particle size and total slag mass did not have a great impact on Ca(+II), Al(+III) and OH release and supports the assumption for a mitigation mechanism that was controlled by the solubility of a mineral phase.

3.4. Conclusion

In batch-type tests, addition of alum-based WTR to steel slag created significant changes on the resulting leachate characteristics; leachate alkalinity, dissolved Ca(+II) and leachate pH decreased and formerly low dissolved Al(+III) concentrations markedly increased (5.3−7.3 mM). Base neutralizing capacity was found to be 72% lower in 10WTR compared to 6M. Reduced alkalinity accompanied with increased Al(+III) concentrations was also observed in effluents from two types of 10WTR columns (98-mL and 2.5-L columns), demonstrating that mitigation effect due to WTR addition was persistent over the long term (70−80 PV) and not significantly affected by changes in particle size and flow rate (Table 3.3). In big column leach tests (V = 2.5 L), bulk dry density of the media (compacted with standard Proctor effort, 600 $kN \cdot m/m^3$) in columns decreased only by 3% on average upon 10% WTR addition (21.3 kN/m^3 for 6M column and 20.6 kN/m^3 for 10WTR column), showing that WTR-modification did not significantly affect the favorable maximum dry density value of aged steel slag.

Dissolved Al(+III) was in the form of aluminate [$Al(OH)_4^-$] and shown to be contributing to alkalinity in WTR/6M leachates. Alkalinity in 6M leachates was almost completely defined by hydroxide alkalinity that was most likely generated by $Ca(OH)_2$ dissolution. While alkalinity in WTR/6M leachates (5−30% WTR based on dry wt.) was 62−73% lower due to decreased amounts of dissolved Ca(+II), 38−103% of it was calculated to originate from dissolved $Al(OH)_4^-$. However, aluminum released from WTR in the form of $Al(OH)_4^-$ at high pH levels was found to be an important factor in decreasing dissolved Ca(+II) release. Al(+III) extracted from WTR using NaOH solutions was able to reduce Ca mobility in pure $Ca(OH)_2$ solutions. When the pH levels were artificially decreased in

10WTR leachates, excessive residual Al(+III) concentration appeared to be alleviated significantly but at the same time Ca(+II) release sharply increased. With decreasing pH (below ~10.3), the positive effects of WTR addition on Ca(+II) release diminished; comparison of 18h and 18h+4h ANC tests implied that pH levels above 10.6 were required to maintain WTR's effectiveness in reducing the alkalinity producing capacity of steel slag.

Based on interpretation of results from calculated saturation indices and SEM and EDX analyses, $Ca(OH)_2$ solubility was found to not govern Ca(+II) and OH^- release in WTR-amended slags; formation of ettringite and monosulfate as secondary mineral phases seemed to explain the reduced Ca(+II) and OH^- release and why the mitigation effect was diminished below pH 10.5. Therefore, it was suggested that $Ca(OH)_2$-solubility-governed alkalinity production in hydrated steel slags was altered upon WTR addition and that calcium sulfoaluminate phases (ettringite and monosulfate) controlled Ca(+II) and OH release in WTR-amended slag samples, reducing the overall alkalinity by over 65%.

Although significant improvements in alkalinity levels were attained, final leachate pH from WTR-amended slag columns was only 0.5 units lower and contaminated by high concentrations of Al (>3−4 mM). To obtain optimal reduction efficiency for alkalinity and Ca(+II) release via WTR addition, the pH of the leachates should be allowed remain above pH 10.5−10.6. In order to further reduce pH, another method should be developed for the leachates after they leave the WTR/6M system.

TABLES

Table 3.1. Association constants ($K_{association}$) at 20°C for the ion association equations.

Species	Formation	log $K_{association}$ (20°C) [a]
OH^-	$H_2O - H^+$	-13.83
$AlHPO_4$	$Al^{3+} + H^+ + PO_4^{3-}$	20.01
$AlOH^{2+}$	$Al^{3+} + 3\,H_2O - 3\,H^+$	-4.85
$Al(OH)_2^+$	$Al^{3+} + 2\,H_2O - 2\,H^+$	-9.93
$Al(OH)_{3\ (aq)}$	$Al^{3+} + 3\,H_2O - 3\,H^+$	-16.16
$Al(OH)_4^-$	$Al^{3+} + 4\,H_2O - 4\,H^+$	-22.45
$Al(SO_4)_2^-$	$Al^{3+} + 2\,SO_4^{2-}$	5.49
$Al_2(OH)_2^{4+}$	$2\,Al^{3+} + 2\,H_2O - 2\,H^+$	-7.47
$Al_2(OH)_4^{5+}$	$2\,Al^{3+} + 4\,H_2O - 4\,H^+$	14.31
$AlCl_2^+$	$Al^{3+} + 2\,Cl^-$	-0.39
$AlSO_4^+$	$Al^{3+} + SO_4^{2-}$	3.78
$CaCl^-$	$Ca^{2+} + Cl^-$	0.41
$CaOH^+$	$Ca^{2+} + H_2O - H^+$	-12.89
$CaSO_{4\ (aq)}$	$Ca^{2+} + SO_4^{2-}$	2.38
HSO_4^-	$H^+ + SO_4^{2-}$	1.93
$H_2PO_4^-$	$2\,H^+ + PO_4^{3-}$	19.52
H_3PO_4	$3\,H^+ + PO_4^{3-}$	21.69
HPO_4^{2-}	$H^+ + PO_4^{3-}$	12.33
$MgCl^+$	$Mg^{2+} + Cl^-$	0.61
$MgOH^+$	$Mg^{2+} + H_2O - H^+$	-11.98
$MgSO_{4\ (aq)}$	$Mg^{2+} + SO_4^{2-}$	2.28
$NaCl_{\ (aq)}$	$Na^+ + Cl^-$	-0.32
$NaSO_4^+$	$Na^{2+} + SO_4^{2-}$	0.74

[a] : Association constants for 25°C listed in the default *Visual MINTEQ ver. 3.1beta* database were recalculated for 20°C (Gustafsson, 2015).

Table 3.2. Thermodynamic data for the solid phases (1 atm, 298 K).

Mineral	Ion Activity Product	$\log(K_{sp})$ 25°C	ΔH_r (kJ/mol)	Reference [a]
Ettringite	$\{Ca^{2+}\}^6\{Al(OH)_4^-\}^2\{SO_4^{2-}\}^3\{OH^-\}^4\{H_2O\}^{26}$	-44.9	204.5	[1]
Monosulfate	$\{Ca^{2+}\}^4\{Al(OH)_4^-\}^2\{SO_4^{2-}\}\{OH^-\}^4\{H_2O\}^6$	-29.43	45.57	[1]
Portlandite	$\{H^+\}^2 / \{Ca^{2+}\}$	-5.18	-17.88	[1]
Gypsum	$\{Ca^{2+}\}\ \{SO_4^{2-}\}^2$	-4.18	-0.46	[1]
Amorphous $Al(OH)_3$	$\{Al^{3+}\}\ \{OH^-\}^3$	-31.2	-111	[2]
Hydrogarnet	$\{Ca^{2+}\}^3\{Al(OH)_4^-\}^2\{OH^-\}^4$	-20.5	243 [b]	[3]

[a]: Listed values were adapted from: [1] Thomas et al., 2003; [2] Perkins and Palmer, 2000; [3] Lothenbach et al., 2012.

[b]: Calculated based on reported K_{sp} and S^0 values, using the following formula:
$\Delta H_r = \Delta G_r + T\Delta S^0 = (-RT\ ln\ K_{sp}) + T\Delta S^0$

Table 3.3. Specification for column leach tests.

Label	Filling Material	Total Dry Weight (g)	Dry Bulk Density (g/cm^3)	Pore Volume (mL)	Moist. Content (%)	Average Flow Rate (mL/min)	Pore Velocity (cm/h)	Contact Time (h)	Test Duration (days)	Volume Passed through (mL)
6M-I	100% 6M	165.4	1.68	50.2	0	0.198	4.73	4.2	12.0	3,244
6M-II	100% 6M	165.8	1.69	50.1	0	0.204	4.88	4.1	12.0	3,267
10WTR-I	10% WTR + 90% 6M	168.8	1.72	46.8	0	0.188	4.82	4.1	12.0	3,250
10WTR-II	10% WTR + 90% 6M	162.3	1.65	48.8	0	0.188	4.63	4.3	12.0	3,418
6M(Big)-I	100% 6M	5484	2.19	910	7	0.980	1.98	15.4	28.2	40,573
6M(Big)-II	100% 6M	5399	2.16	935	7	0.870	1.71	17.9	50.6	72,857
10WTR(Big)-I	10% WTR + 90% 6M	5355	2.14	805	13	1.170	2.67	11.4	50.6	66,142
10WTR(Big)-II	10% WTR + 90% 6M	5165	2.07	865	13	0.940	1.99	15.3	50.6	59,621

Table 3.4. Elemental leaching from WTR, 6M and alum precipitate in 18hLTs and ammonium oxalate extractions.

	Water Treatment Residual (WTR)	Steel Slag (6M)	Alum Precipitate
pH [1]	6.9	12.4	5.6
Water Soluble Content (mg/kg) [1,2]			
Aluminum (Al)	<20	30	*n/a*
Calcium (Ca)	870	14,000	*n/a*
Sulfur (S)	370	170	*n/a*
Phosphorous (P)	<7	<7	*n/a*
Iron (Fe)	<5	<5	*n/a*
Magnesium (Mg)	66	<20	*n/a*
Potassium (K)	64	23	*n/a*
Silicon (Si)	<4	<4	*n/a*
Ammonium Oxalate Extractable Content (mg/kg) [2,3]			
Aluminum (Al)	113,000	940	236,000
Sulfur (S)	6,300	230	75,800
Phosphorous (P)	1,000	7,500	*n/a*
Iron (Fe)	6,700	36,500	*n/a*

[1]: Values were measured in leachates from 18hLTs using DI water as extraction liquid with a L:S ratio of 20 mL/g.

[2]: Concentrations were calculated based on dry weight.

[3]: Values were measured in leachates from 2-hour acid ammonium oxalate extractions.

Table 3.5. Concentrations of the major elements detected in the leachates from 18hLTs using DI water as extraction liquid and the activities of the major ionic species of these elements.

	6M	5WTR	10WTR	20WTR	100WTR
pH	12.4	11.7	11.1	10.5	6.9
Concentrations (mM) [1]					
Ca	17.96	7.06	4.33	3.44	1.08
Al	0.05	5.32	7.28	5.78	0.02
Na	0.12	0.05	0.09	0.07	0.16
S	<0.01	0.12	0.26	0.50	0.57
Cl	0.06	0.07	0.12	0.16	0.45
Ionic Strength (M)	0.042	0.018	0.013	0.011	0.004
Activities of the Major Species (mM) [2,3]					
H^+	4.12e-10	1.95e-09	7.24e-09	3.16e-08	1.29e-04
OH^-	16.64	3.52	0.947	0.217	5.32e-05
Ca^{2+}	7.30 (84.7%)	3.95 (97.1%)	2.65 (97.1%)	2.18 (96.2%)	0.78 (93.8%)
$CaOH^+$	2.289 (15.3%)	0.261 (1.23%)	0.047 (1.23%)	0	0
Na^+	0.098 (98.3%)	0.043 (99.8%)	0.076 (99.8%)	0.061 (99.8%)	0.151 (99.8%)
$Al(OH)_4^-$	0.043 (100%)	4.656 (100%)	6.491 (100%)	5.206 (100%)	0.012 (71.8%)
Cl^-	0.053 (98.2%)	0.064 (99.4%)	0.104 (99.4%)	0.144 (99.5%)	0.425 (99.8%)
SO_4^{2-}	0	0.05 (73.3%)	0.12 (73.3%)	0.25 (76.2%)	0.39 (87.3%)
Sum of Cations [4] (mEq)	17.0	8.19	5.43	4.43	1.72
Sum of Anions [4] (mEq)	-16.7	-8.33	-7.79	-6.07	-1.21
Charge Difference (mEq)	0.26	-0.14	-2.36	-1.65	0.50

[1]: Elemental dissolved concentrations measured using ICPE.

[2]: Speciation calculated for 20°C using *Minteq Visual* (Gustafsson, 2015). Concentrations the detections limits were assumed to be 0 in these calculations.

[3]: Percentage values between parentheses under the listed activities denotes the fraction of the species compared to total activity of the element.

[4]: Calculated using Eq. 3.1.

Table 3.6. Leachate alkalinity at pH 7 and $Al(OH)_4^-$, $CaOH^+$ and OH^- concentrations in the leachates from 18hLTs using 0.02 M NaCl as extraction liquid.

	6M	5WTR	10WTR	20WTR	30WTR
Leachate pH	12.5	12.2	11.5	10.8	10.4
Ionic Strength (M) [1]	0.0649	0.0387	0.0361	0.0354	0.0323
Alkalinity at pH 7 (mEq/L) [2]	31.29	12.03	9.06	8.35	8.46
Concentrations (mmol/kg) [1]					
Consumed H^+ at pH 7, $[H^+]$ [2]	658	244	208	174	171
$[Al(OH)_4^-]$ [3]	1.28	93.4	168	180	118
$[CaOH^+]$ [3]	63.6	11.7	2.36	0.45	0.19
$[OH^-]$ [3]	534	238	49.6	9.50	4.25
$[CaOH^+] + [OH^-] + [Al(OH)_4^-]$	599	343	220	190	122
Ratios					
$\frac{[CaOH^+] + [OH^-] + [Al(OH)_4^-]}{[H^+]}$	91%	141%	106%	109%	72%
$\frac{[Al(OH)_4^-]}{[H^+]}$	0.2%	38%	81%	103%	69%

[1]: Calculated in *Minteq Visual*.

[2]: Values are from leachate alkalinity tests.

[3]: Concentrations were estimated in *Minteq Visual* based on elemental concentrations of Al, Ca, S, P, Mg, K and Na and leachate pH. Cl concentrations were assumed to be 0.02 M.

Table 3.7. Acid or base neutralizing capacities of 6M, 10WTR and 100WTR.

	Neutralizing Capacity at pH 7 [1] (mEq/kg)	Neutralizing Capacity at pH 8.5 [1] (mEq/kg)
6M (18h)	2050	1400
6M (18h+4h)	2080	1700
10WTR (18h)	1600	870
10WTR (18h+4h)	780	570
100WTR (18h)	- -	-250

[1]: Values were estimated by interpolation of available data points that were given in Figure 3.3.

Table 3.8. Leachates from NaOH extractions and 18hLTs using NaOH extracts as extraction liquid.

18-h Test Type	pH	Al (mM)	Ca (mM)
2.50 g 6M in DI water	12.38	<0.02	18.0±0.7
NaOH Solution	12.50	<0.02	<0.02
2.50 g WTR in 0.5 L-NaOH solution at pH 12.5	12.46	32.8±0.4	<0.02
1.25 g Alum-precipitate in 0.5-L NaOH solution at pH 12.5	12.45	31.4±0.3	<0.02
2.0 g 6M in 50-mL NaOH solution at pH 12.5	12.61	<0.02	7.2±0.3
2.0 g 6M in WTR-extract	12.56	31.4±0.4	0.67±0.01
2.0 g 6M in Alum-precipitate-extract	12.53	29.8±0.6	0.25±0.01

Table 3.9. Results from 18hLTs using 2.5-g WTR and $Ca(OH)_2$ or CaO mixtures in DI water.

Ca Source	Added Mass (g)	Added Ca, Theoretical [1] (mM)	Added Ca, Measured [2] (mM)	Leachate pH	Dissolved Ca [3] (mM)	Dissolved Al [3] (mM)
$Ca(OH)_2$	0.065	17.5	18.5	9.4	3.9±0.1	0.48±0.05
CaO	0.050	17.8	16.8	9.5	3.9±0.1	0.52±0.07
CaO	0.10	35.7	33.8	10.1	4.4±0.0	2.2±0.2

[1] : Theoretical soluble Ca(+II) concentration that was in the mixture was calculated based on the added mass and the formula weight of the chemicals; 74.09 g/mol for $Ca(OH)_2$ and 56.08 g/mol for CaO.

[2] : Values were measured in 50-mL DI water containing dissolved Ca-compound at its listed mass.

[3] : Concentrations measured in the leachates from 18hLTs.

FIGURES

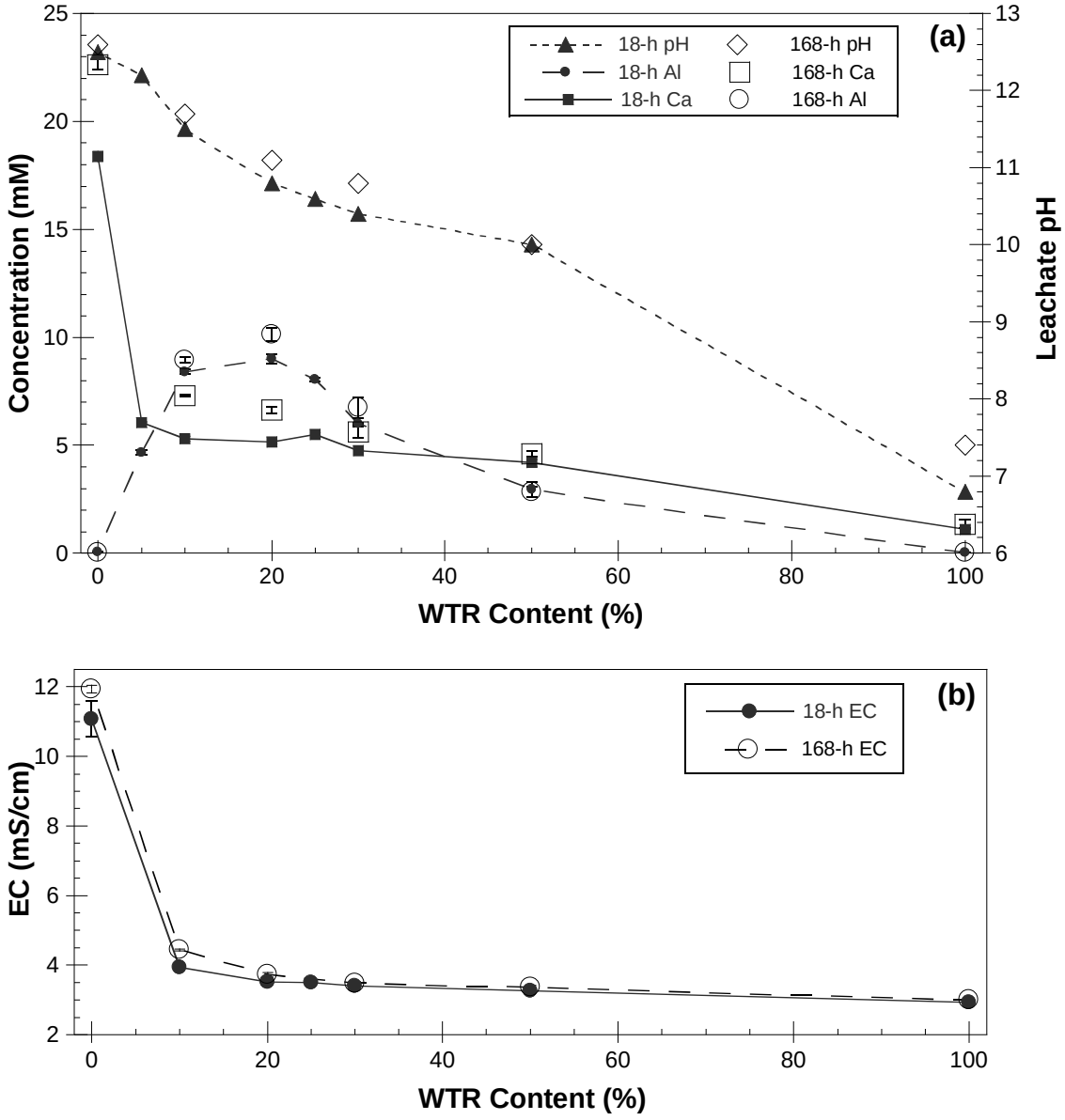

Figure 3.1. (a) Leachate pH, dissolved Al and Ca concentrations; (b) electric conductivity (EC) from 18hLTs and 168hLTs using 0.02 M NaCl solution as extraction liquid.

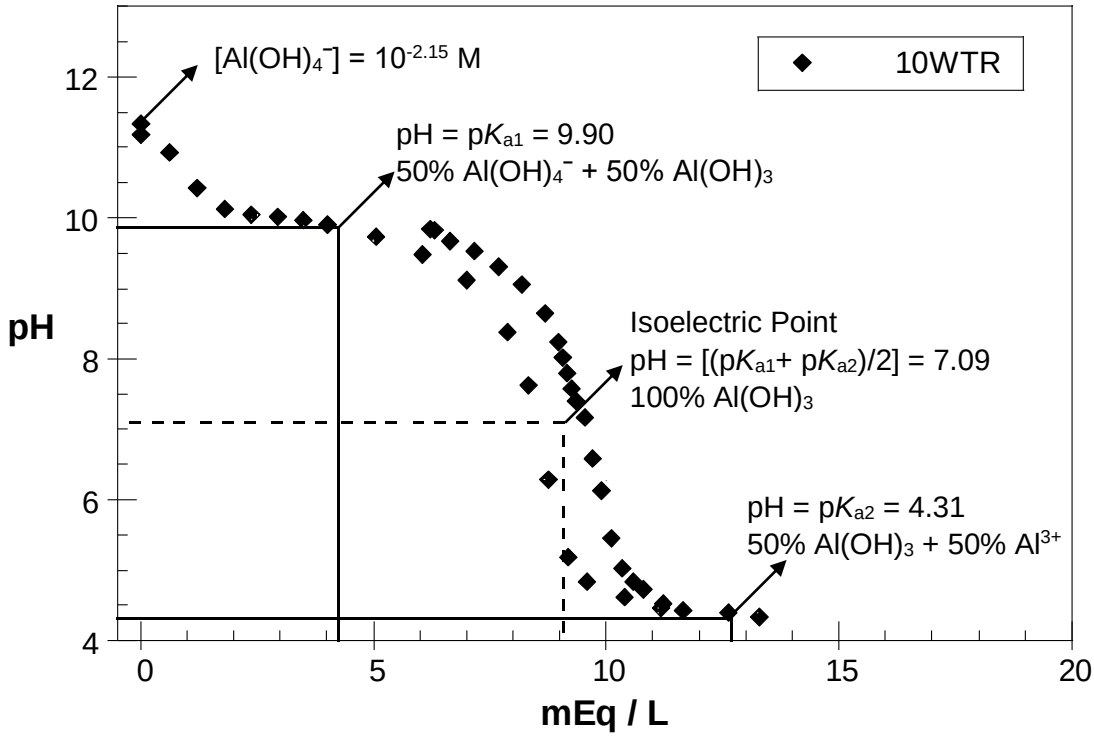

Figure 3.2. Middle points for $Al(OH)_3$ precipitation and Al^{3+} dissolution reactions in 10WTR leachates during acid-titration.

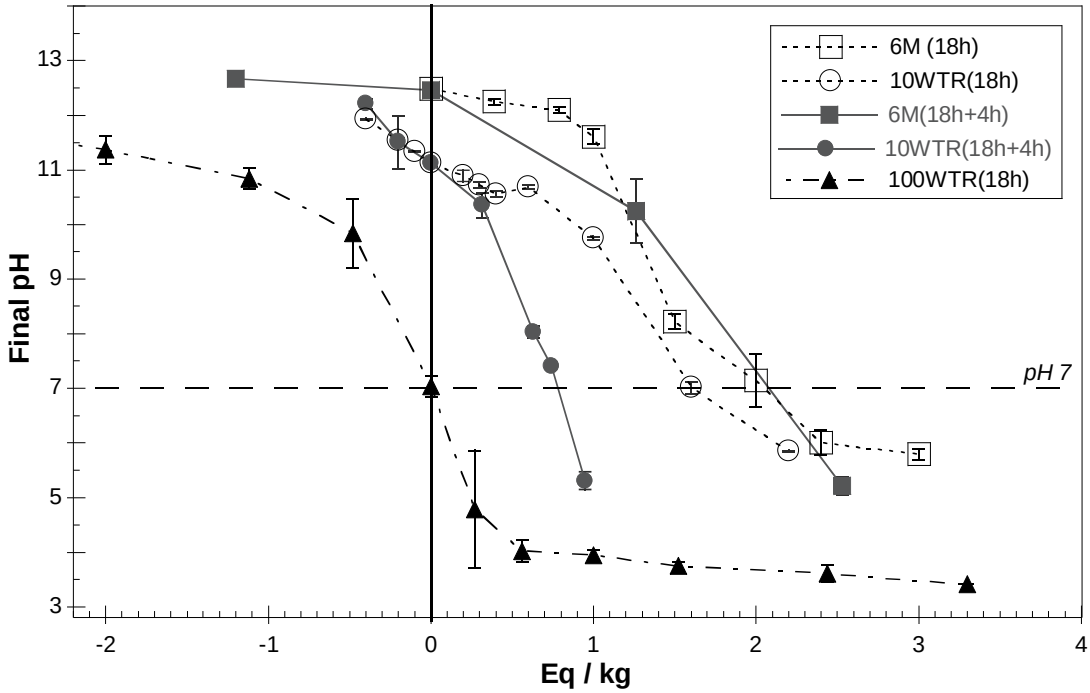

Figure 3.3. A comparison of neutralization capacities of 6M, 10WTR and 100WTR mixtures measured in 18h and 18h+4h tests [1].

[1] The values between parentheses in the labels define type of the buffering capacity test; (18h): acid/base was introduced at the start of the test and the specimen was tumbled contacting acid/base for 18 hours; (18h+4h): after 18-hour tumbling, acid/base was introduced and the specimen was tumbled for an additional 4 hours. Positive and negative values on the x-axis indicate the concentration of added H^+ and OH^-, respectively; Eq/kg = mol H^+ or OH^- per kg solid material based on dry weight.

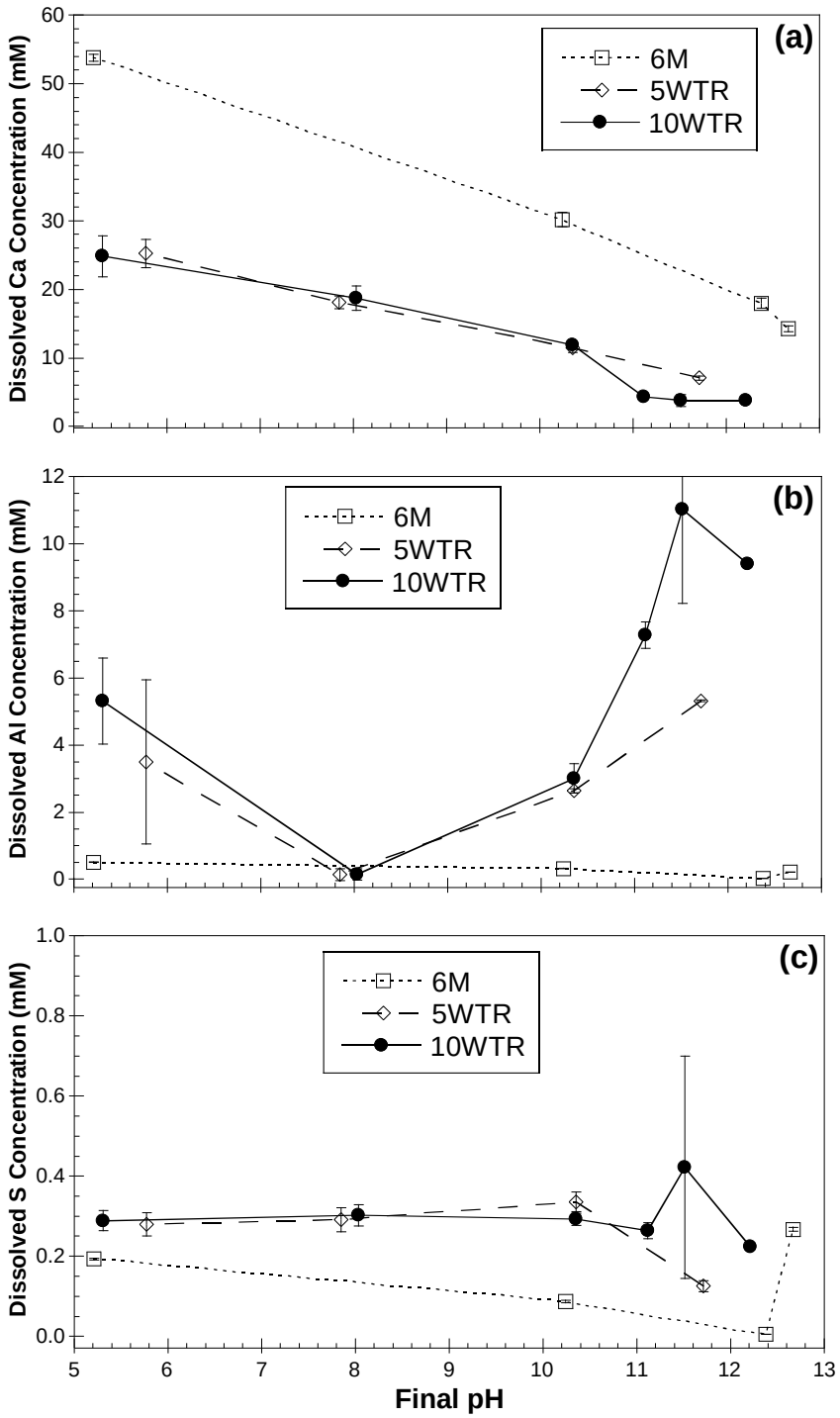

Figure 3.4. (a) Dissolved Ca; (b) dissolved Al; and (c) dissolved S concentrations from 6M, 5%WTR and 10%WTR leachates with modified final leachate pH values (18h+4hLTs).

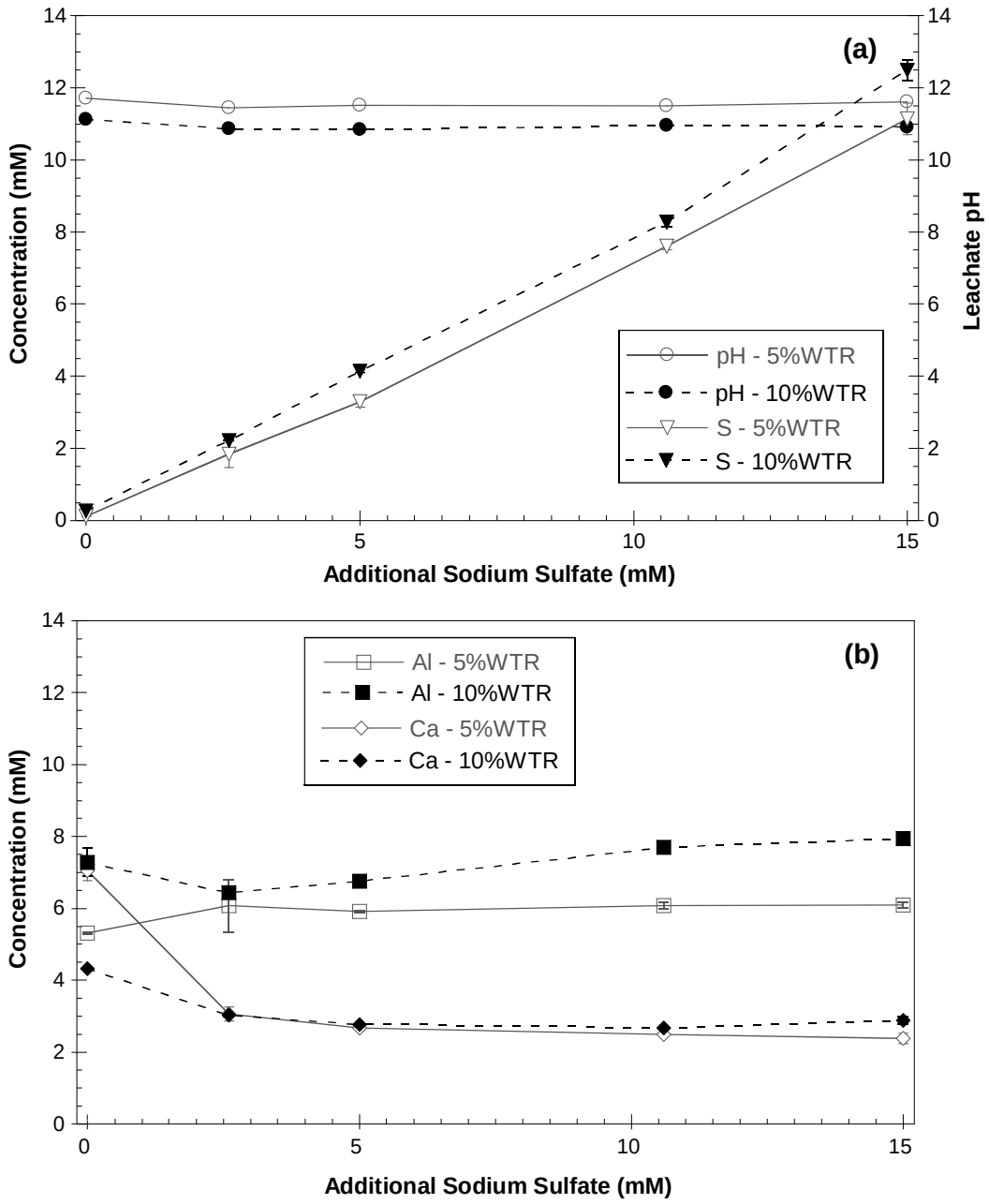

Figure 3.5. Dissolved elemental concentrations and leachate pH in 5WTR and 10WTR against the amount of added $Na_2(SO_4)$.

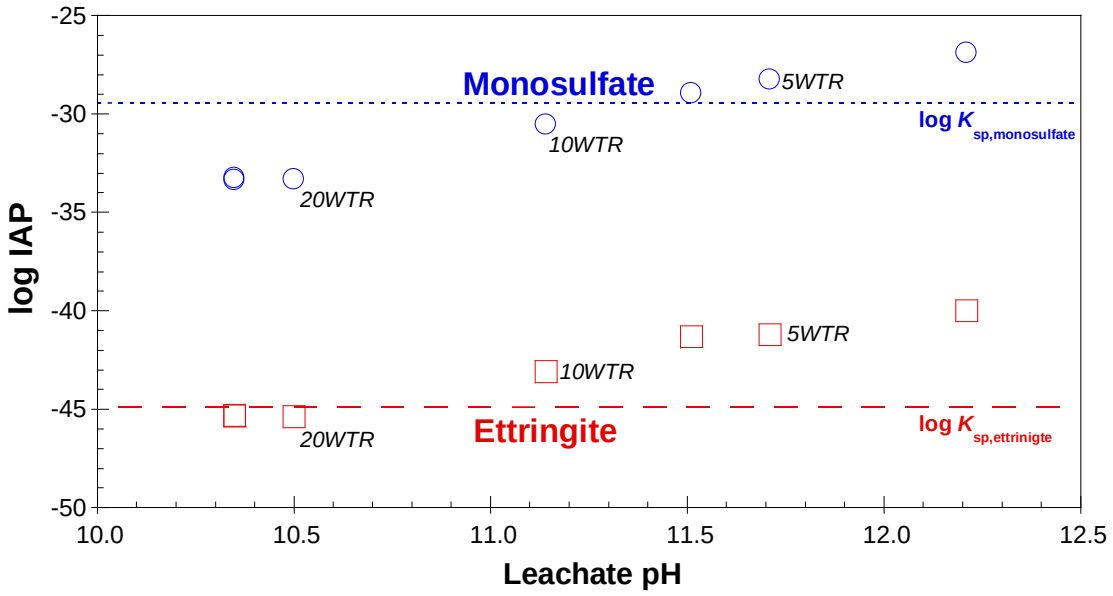

Figure 3.6. IAP values calculated for ettringite and monosulfate using the dissolved elemental concentrations in different WTR/6M leachates from 18hLTs using only DI water and 18h+4hLTs with acid/base addition. Samples at their original pH are labeled.

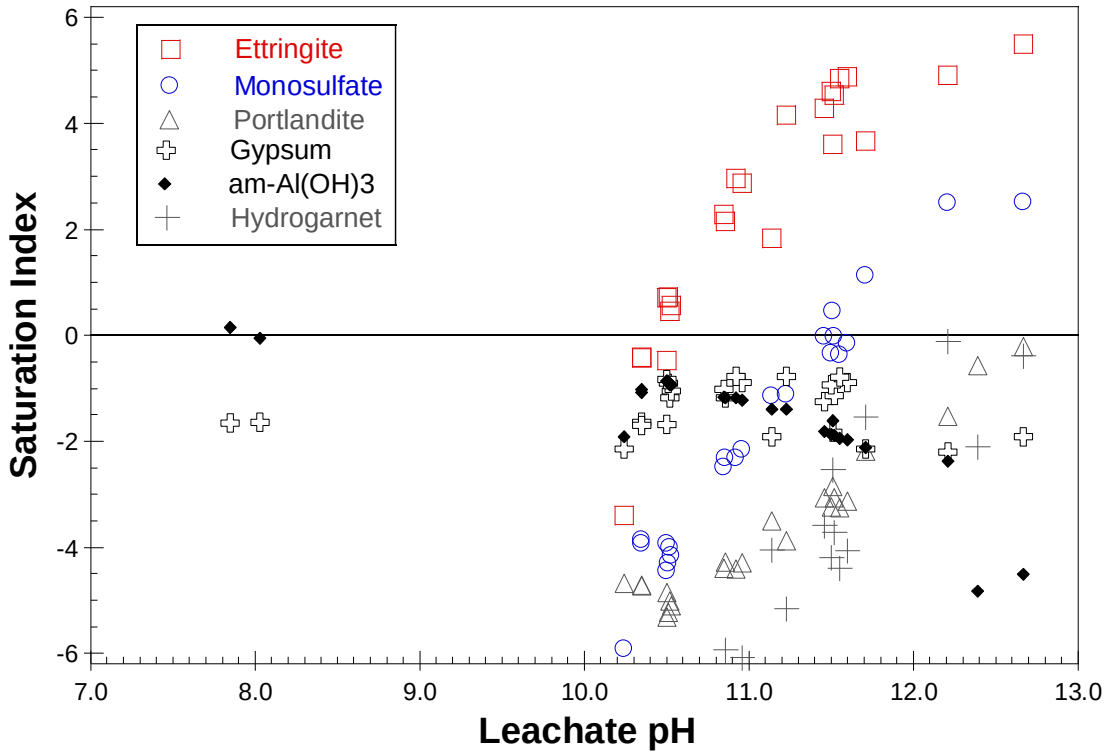

Figure 3.7. Saturation indices calculated for the leachates from 6M and WTR/6M leachates from 18hLTs using only DI water; 18h+4h leach tests with acid/ base addition; and 18hLTs with sulfate additions.

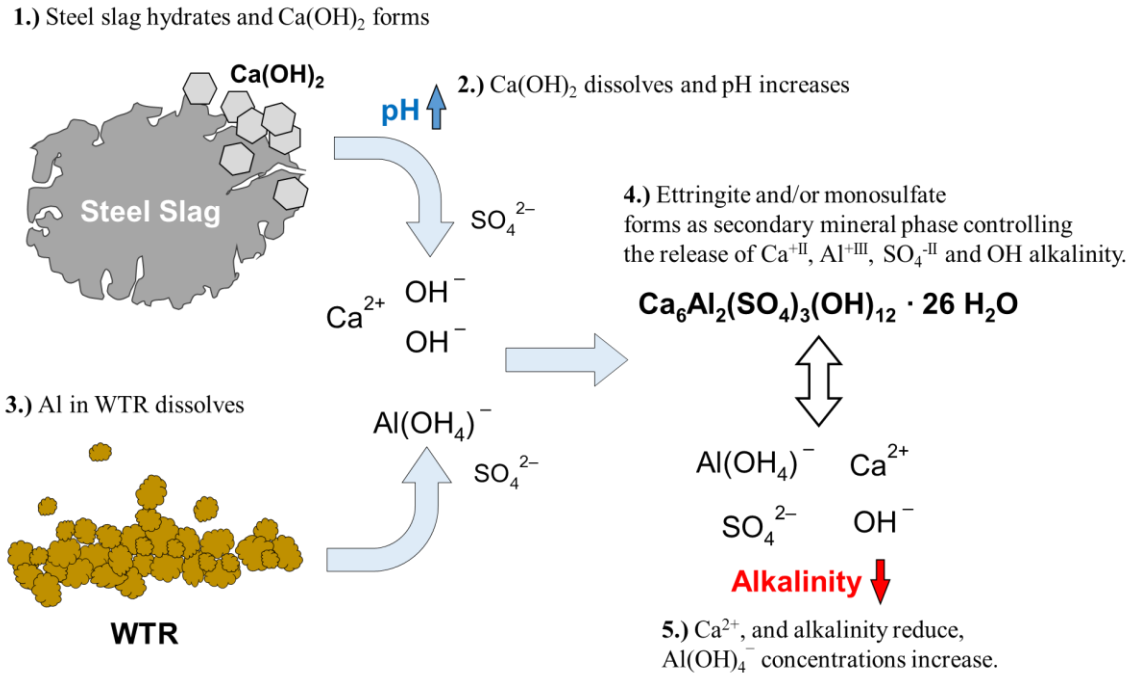

Figure 3.8. Proposed alkalinity mitigation mechanism for WTR-amended aged steel slags.

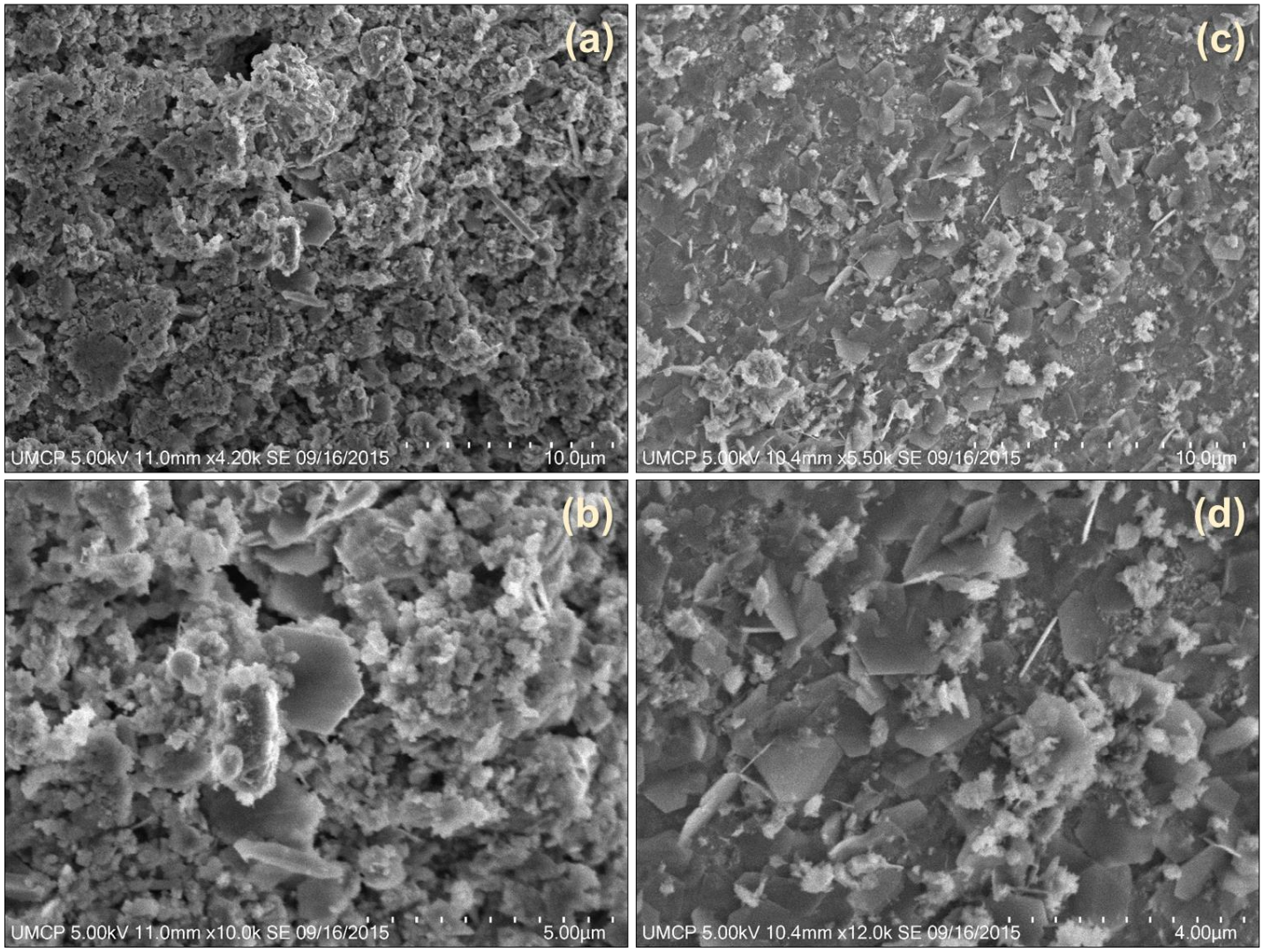

Figure 3.9. SEM images of the steel slag particles in 6M mixture after 18 hours of hydration.

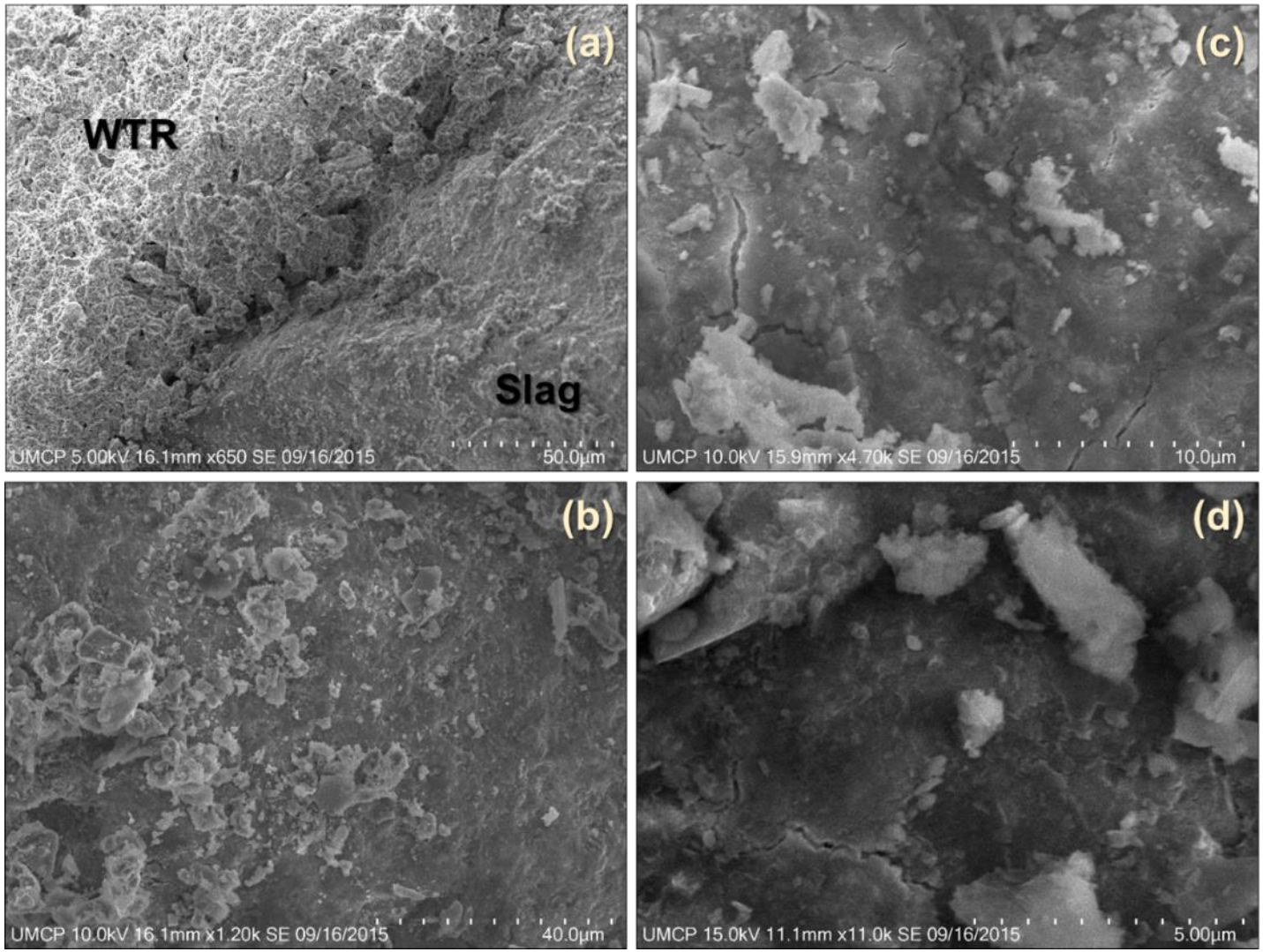

Figure 3.10. SEM micrographs of the steel slag particles in 10WTR mixture after 18 hours of hydration.

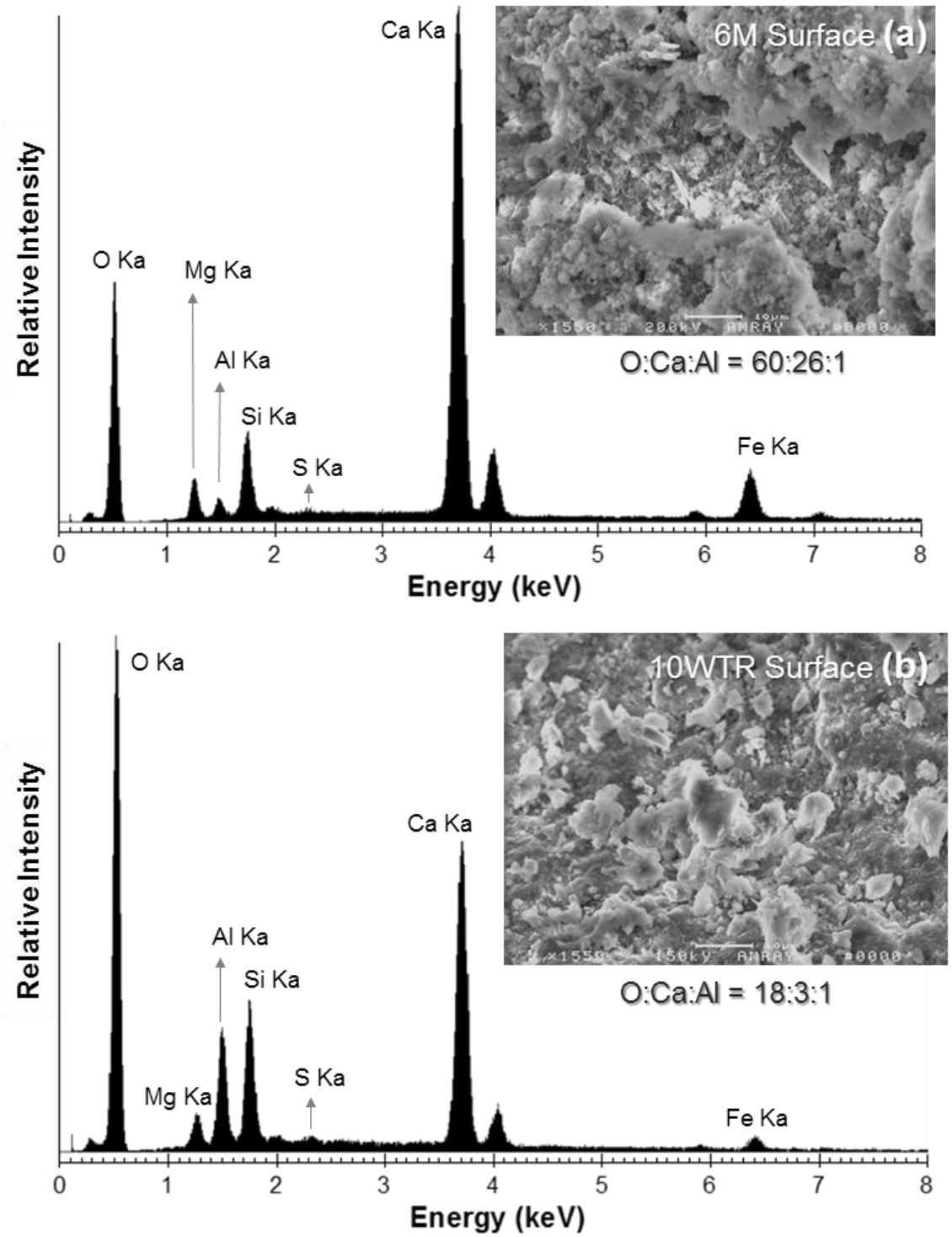

Figure 3.11. Results of EDX analyses employed on steel slag particles in **(a)** hydrated 6M and **(b)** hydrated 10WTR mixtures.

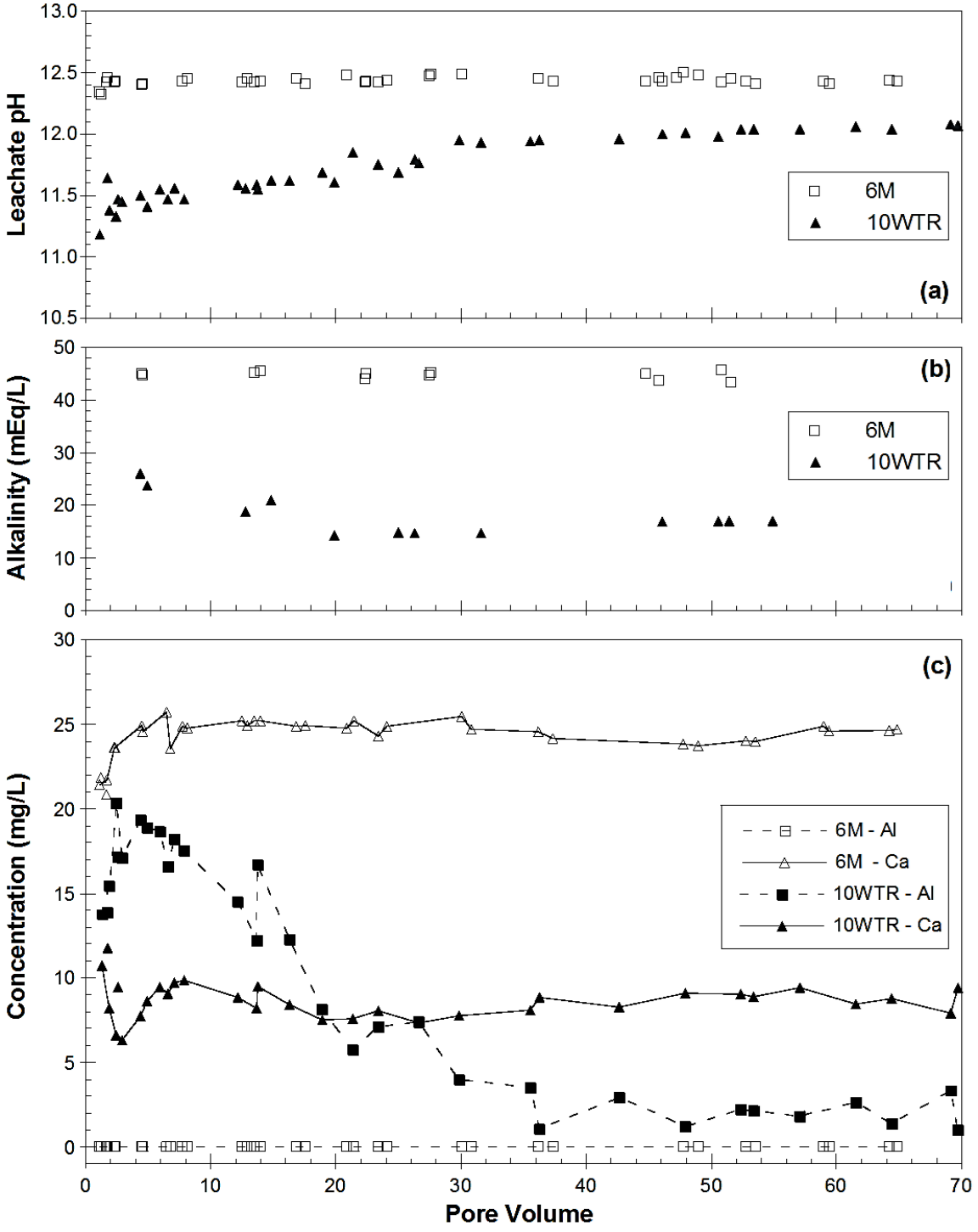

Figure 3.12. Effluent pH **(a)**; alkalinity **(b)**; and dissolved Al and Ca concentrations **(c)** measured in the effluent from the columns leach tests.

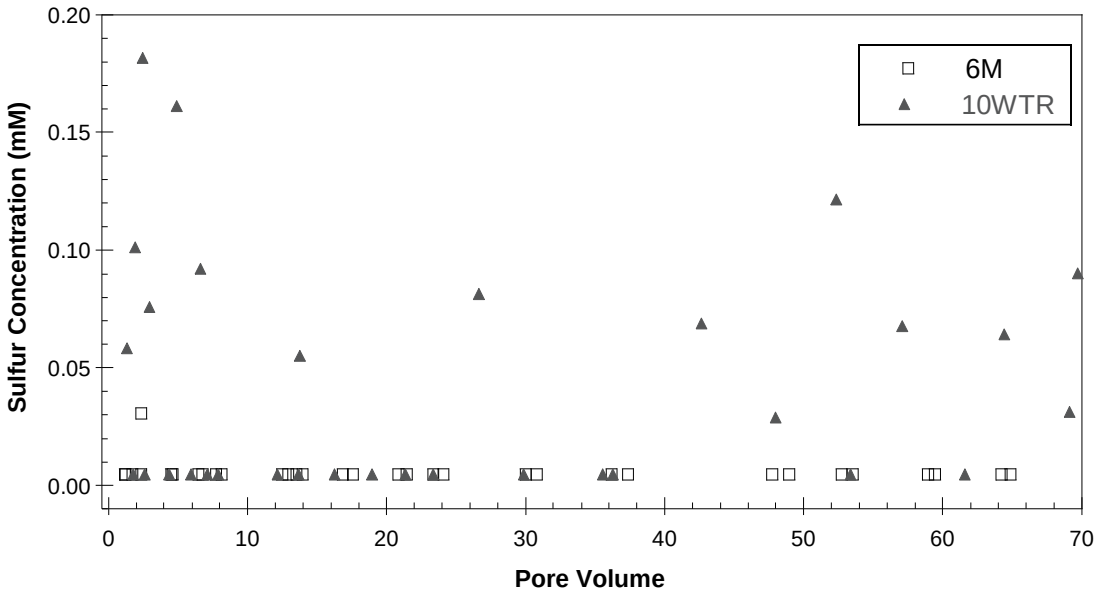

Figure 3.13. Dissolved S release from 10WTR and 6M columns.

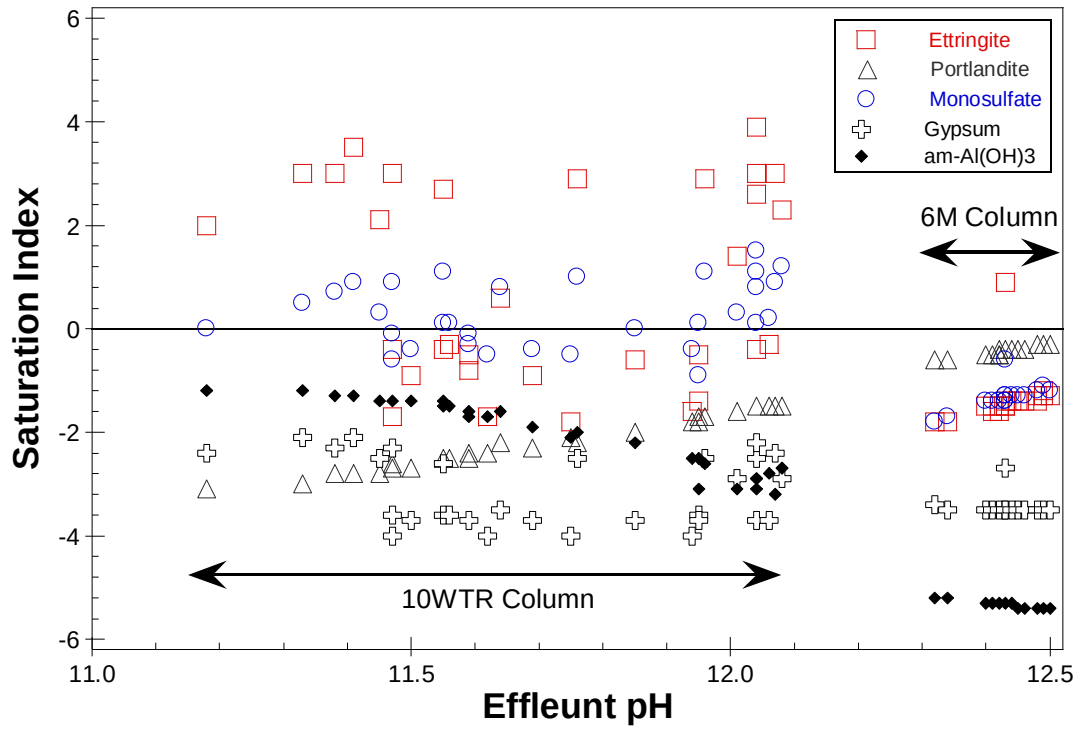

Figure 3.14. Saturation indices calculated for the effluents from 6M and 10WTR columns.

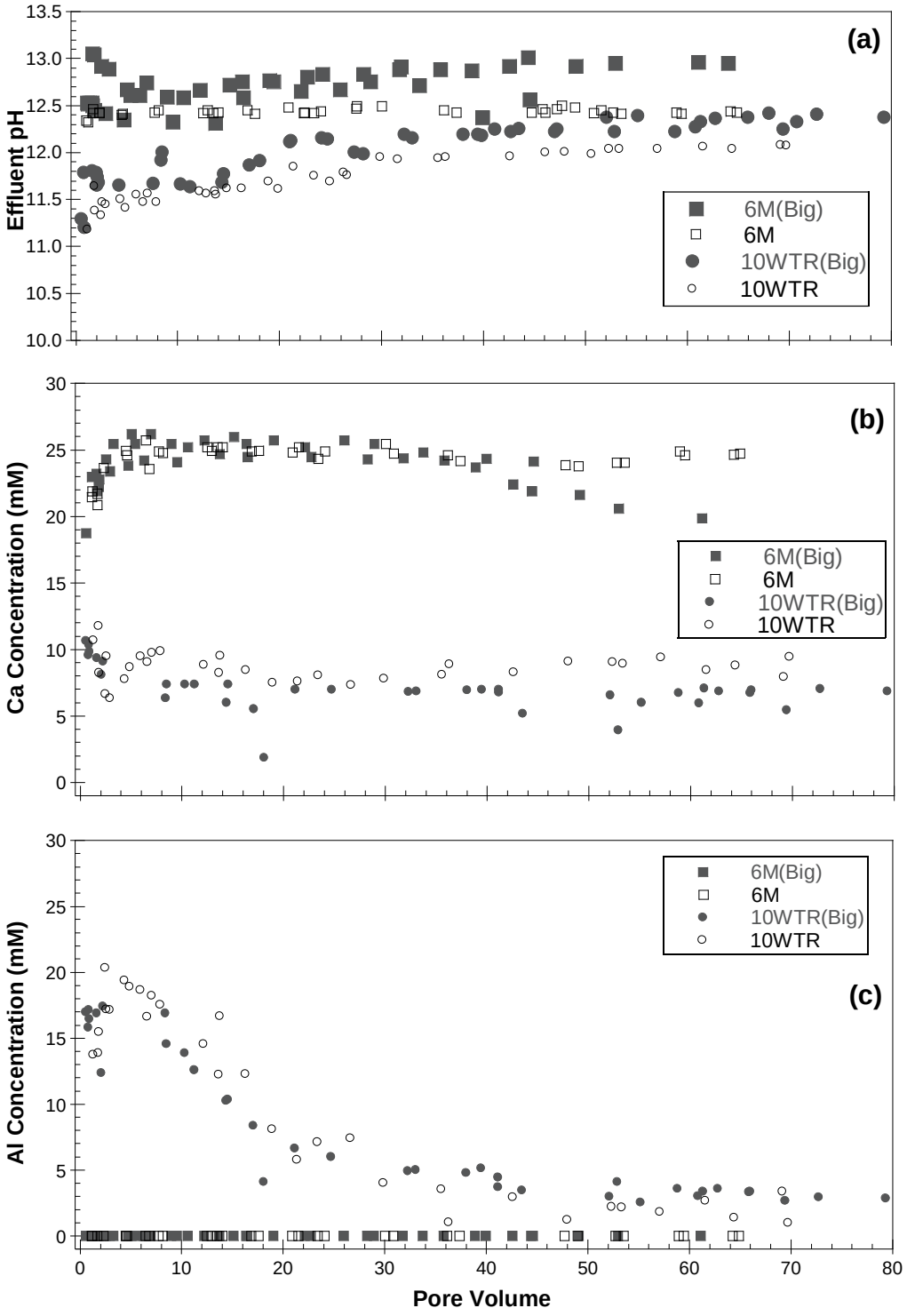

Figure 3.15. Comparison of effluents from big (2.5 L) and small columns (98 mL); **(a)** effluent pH; **(b)** dissolved Ca concentrations; and **(c)** dissolved Al concentrations.

CHAPTER 4: REMOVAL OF RESIDUAL ALKALINITY AND ALUMINUM IN THE LEACHATE OF AGED STEEL SLAG−WATER TREATMENT RESIDUE MIXTURES UTILIZING COMPOST

4.1. Introduction

Water treatment residual addition provided a reliable mitigation method for the high alkalinity problem in aged steel slag leachates that apparently depending on the formation of calcium sulfoaluminate hydrates. Compared to pristine aged steel slag leachates, alkalinity in WTR-amended slag leachates was ~70% lower, and these reduction levels were reproducible in both batch-type and column tests. However, final effluent pH values were still unacceptably high (>11.5) and the leachates from WTR/6M mixtures were contaminated with high concentrations of dissolved Al^{III}. In addition to high pH levels, Al^{III} release from WTR can be problematic, since high concentrations of dissolved Al present in soil porewater is shown to be phytotoxic adversely effecting plant growth (Hue et al., 1986; Lombi et al., 2010). Dissolved Al^{III} in the leachates, mainly in form of $Al(OH)_4^-$, were caused by mobilization of aluminum in WTR at high pH levels. On the other hand, high pH levels, above 10.5−10.6, are found to be required for formation of calcium sulfoaluminate hydrates as secondary mineral phases in WTR/6M system. It was also shown that the majority of the alkalinity in the WTR-amended slag leachates originated from $Al(OH)_4^-$ that was acting as a base.

Based on these findings, two different approaches were formulated to remove residual alkalinity and dissolved Al^{III} concentrations in WTR-amended slag leachates. The first approach was to decrease Al solubility inside WTR/6M systems by introducing a chemical that can complex with Al and precipitate, removing Al and associated alkalinity from the

solution. The second approach was to decrease pH to circumneutral range where $Al(OH)_4^-$ precipitates in form of Al-hydroxides. However, this neutralization process should be carried out without interfering with the high pH levels occurring in the WTR/6M system, and thus it should be employed after the leachate was formed and leave the WTR/6M system.

Phosphates can precipitate dissolved Al in the solution and complex with Al in the WTR (Pa Ho, 1975; O'Neill and Davis, 2012). It was assumed that introduction of PO_4(-III) in form of sodium phosphate might result in removal of excessive Al in the leachates of WTR-amended steel slag. Batch-type 18-h leach tests, where sodium phosphate solution at different concentrations were used as extraction liquid, were conducted to find the effective PO_4(-III) dosage. The findings were used to construct 10%WTR-amended steel slag columns with sodium phosphate powder. Dissolved Al, Ca, S, P and Na concentrations in the effluents from these columns were measured to evaluate the success of PO_4(-III) treatment.

A class-A (U.S. EPA standards) biosolids compost that was produced by composting sewage sludge found to produce acidic leachates (USEPA, 1994). The high base neutralizing capacity of the compost was characterized and its ability of mitigating alkalinity in WTR-amended slag leachates were tests in sequential batch-type tests. An experimental setup, where two columns were connected in series, was devised to test a column of biosolids compost's ability for neutralizing alkalinity in the effluents from the first columns containing WTR-amended steel slag. In these two-column-in-series tests using different amounts of biosolids composts and flow rates, the breakthrough point for the base neutralizing capacity of compost was determined by analyzing alkalinity and pH

levels in the effluents. Dissolved Al, Ca, S and P concentrations in the effluents from these columns were also measured mainly to evaluate the success of Al removal.

4.2. Materials and Methods

4.2.1. Composts and Sandy Soil

A class-A biosolids compost (BC) that was produced by composting sewage sludge was collected from Baltimore, MD. The raw biosolid was originated from the anaerobic digester unit of Back River wastewater treatment plant in Baltimore, MD. It was brought to the laboratory and sieved through a U.S. #10 sieve (opening size =2.00 mm). Only the fraction that passed through the U.S. #10 sieve was used in the tests described in this chapter. Sieved composts were stored in sealed plastic 5-gallon buckets to maintain its moisture content. The moisture content was frequently checked to before each test to calculate the right dry mass of composts used. Throughout the experimental studies, moisture of BC was changed from 46% to 43%. The loss on ignition (LOI) at 550°C was 52% for BC. The dry density of BC was estimated at 1.72 g/cm^3 based on the value of its LOI content (volatile solids =1.0 g, fixed solids =2.5 g). Soluble constituents of BC under different conditions are listed in Table 4.1.

Sandy soil used in this study is commonly used in embankment construction by the Maryland State Highway Administration (SHA) and was collected from a pit in Denton, Maryland. The sandy soil was classified as poorly graded sand with silt (SP-SM) according to the unified soil classification system and A-3 (fine sand) according to the AASHTO classification system (AASHTO, 2000). Sandy soil was mixed with composts at different proportions and this mixtures used to fill columns. The particle size of sand used in these mixtures was 0.25 mm−2.00 mm. The total elemental analysis results for sandy soil used

in this study are listed in Table 4.2; Elemental leaching from sandy soil in 18hLTs and ammonium oxalate extractions, along with its other properties are given in Table 4.3.

4.2.2. Sodium Phosphate Additions

Presence of phosphate was thought to help to remove excessive Al concentration through precipitation reactions. $NaH_2PO_4 \cdot H_2O$ (≥99.5%, Fisher Scientific, Waltham, MA) was used as the phosphate source. $NaH_2PO_4 \cdot H_2O$ solutions with different concentrations were used as extraction liquid in 18hLTs that were employed using WTR/6M mixtures.

4.2.3. Loss on Ignition

The compost samples used in this study were subjected to LOI tests that were conducted following ASTM D7348 (ASTM, 2008). LOI tests were employed on oven-dried 20-g compost samples at 550ºC in a muffle furnace. All tests were triplicated.

4.2.4. Sequential Batch-type Leach Tests

Sequential batch-type water leach tests are conducted as two-stage 18hLTs (Figure 4.1). First, untreated or treated steel slag was used to conduct an 18hLT. Then the leachate from the first 18hLT was filtered through a 0.22-µm pore-sized membrane filter and used as the extraction liquid in the second 18hLT. In second leach test, biosolids compost was used as the solid phase. Liquid-to-solid ratio was kept same (L/S=20 mL/g). The final leachates from the second leach test were preserved and stored same as leachates from regular 18hLTs, as described above.

4.2.1. Column Leach Tests

Columns leach tests using single column setup and two-columns-in-series setup was employed in this part of the study. Columns leach tests using single column setup were

using 6M, WTR and sodium phosphate monobasic powder as filling material were conducted as described in the previous chapter (Figure 4.2). Glass tubes having a 25-mm inside diameter and 200-mm height were used as columns. The columns were filled without any compaction other than tapping the column while it was being filled. 0.02 M NaCl dissolved in deionized (DI) water was used as the influent to simulate the ionic strength of water percolating through soil. The volume of water passed through the columns were normalized by the pore volume (PV) of the column and reported in units of PV. The specifications for these column leach tests were listed in Table 4.4.

Columns leach tests with two-columns-in-series setup were utilized to tests the performance of columns containing compost (Figure 4.3). Again glass tubes having a 25-mm inside diameter and 200-mm height were used as columns. Particle size of wet composts was <2.00 mm. 0.02 M NaCl dissolved in deionized (DI) water was used as the influent for first columns and effluent of the first columns were used as the influent for the second columns. The volume of water passed through the columns were normalized by the pore volume of the first column in the two-column-in-series system and reported in units of PV of the first column in the system. The specifications for the first columns and the second columns in two-columns-in-series system were listed in Table 4.5 and Table 4.6.

4.3. Results and Discussions

4.3.1. Sodium Phosphate Addition to Inhibit Aluminum Leaching

Figure 4.4 shows that NaH_2PO_4 addition to 6M and 6M/WTR mixtures at sufficient dosages had the potential of decreasing dissolved Al(+III) and Ca(+II) concentrations and leachate pH at the cost of creating high residual P concentrations. Addition of 5 mM PO_4(-III) to 5WTR and 10WTR mixtures decreased dissolved Ca(+II) concentrations to 2.1 mM

from 7.1 mM and 2.2 mM from 4.3, respectively, while making little change in Al(+III) concentrations and leachate pH; dissolved P concentration in 5WTR leachates increased became 0.06 mM, whereas dissolved P concentration in 10WTR leachate stayed the below detection limit (<0.001 mM). 8 mM PO_4(-III) addition dropped the Ca(+II) concentrations below detection limit (<0.025 mM) both in 5WTR and 10WTR leachates. When 10 mM PO_4(-III) was added to 10WTR, Ca(+II) concentrations decreased below detection limit (<0.0025 mM), Al(+III) concentration reduced to 0.54 mM, residual P concentration was 3.9 mM and the leachate pH was 10.6. 10 mM $NaHPO_4$ addition to 5WTR caused Al(+III) concentration to become 1.4 mM and adding more PO_4(-III) decreased pH below 10.3 range. When 12 mM PO_4(-III) was added, the majority of Ca(+II) and Al(+III) in 5WTR (0.05 mM Al, 0.03 mM Ca) and 10 WTR (<0.02 mM Al, 0.06 mM Ca) was immobilized; the pH of 5WTR and 10WTR leachate became 10.1 and 9.7, respectively and residual P concentrations increased to 5.5 mM for 5WTR and 5.8 mM for 10WTR.

According to these results, by adding NaH_2PO_4, it was not possible that obtaining Al(+III) concentrations below detection limit (<0.02 mM) in 5WTR and 10WTR leachates without creating residual P concentration. Due to residual P creation problem, NaH_2PO_4 dosage should be as low as possible. Since added PO_4(-III) was also consumed by dissolved Ca^{2+}, having a lower total amount of dissolved Ca(+II) and Al(+III) in the original leachates seemed to be more advantageous. 10WTR was containing a lower amount of total dissolved Al(+III) and Ca(+II) compared to 5WTR (11.6 mM vis-à-vis 12.4 mM) and thus, it had a slightly lower dissolved Al(+III) concentrations between 8−12 mM upon $NaHPO_4$ addition. Another criterion that had to be considered was maintain final leachate pH levels above 10.5−10.6 to avoid calcium sulfoaluminates dissolution in WTR/6M system. To

achieve this, the NaH_2PO_4 dosage should be at ≤10 mM for 10WTR and ≤8 mM for 5WTR. Therefore, it appears that the optimum reduction in Al(+III) concentration without sacrificing the benefits of ettringite/monosulfate formation was achieved in 10 mM NaH_2PO_4 added 10WTR leachates.

≥10 mM $NaHPO_4$ addition decreased dissolved Ca(+II) concentration below detection limit in 6M leachates and decreased leachate pH from 12.4 to 11.6, but residual P concentration became 2.5 mM. The leachate pH in 10WTR with 10 mM NaH_2PO_4 was 10.6 and it was previously shown during passivation trials that presence of PO_4(-III) in 6M leachates did not remove alkalinity effectively while decreasing Ca(+II) concentrations, significantly. Thus, addition of $NaHPO_4$ to 6M was not preferred over the NaH_2PO_4 addition to WTR/6M mixtures.

10 mM phosphate addition in batch-type tests corresponds to 200 mmol per kg 10WTR mixture. 200 mmol/kg $NaHPO_4$ (FW: 139.98 g/mol) corresponds to 2.8% (wt./wt.). 2% NaH_2PO_4 powder containing 10WTR columns were prepared and duplicated CLTs were conducted. In Figure 4.5a shows that 2% NaH_2PO_4 addition to 10WTR columns resulted in excessive S, P, Na and Al release from 10WTR columns during the first 10 PV, while effluent pH levels were ~11.5 and dissolved Ca(+II) concentrations were below 0.3 mM. The reason of high Al(+III) and S release was not determined but high Na and P suggested that NaH_2PO_4 was rapidly dissolved and flushed out. After the first 10 PV, 2% and 4% NaH_2PO_4-added 10WTR columns started to operate similar to 10WTR columns without NaH_2PO_4 (4.4−6.7 mM Ca at pH 11.8−12). 4% NaH_2PO_4-added 10WTR columns leached ~0.4 mM Ca(+II) during the first 15 PV and ~5 mM Ca(+II) between 15−62 PV (Figure 4.5b). Figure 4.6 shows that leachate alkalinity from the columns were also high (>40

mEq/L) during initial stages of the columns tests and the effluent alkalinity values decreased to levels (11−17 mEq/L) comparable to regular 10WTR columns after 10−15 PV. Therefore, it can be concluded that residual Al(+III) removal by NaH_2PO_4 addition was not possible in dynamic systems, thus field application is not feasible.

4.3.2. Residual Al and Alkalinity Removal Using Biosolids Compost

4.3.2.1. Base Neutralizing Capacity of Compost

In Table 4.7, leachate pH and dissolved Al(+III) and Ca(+II) concentrations measured in the leachates from 18hLTs that were conducted using oven-dried biosolids compost and WTR/6M mixtures are listed. In 18hLTs, 100% biosolids compost (BC) produced an acidic leachate at pH 5.0 with a high concentration of dissolved Ca(+II) (9.7 mM). The high Ca(+II) concentration was likely to be a result of liming practice that was carried out during composting. A comparison of 10% BC+10% WTR+80% 6M and 20%WTR+80% 6M demonstrates that biosolids compost did not perform better than WTR in terms of reducing leachate pH when it was directly added to the WTR/6M mixtures; pH for both mixtures were pH 10.5.

In Table 4.8, leachate pH and dissolved Al(+III) and Ca(+II) concentrations measured in the leachates from different amounts of oven-dried BC that were mixed with 18hLTs were conducted using in 10WTR and 6M leachates are given. For the leachates from 1.0-g, 2.0-g and 3.0-g biosolids compost samples contacting 10WTR leachate for 18 hours, the final pH values were 7.0, 6.1 and 5.7, respectively. Dissolved Al(+III) concentrations were <0.02 mM. Dissolved Ca(+II) concentrations varied within the range of 6.4−14 mM which were significantly higher compared to 4.9 mM dissolved Ca(+II) in 10WTR leachate. When 1.0-g BC was allowed to contact with 40-mL 6M leachate at pH 12.4, the final pH

was 7.2; dissolved Al(+III) concentrations were decreased from 0.1 mM to <0.02 mM and dissolved Ca(+II) concentrations increased from 18.4 mM to 19.1 mM. Results show that even 1.0-g BC was able to significantly reduce the alkalinity and Al mobility both in 40 mL of 10WTR and 6M leachates, but dissolved Ca(+II) concentrations increased.

Base neutralizing capacity (BNC) of wet and oven-dried biosolids compost was tested in 18-h tests and results are plotted in Figure 4.7. For comparison, also two green waste composts were tested for their BNC. The BNC values for the composts were calculated interpolating the data in the graph (Table 4.9). Although oven-dried BC was used in batch-type tests that are presented above, drying compost prior to field applications is unpractical and not necessary. Thus the BNC of wet biosolids compost was also tested and it was noticed that wet compost had a much higher BNC compared to its oven-dried form. Oven-dried BC had a 530 mEq/kg BNC at pH 7, whereas wet BC with its original moisture content of 43% had a 1270 mEq/kg BNC at pH 7. On the other hand, both greenwaste composts (GWC1 and GWC2) produced leachates at pH ~7.8 and their BNC calculated for pH 8.5 was extremely small within the range of 40−100 mEq/L compared to BNC of wet biosolids compost was 2320 mEq/kg at pH 8.5. Considering the alkalinity was 31.3 mEq/L in filtered 6M leachates and 9.1 mEq/L in filtered 10WTR leachates, 1-grams of wet biosolids compost could theoretically neutralize ~40 mL of 6M leachate and ~140 of mL 10WTR leachate in 18hLTs.

Organic acids in BC are suspected to be the source of its high base buffering capacity. Apparently, these organic acids are found in BC at much higher concentrations compared to green waste composts. The LOI at 550°C for BC was 52%, implying a very rich organic content; the LOI at 550°C for GWC1 was 25%. Due to the microbial activity during the

composting process, organic matter in the raw feed material is degraded and some of the end-products of this process are low-molecular-weight organic acids (Song et al., 2015; Wang et al., 2015). The structure of these organic acids in composts are similar to humic substances in soils (Manser and Keeling, 1996; Sparks, 2003; Zhou and Haynes, 2010).

4.3.2.2. Alkalinity Reduction in Compost Columns

After biosolids compost (BC) were observed to successfully decrease pH and dissolved Al(+III) concentrations in 6M and 10WTR leachates during batch-type tests, the base neutralizing capacity of BC was also investigated in column leach tests (CLT) with two-column-in-series setups. The results of pH measurements on the effluents of first and second columns in these two-column-in-series systems are given in Figure 4.8 as a function of pore volumes (PV) of the first columns. In this graph, the effluent data labeled as 10WTR and 6M delineate the pH measurements made in the effluents from the first columns in the two-column systems. It should be noted that the leachate pH data for 10WTR was constructed combining the data from 5 different first columns containing 10%WTR+90%6M slag mixture in two-column systems whose effluents were directed into BC15, BC30-I, BC30-II, BC50 and GWC1. Despite 10WTR data was a combination of pH measurements from columns with pore velocities that were varying within the range of 7.1−10.3 cm/h (Table 4.5), the pH data from all 5 columns were matching well and hence, it was considered to be appropriate to present them combined. The data from same type of CLTs using 6M and 10WTR mixtures that were presented in the previous chapter are also given as a comparison.

Effluent pH of 10WTR increased from pH 11.5 to pH 12.1 during the duration of the CLT. BC30(single) column maintained its acidic nature throughout the CLT (pH 4.1 at 1 PV and

5.7 at 157 PV). In the other BC columns that were fed with effluents from the first columns contained 10WTR (pH >11.5), the effluent pH levels were all initially at ~4.4 and kept below pH 6.1 during the first 48−71 PV until an apparent "breakthrough point" for the base neutralizing capacity of BC columns was reached and effluent pH values started to increase sharply becoming pH ≥7. Effluent pH values from BC15, BC30-I, BC3-II and BC50 passed pH 7 threshold at 58 PV, 74 PV, 65 PV and 74 PV, respectively (Table 4.10). Notice that there was a 30-PV gap between the points where pH was 5.7 (60 PV) and 8.5 (90 PV) for BC30-I column; considering the behavior of other BC columns, the point where pH 7 was reached in BC30-I could be as high as 80 PV.

The effluent pH from 6M was averaging at pH ~12.5. 6M/BC30 received effluent from 6M column as influent. For 6M/BC30, the pH influent was higher compared to other BC30 columns (i.e., BC30-I and BC30-II) and accordingly, the effluent pH of 6M/BC30 reached pH 7 relatively earlier at 42 PV.

GWC1 contained 28 g (based on dry wt.) of greenwaste compost with a very weak BNC compared to biosolids compost and was also fed with the effluent from 10WTR column. The initial effluent pH of GWC1 columns was 7.6 and reached pH 11.5 at 42 PV. These results demonstrate that a compost with low base neutralizing capacity and a leachate pH above 7 was generally ineffective in neutralizing 10WTR effluents.

Overall, the column that was containing compost with lower base neutralizing capacity (GWC1) failed first and the column that was receiving influent with higher pH (6M/BC30) failed earliest. But the columns that were all fed with 10WTR leachate and containing different amounts BC based on dry weight were all failed very close together, within the

range of 58−74 PV. However, it was expected that the presence of greater BC mass in columns would be resulted in higher amount of BNC availability to neutralize more number of pore volumes proportional to their BC content. BC30-I contained 34% more BC (based on dry weight) compared to BC15 but it only neutralized 22% more PV. BC50 contained 22% more BC compared to BC30-II, but it only neutralized 12% more PV.

The effluent alkalinity from first and second columns in the two-column systems are plotted in Figure 4.9. The effluent alkalinity values from 10WTR and 6M columns and the data from same type of CLTs were given together. The alkalinity in the effluents from 10WTR columns were >13 mEq/L, whereas 6M column released ~45 meq/L. In spite of high alkalinity coming from 10WTR and 6M columns, all BC columns were able to completely neutralize the received alkalinity and even released small amounts of acidity within the range of 0 and 2.6 mEq/L (shown as negative alkalinity values in the graph) until effluent pH values reached ≥7. Even GWC1 appeared to neutralize the majority of the alkalinity it was receiving from 10WTR column during the first 14 PV.

The cumulative alkalinity mass (mEq) released from 6M and 10WTR columns were calculated as a function of the volume of water using the combined alkalinity data from all 6M and 10WTR columns. For each BC column, these cumulative alkalinity values were used to estimate the amount of “total received alkalinity” until the effluent leachates of the BC columns reached pH 7. “Total received alkalinity” was then divided by the “weight of BC” in each column to calculate the amount of “total neutralized alkalinity” per kg of dry BC. All the calculated values are listed in Table 4.10. In these calculations were simplified by omitting the acidity released by the BC columns, since the acidity released from BC columns were relatively very low compared to received alkalinity.

For the 5 BC columns, the correlations between biosolids compost mass (dry wt.) and the total neutralized alkalinity (mEq) until pH reached 7 was weak; Pearson correlation coefficients, R, was 0.39 (Figure 4.10a). When the 6M/BC30 column was omitted, the correlation coefficient increased to 0.75 (Figure 4.10b). When average contact time and neutralized alkalinity mass correlated the overall relationship for 5 columns was low again (R=0.46) (Figure 4.10c). When average contact time and neutralized alkalinity per kg BC (based on dry weight) were plotted together, the most strong correlation involving all 5 columns was obtained (R=0.91) (Figure 4.10d). Average contact time was a function of flow rate, column height and porosity of the column. Average contact time represents the amount of time that took for water to travel the whole distance of the column height. However, when the columns with similar contact times and similar influents were grouped together (BC15 and BC30-I; BC30-II and BC50) and examined, it was seen that the columns with less BC content neutralized alkalinity from the first columns more efficiently (higher mEq/kg values). For example BC50 with 29-g BC content neutralized alkalinity less efficiently compared to BC30-II which has the same contact time and only 22.6-g BC content. The same was true for BC15 compared to BC30-I. Therefore, contact time appeared to be the most important parameter to describe BNC performance.

A possible explanation for these observations can be due to a BNC loss due to water flow since contact time seemed to be more important (Figure 4.11). Evidence of organic matter leaching from the biosolids compost columns was visible in effluent samples; the effluents from compost columns had a dark brown color at the start of the tests and the color eventually became yellow on the later stages of the tests. To test this theory, 2.0-g BC samples were washed in sequential 18hLTs using 0.04 M NaCl as extraction liquid and

then the drained washed composts were subject to BNC tests (Figure 4.12). Each wash run corresponded to contacting approximately 19 PV worth of water. After the first wash, it was calculated that 856 mEq/kg of the BNC was lost compared to unwashed samples, corresponding to a 67% loss. After the two washes (equivalent of 38 PV), it was calculated that 802 mEq/kg of the BNC was lost compared to unwashed samples, corresponding to a 63% loss. After three washes (equivalent of 38 PV), it was calculated that 975 mEq of the BNC was lost compared to unwashed samples, corresponding to a 77% loss. In summary, it seems possible to lose 63−77% of BNC measured in 18-h tests without using it due to water flow that was worth of 57 PV. Relatively small differences between 3 washing runs implied that the majority of BNC loss occurred when the compost was submersed for the first time.

When different amounts (0.25−3.0 grams) of pristine and one-time-washed BC samples were tumbled contacting with filtered 10WTR leachates for 18 hours, the final leachate pH values were 0.3 pH units lower on average (corresponding to 50% less proton activity) for washed BC samples that contacted 10WTR leachates and compared to pristine BC samples (Figure 4.13). This indicates that ~50% of base neutralizing potential could be lost independent of the total mass.

Composts can release some of their organic matter content in form of particulate organic carbon and dissolved organic carbon (DOC) (Iqbal et al., 2015). A study on compost/sand mixture use in bioretention systems shows that increasing compost fraction in the mixtures caused increased dissolved organic carbon release from the composts (Beesley, 2012). The DOC compounds in compost leachates consist mainly of organic acids (Wershaw et al.,

1996). Therefore, it seems possible that composts can lose its BNC due to leaching DOC once the compost columns were wetted.

Based on the average value for the BNC loss values from each step of washing, the loss rate of base neutralizing capacity was estimated at 878 mEq/kg BC (dry wt.). This value was multiplied by BC weight (dry wt.) in the columns and the lost (washed away) BNC values were calculated for each column assuming the loss was solely a function BC mass not related to the amount of water passed through the system. The calculated value was added the amount of neutralized alkalinity mass that was in the effluent of the first column (Table 4.11). According to these calculations, 27±5% of total BNC capacity was lost due to water flow.

The average 10WTR mass in the first columns were 175 g (dry wt.); the average breakthrough point where pH reach 7 in BC column receiving effluents of 10WTR (BC15, BC30-I, BC30-II and BC50) was 68 pore volumes. The average contact time in these columns were 3.1 hour, corresponding to 6.9 cm/h. The average porosity in BC columns was 0.51 and the average biosolids compost mass was 22.3 g. On average 2.6 Eq alkalinity per kg dry compost was neutralized. When an estimation for the amount of compost required to neutralize 10WTR leachates was made based on these average values, it was calculated that 0.128 kg dry biosolids compost was required per kg 10WTR mixture to treat 68 PV worth of water at a flow rate of 17.5 mL/h before the neutralization capacity of compost was depleted. The strong relationship between neutralized amount of alkalinity per kg compost and contact time is considered, it seem likely to attain better neutralizing performances at slower flow rates.

4.3.2.3. Al and Ca Retention in Compost Columns

Figure 4.14a shows the dissolved Al(+III) concentrations measured in the effluents from BC30(single), 6M and 6M/BC30 columns. Although BC30(single) was fed with 0.02 M NaCl in DI water, it leached 0.46 mM Al(+III) at 1.1 PV (pH 4.1) and 1.1 mM Al(+III) at 2.9 PV (pH 4.4) and dissolved Al(+III) concentrations stayed below 0.08 mM between 2.9−144 PV (pH 4.4−5.7). BC compost had a 2200 mg/kg ammonium oxalate extractable Al(+III) content (Table 4.1). Therefore, it can be said that BC/sand mixture has a tendency of leaching low amounts of Al(+III) upon wetting, regardless of the influent Al(+III) concentrations.

6M column leached 0.24 mM Al(+III) at 1.8 PV and ≤0.02 mM at rest of the test (pH ~12.5). 6M/BC30 leached ≤0.06 mM Al(+III) until pH started to increase above pH 7 (beyond 42 PV). 6M/BC30 leached 0.3 mM at 44 PV (pH 8.8), 1.2 mM Al(+III) at 64 PV (pH 12.0) and 0.45 mM Al(+III) at 71 PV (pH 12.4). The difference between received and released Al(+III) concentrations for 6M/BC30 indicated elevated Al(+III) release from 6M/BC30 at pH >8.8 should be mainly originated from the BC/soil content, as in the case of BC30(single).

Figure 4.14b shows the dissolved Al(+III) concentrations measured in the effluents from BC columns that received the effluents from 10WTR columns. Al(+III) leaching from 10WTR peaked at around 12–14 mM at 2–8 PV. Between 10 PV and 100 PV, dissolved Al(+III) concentration in 10WTR effluent decreased from 13 mM to 1 mM and was 0.9±0.2 mM at 100–157 PV.

Biosolid compost columns where the inflow was the effluent of 10WTR, effluent Al(+III) concentrations with the range of 0.08−0.27 mM were measured at during the first 4 PV (pH <4.4). After the first 4 PV, Al(+III) concentrations were mostly ≤0.08 mM as long as the effluent pH stayed below 6.1, despite receiving high concentrations of dissolved Al(+III) from 10WTR columns. Once the effluent pH rose above 7, Al(+III) release started to increase rapidly to levels above influent Al(+III) concentrations. For example, Al(+III) release from BC30-I increased to from 0.17 mM (pH 8.5) to 1.5 mM at 90 PV (pH 9.3), reached to 3.3 mM at 118 PV (pH 10), and finally decreased to 2.3 mM at 135 PV (pH 11.5), while the influent Al(+III) concentrations were always at around 1 mM. Some of this Al(+III) release that was higher than influent Al(+III) concentrations can be explained by Al(+III) dissolution originated from the BC/soil mixture inside these columns. Another source of Al(+III) release at alkaline pH could be dissolution of previously immobilized Al(+III) in the second columns as the pH increased.

In Figure 4.15, the cumulative Al(+III) mass released from 10WTR and BC30-I columns as a function of water volume are plotted. The difference between total received Al(+III) mass and total released Al(+III) mass in BC30-I was 18.7 mmol Al (corresponding to 0.83 mol Al/kg biosolids compost) at 74 PV where effluent pH from BC30-I was estimated to reach 7. Even at 135 PV where effluent pH of BC30-I was 11.5, the difference was 16.9 mmol Al. These values indicate that BC had the capacity to retain the majority of the Al(+III) influx both below and above pH 7.

Al(+III) release from GWC1 column columns rapidly increased as the effluent pH approached to influent pH; it leached 0.62 mM Al at 14 PV (pH 8.75), and 3.8 mM Al at 42 PV (pH 11.5) matching the influent Al(+III) concentrations from 10WTR column. It

appears that GWC1 also managed to retain majority of the received Al(+III) concentrations but at a much lower extent compared to BC containing columns.

Figure 4.16 shows dissolved Al(+III) concentrations measured in the effluent of all columns as a function of pH, along with a solubility curve for total dissolved Al(+III) in an amorphous-$Al(OH)_3$–H_2O system. The curve for the total dissolved Al(+III) concentration was calculated using the K values at 20°C that were reported in Stumm and Morgan (1996) for Equations 4.1–4.4. The ionic strength was assumed to be equal to 0.05 M and Davies Equation (Eq. 3.1) was used to calculate the activity coefficients (1 atm, I=0.05 M). Comparison of the am-$Al(OH)_3$ solubility curve and the dissolved Al(+III) concentrations from compost columns demonstrates that Al(+III) concentrations both under acidic (pH <5) and alkaline conditions (pH >8.5) were greatly lower relative to a predominantly solubility controlled Al(+III) release mechanism would allow. The majority of the Al(+III) in 10WTR effluent were immobilized inside biosolids compost column at pH values ranging from 4.4 to 7, implying the presence of a retention mechanism for Al(+III) other than precipitation in form of Al-hydroxides.

$$Al^{3+} + H_2O \leftrightarrow Al(OH)^{2+} + H^+ \qquad \log K_1 = -5.15 \text{ at } 20°C \qquad (4.1)$$

$$Al^{3+} + 2\ H_2O \leftrightarrow Al(OH)_2^{+} + 2\ H^+ \qquad \log \beta_2 = -10.46 \text{ at } 20°C \qquad (4.2)$$

$$Al^{3+} + 4\ H_2O \leftrightarrow Al(OH)_4^{-} + 4\ H^+ \qquad \log \beta_4 = -23.21 \text{ at } 20°C \qquad (4.3)$$

$$(am)Al(OH)_{3\,(s)} + 3\ H^+ \leftrightarrow Al^{3+} + 3\ H_2O \qquad \log K_{so} = 11.13 \text{ at } 20°C \qquad (4.4)$$

Aluminum is well known to be complex with natural organic materials and is removed from the aqueous phase at low pH values (Sparks, 2003). Composts are rich in organic matter with organic surface functional groups that serve as a sink for dissolved metal

cations; cations and the negatively charged functional groups can form strong inner-sphere complexes (Madrid, 1999; Zhou and Haynes, 2010). Kerndorff and Schnitzer (1980) studied sorption of 11 metals, including Al, onto humic acids within the pH range of 2.4−5.8 and reported that the sorption efficiency increased with rise in pH, decrease in metal concentration and increase in humic acid concentration. Hagvall et al. (2015) reported that complexes between carboxylic functional groups in natural organic matter and Al(+III) were favored more within the range of pH 3−6. Therefore, the Al immobilization under acidic conditions can be explained by Al(+III) retention on organic matter; dissolved Al(+III) strongly bound to the organic matter in the compost and the majority of Al(+III) remained immobile even when the alkaline conditions prevailed in the system.

Dissolved Ca(+II) concentration in the effluents are given in Figure 4.17. 10WTR(two) was within the range of 6−8 mM at 1−157 PV, whereas 6M(two) leached 20−23 mM Ca(+II) at 1.8−85 PV. During the first 5 PV, all columns containing BC leached Ca(+II) concentrations within the range of 17−28 mM −much higher than their respective influent concentrations. This “first flush” behavior in Ca(+II) release was matched by an equally high S release from the BC columns (Figure 4.18). S releases were also much higher that the influent S concentrations; highest S releases from 6M and 10WTR columns were 0.54 mM and 0.72 mM, respectively. Both the highest Ca(+II) and S release were from BC30(single) (28 mM Ca and 31 mM S), suggesting that Ca(+II) and S was mainly released from BC/Soil mixture. After the initial high release period during the first 20 PV, Ca(+II) concentrations in the effluent of second columns fell to <1 mM, despite the steady flow of Ca(+II) at 6−8 mM from 10WTR(two). Once the pH of the columns rose above 7, Ca(+II)

release from compost columns increased again to 3−5 mM. Even when pH of the effluent approached influent pH of 11.5, effluent Ca(+II) concentrations did not match influent concentrations. Therefore, excluding the first flush, Ca(+II) was predominantly retained in compost column and it was bound to compost strong enough that it was not extracted even at high pH levels, similar to the case of Al retention. Dissolved Ca(+II) concentrations were not a source of concern but its strong sorption onto compost confirms that compost had a high capacity to retain cations.

Unlike BC columns, GWC1 only leached 3.6 mM Ca(+II) and 1.1 mM S initially (1.5 PV) and concentrations of Ca(+II) and S stayed below 1 mM until pH was reached 11.5. At pH 11.5, GWC1 leached 3.6 mM Ca(+II) and 0.1 mM S (42 PV).

4.3.2.4. P Release from Compost Columns

Figure 4.19 shows the dissolved P concentrations from the second columns in two-column-in-series systems and BC30(single). The highest initial and overall P release was from BC30 (single). Between 1 and 34 PV, P concentrations in BC30(single) effluent ranged from 3.0 mM to 0.27 mM and it stayed at around 0.14±0.06 mM until 144 PV. Trend in P release for other BC columns were similar to BC30(single). Compared to dissolved P concentrations from BC columns, dissolved P concentration were relatively very low in 6M and 10WTR effluents (<0.019 mM P). GWC1 column released P at concentration varying from <0.02 mM to 0.22 mM P (1−42 PV). These observations suggest that the P release was predominantly originated from BC composts and that P release from columns seems to be independent the properties of the influents. Therefore, dissolved P release was naturally occurring for BC and neutralization of highly alkaline effluents from 10WTR and 6M columns by BC did not appear to have negative impact on dissolved P leaching.

Dissolved P leaching from composts were also observed in other studies (Glanville et al., 2003; Kim, 2010; Gleason, 2013). P contamination in surface water bodies can cause eutrophication and hypoxia (Boesch et al., 2001). U.S. EPA recommends maintaining concentrations below 31.25 µg/L in rivers and streams in MD, as part of ecoregion 66 XIV (Eastern Coastal Plain), to protect aquatic life in the Chesapeake Bay (USEPA, 2000). In addition to dissolved P release, dissolved nitrogen leaching from compost is also possible (King and Torbert, 2007). Therefore, direct discharge of the leachates from the biosolids compost into surface waters should be avoided (Gleason, 2013).

4.4. Conclusion

In batch-type tests, PO_4(-III) addition to 10WTR decreased the Al and Ca(+II) release even further, at the cost of creating residual dissolved P in the leachate. Despite the promising results that were observed during batch-type tests in terms of reductions in dissolved Al(+III) and Ca(+II) release, in column tests, NaH_2PO_4 addition to 10WTR in powder form caused extremely high Al(+III) release (>40 mM) during the first 5 PV compared to regular 10WTR columns. After the sodium phosphate monobasic was flushed out, the columns started to behave similar to regular 10WTR columns in terms of effluent pH, dissolved Al(+III) and Ca(+II) concentrations.

The residual alkalinity and Al(+III) in WTR-amended slag leachates were successfully minimized utilizing a biosolids compost with high base neutralization capacity. In CLTs with two columns in series, directing the effluents of the columns containing 10WTR to biosolids compost columns reduced the pH level of the effluents by ≥6 log units. This significant reduction in pH level was maintained until the breakthrough point for neutralizing capacity was reached. Biosolids compost was able to neutralize 58−74 PV

worth (68 PV on average) of leachate from 10WTR columns by completely removing the alkalinity of the leachate. Until the breakthrough point was reached, effluent pH mostly stayed within the range of pH 4.4−6.1 and the effluent acidity was >3 mEq/L. This was a good improvement compared to 10WTR effluents in terms of these parameters. The pH of effluents from 10WTR column was 11.5 and alkalinity ranged from 14−26 mEq/L. On average, 2.6 Eq alkalinity per kg dry compost was neutralized.

However, results from batch-type tests of compost washed with 0.04 M NaCl solution demonstrated that BNC of biosolids composts could be washed away solely by the percolating water and that the majority of the BNC loss appeared to occur upon the biosolids compost being wetted for the first time (Figure 4.11). The average contact time seems to be a more important design parameter that was affecting the neutralizing performance compared to the mass of the biosolids compost in the columns. On average, it was calculated that ~0.13 kg dry biosolids compost was required per kg 10WTR mixture to treat 68 PV worth of water at a flow rate of 17.5 mL/h before the neutralization capacity of compost was depleted. Considering the strong relationship between neutralized amount of alkalinity per kg compost and contact time, it seems likely to obtain better neutralizing performances at slower pore velocity levels, which is likely to occur in the field.

Column tests are considered to be the best method to imitate percolation of leachates through porous media, study its long-term leaching behavior, and approximating particle size distribution, porosity of the media and the dynamic mass-transfer conditions in the field. But, in the literature, there are no clear definitions for translating results of column tests to actual spans of time that were simulated. Nevertheless, rough estimations were made to speculate on what would be the equivalent of one pore volume's worth of leaching.

The annual precipitation rate for Maryland is ~1 m (Cetin et al., 2012) and 15% of it was assumed to infiltrate into the embankment under the asphalt road (imperviousness =75−100%) (USEPA, 1993; USEPA, 2005), corresponding to 15 cm/yr. Since the average porosity of the small 10WTR columns (20-cm diameter, V = 98 mL) was 47% and the column height was 20 cm, 1 PV was reached in 0.63 years [20 cm·PV^{-1}/(15 cm·yr^{-1}/0.47)]. Bin-Shafique et al. (2006) measured that 5% of the annual precipitation (~1 m/year) infiltrated to a fly ash-stabilized subgrade layer under the road and estimated that approximately 1 pore volume in the columns tests correspond to 1 year in the field based on the infiltration rate.

Another estimation method is based on liquid-to-solid ratios (L:S) in the columns. It is assumed that a L:S of 1 corresponded to 5 years of leaching that may take place in the field (Ram et al., 2007). The average solid mass in 10WTR columns was 172 g and the average pore volume was 45.8 mL (Table 4.5). Based on of these values, an L:S ratio of 1 is estimated to be reached when 3.7 PV worth of water passed through 10WTR columns. Therefore, it can be concluded that one PV of water that passes through the small columns is equivalent to 1.35 years (=5 years/3.7 PV) of leaching under field conditions. Based on the average of the values calculated for small columns (0.63 PV·yr^{-1} and 1.35 PV·yr^{-1}), it can be roughly estimated that 1 PV is equivalent to 1 year of leaching in the field for the 10WTR columns. In this case, ~0.13 kg of dry biosolids compost per kg of 10WTR (10% WTR + 90% 6M slag) that is used in the embankment can be expected to last for ~68 years before its breakthrough point is reached.

Although it is hard to make accurate estimations without further research, results of the column tests showed that the partial alkalinity mitigation effect of WTR-addition was

persistent over the long term (157 PV) and that the compost column was very effective in maintaining pH levels below 7 and retaining Al(+III) to the point where base neutralization capacity of biosolids-based compost was depleted (at least 55 PV). Therefore, it seems possible to maintain low effluent pH levels in a system as long as the biosolids compost is replaced when its BNC is depleted.

In BC columns, the majority of dissolved Al(+III) was removed from the aqueous phase, in spite of the significantly high influx of dissolved Al(+III) (especially during the first 10–20 PV) from 10WTR and 6M columns. As long as the BC columns neutralized the alkalinity (pH <7, alkalinity ≤0) from the first columns , high concentrations of dissolved Al(+III) (0.25−14 mM) coming from the columns containing 6M or 10WTR were mostly immobilized (<0.1 mM). Until the effluent pH values became >7, high rate of dissolved Ca(+II) removal was also obtained after the initial high Ca(+II) release (6−24 mM) during the first 10 PV in the BC columns. The results indicate that Ca(+II) and Al(+III) were removed from the aqueous phase and retained in the compost columns, possibly through a sorption mechanism. After breakthrough points were reached, the soluble Al(+III) in the compost/sand mix and some of the Al(+III) accumulated on the compost column seemed to be mobilized, but the majority of removed Al(+III) stayed bound to the compost, indicating that the complexation of Al(+III) was effective within a large pH range from 4.4 to 11.5. However, dissolved P was released from BC columns. Dissolved P release was highest in the BC column receiving 0.02 M NaCl, suggesting that 10WTR leachate did not contribute to dissolved P release but that dissolved P release was inevitable in a system utilizing biosolids compost.

TABLES

Table 4.1. Elemental leaching from biosolids compost under different conditions.

	18hLT [1]	Ammonium Oxalate Extraction [2]	18hLT at pH 12.5 [3]
pH	5.0	3.0	12.5
Dissolved Concentrations (mg/kg)			
Al	<20	2200	10
Ca	7700	<10	940
K	<20	520	590
Mg	9860	850	350
Na	<20	240	18000
S	8900	2240	10700
P	250	7800	200
Fe	27	15200	130

[1]: 18-hour leach tests using DI water as extraction liquid, L:S=20 mL/g.

[2]: 2-h acid ammonium oxalate extractions, L:S=50 mL/g.

[3]: 18-hour leach tests using NaOH solution at pH 12.5 as extraction liquid, L:S=20 mL/g.

Table 4.2. According to total elemental analyses (TEA), chemical composition of sandy soil that was mixed with composts.

Element (mg/kg) [a]	Sandy Soil
Al	28800
B	2.86
Ca	280
Cu	1.28
Fe	10800
K	548
Mg	373
Mn	38.2
Na	33
P	161
S	68.8
Zn	15.0
Ag	<0.001
As	<3
Cd	<0.4
Co	4.62
Cr	15.5
Hg	<0.001
Li	4.02
Mo	<0.4
Ni	<0.3
Pb	<2
Sb	0.02
Tl	<0.001
V	16.5

[a] **:** All values are based on dry weight (wt./wt.).

Table 4.3. Elemental leaching from sandy soil in 18hLTs and ammonium oxalate extractions, along with its other properties.

	Sandy Soil
pH [1]	5.3
Specific Gravity [2]	2.6
Moisture Content	0.2%
LOI at 550ºC	0.9%
Water Soluble Content (mg/kg) [1,3]	
Calcium (Ca)	94.4 ±3.1
Phosphorous (P)	0.82 ±0.03
Ammonium Oxalate Extractable Content (mg/kg) [3,4]	
Phosphorous (P)	2.12 ±0.35
Iron (Fe)	890 ±250

[1]: Values were measured in leachates from 18hLTs using DI water as extraction liquid with a L:S ratio of 20 mL/g.

[2]: ASTM D-854 (ASTM, 2010b).

[3]: Concentrations were calculated based on dry weight (wt./wt.).

[4]: Values were measured in leachates from 2-hour acid ammonium oxalate extractions.

Table 4.4. Specifications of the columns used in CLTs with sodium phosphate addition.

Column Label	Filling Material	Sodium Phosphate (g)	Total Dry Weight (g)	Dry Bulk Density (g/cm^3)	Pore Volume (mL)	Average Flow Rate (mL/min)	Pore Velocity (cm/h)	Average Contact Time (h)	Test Duration (days)	Volume Passed through (mL)
2%NaP-I	10% WTR + 90% 6M + 2% NaH_2PO_4	3.3	170.3	1.73	45.9	0.27	7.0	2.9	8.0	3,059
2%NaP-II	10% WTR + 90% 6M + 2% NaH_2PO_4	3.3	170.7	1.74	45.8	0.21	5.5	3.7	9.6	2,899
4%NaP-I	10% WTR + 90% 6M + 4% NaH_2PO_4	6.6	172.4	1.76	44.9	0.17	4.6	4.4	11.6	2,850
4%NaP-II	10% WTR + 90% 6M + 4% NaH_2PO_4	6.4	165.9	1.69	46.9	0.26	6.6	3.0	8.1	3,015

Table 4.5. Specifications of the first columns in two-column-in-series systems.

Parameters for 1st Columns	Two-Column-in-series Systems						
	BC30-I	BC30-II	6M/BC30	BC15	BC50	$BC30_{(Single)}$	GWC-1
Filling Material	10% WTR + 90% 6M	10% WTR + 90% 6M	100% 6M	10% WTR + 90% 6M	10% WTR + 90% 6M	*none*	10% WTR + 90% 6M
Fill Height (cm)	20	20	20	20	20		20
Total Weight (g)	174.1	174.1	167.8	175.3	175.2		174.8
Bulk Density (g/cm^3)	1.77	1.77	1.71	1.79	1.78		1.78
Porosity	0.46	0.46	0.50	0.46	0.46		0.45
Pore Volume (mL)	45.2	45.2	49.5	44.8	44.9	45.8 [1]	45
Pore Velocity (cm/h)	10.33	6.83	5.5	8.11	7.17		7.09
Average Contact Time (h)	1.9	2.9	3.6	2.5	2.8		2.8
Total Duration (day)	14.1	14.7	13.4	12.4	18	18	6
Weighted Average of Flow Rate (mL/min)	0.39	0.26	0.22	0.32	0.26	0.33	0.26

1 : The average pore volume of all 10WTR columns was chosen as the pore volume of the first column for BC30(single).

Table 4.6. Specifications of the second columns in two-column-in-series system.

Parameters for 2nd Columns	Column Label						
	BC30-I	BC30-II	6M/BC30	BC15	BC50	$BC30_{(Single)}$	GWC1
Filling Material	BC+Soil	BC+Soil	BC+Soil	BC+Soil	BC+Soil	BC+Soil	GWC1+Soil
Fill Height (cm)	20	20	20	20	20	20	19
Total Weight of the Fill (g)	94.1	92.6	94.7	112.2	80.4	93.6	100.0
Soil Weight (g)	52.4	52.8	52.8	84.5	29.2	53.4	65
Compost Moisture	0.46	0.43	0.46	0.46	0.43	0.43	0.2
Dry Compost Weight (g)	22.5	22.7	22.6	14.9	29.2	22.9	28
Bulk Density (g/cm^3)	0.96	0.94	0.96	1.14	0.82	0.95	1.07
Porosity	0.54	0.55	0.53	0.45	0.56	0.54	0.55
Pore Volume (mL)	52.6	53.9	52.3	43.8	54.5	53.4	51
Pore Velocity (cm/h)	8.8	5.7	5.0	8.6	5.8	7.3	5.7
Average Contact Time (h)	2.3	3.5	4.0	2.3	3.5	2.7	3.3

Table 4.7. Results from 18hLTs using WTR/6M mixtures amended with 10% BC under dry conditions.

BC Content[1],[2] (%)	WTR Content[2] (%)	6M Content[2] (%)	L:S [3] (mL/g)	Leachate pH	Al (mM)	Ca (mM)
0	10	90	20	11.1	7.3±0.4	4.3±0.02
0	20	80	20	10.5	5.8±0.6	3.4±0.3
10	10	80	20	10.5	4.0±0.2	4.3±0.1
10	30	60	20	9.8	1.6±0.8	4.1±0.1
100	0	0	20	5.0	<0.02	9.7±0.5

1 : Biosolid compost was dried in oven at 105°C for 24 hours.

2 : Given percentages are based on the dry weight of the components relative to the total weight of the mixture (wt./wt.).

3 : Liquid-to-solid ratio. Extraction liquid was 50-mL DI water and total solid material weight was 2.50 g.

Table 4.8. Results from 18-h batch-type leach tests using BC in 10WTR or 6M leachate.

BC Weight[1] (g)	Extraction Liquid[2]	L:S [3] (mL/g)	Leachate pH	Al (mM)	Ca (mM)
0	10WTR Leachate	n/a	11.1	7.2±0.3	4.9±0.3
1.0	10WTR Leachate	40	7.0	<0.02	6.4±0.1
2.0	10WTR Leachate	20	6.1	<0.02	10.6±0.9
3.0	10WTR Leachate	13.3	5.7	<0.02	14.0±0.8
0	6M Leachate	n/a	12.4	0.1±0.0	18.4±0.7
1.0	6M Leachate	40	7.2	<0.02	19.1±0.7

1 : Biosolids compost was oven dried (105°C, 24 hours).

2 : Extraction liquid was either 40-mL 6M leachate or 40-mL 10WTR leachate from another 18hLT.

3 : Liquid-to-solid ratio.

Table 4.9. Estimated base neutralizing capacities for the composts.

Material	mEq/kg at pH 7*	mEq/kg at pH 8.5*
10WTR(18h)	1600	870
10WTR(18h+4h)	780	570
BC (18h)	-1270	-2320
BC, Dried (18h)	-530	-1020
GWC1	- -	-40
GWC2	- -	-100

***** : Values were estimated based on interpolated data points. Negative values indicate base addition, whereas positive values indicate acid addition.

Table 4.10. Parameters calculated for second columns based on the results from CLTs.

Second Column	PV at pH 7	Total Volume at pH 7 (L)	Total Received Alkalinity (mEq)	Mass of BC (g, dry wt.)	Total Neutralized Alkalinity (Eq/kg BC, dry wt.)	Average Contact Time (h)	Total Contact Time (h)
BC15	58	2.58	46.0	14.9	3.09	2.3	136
BC30-I	74	3.32	59.3	22.5	2.64	2.3	143
BC30-II	65	2.96	52.8	22.7	2.32	3.5	193
BC50	74	3.15	56.1	29.2	1.92	3.5	200
6M/BC30	42	2.07	93.8	22.6	4.15	4.0	157

Table 4.11. Estimated base neutralizing capacities that were washed away.

	Neutralized Alkalinity [1] (mEq)	Lost to Water Flow [2] (mEq)	Total Consumed BNC [3] (mEq)	Lost BNC divided by Total Consumed BNC [4]
BC15	48	13	62	0.21
BC30-I	62	20	82	0.24
BC30-II	56	20	76	0.26
BC50	59	26	85	0.31
6M/BC30	39	20	59	0.34

[1] : Neutralized alkalinity mass until pH reached 7.

[2] : Calculated by assuming a loss rate of 878 mEq BNC per kg dry biosolids compost.

[3] : The sum of BNC loss due water flow and neutralized alkalinity mass.

[4] : The ratio between BNC loss due to water flow and total consumed BNC.

FIGURES

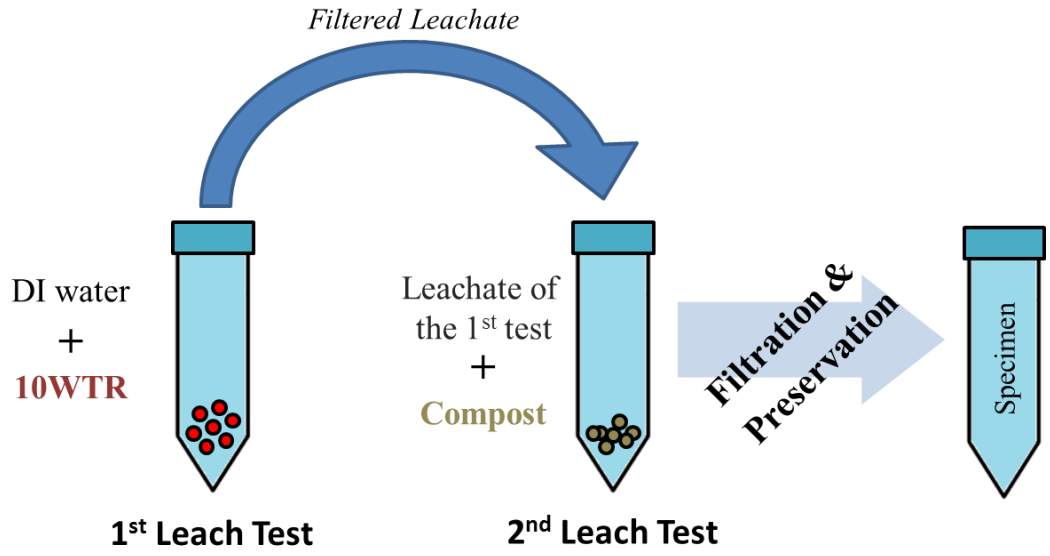

Figure 4.1. Sequential batch-type leach tests.

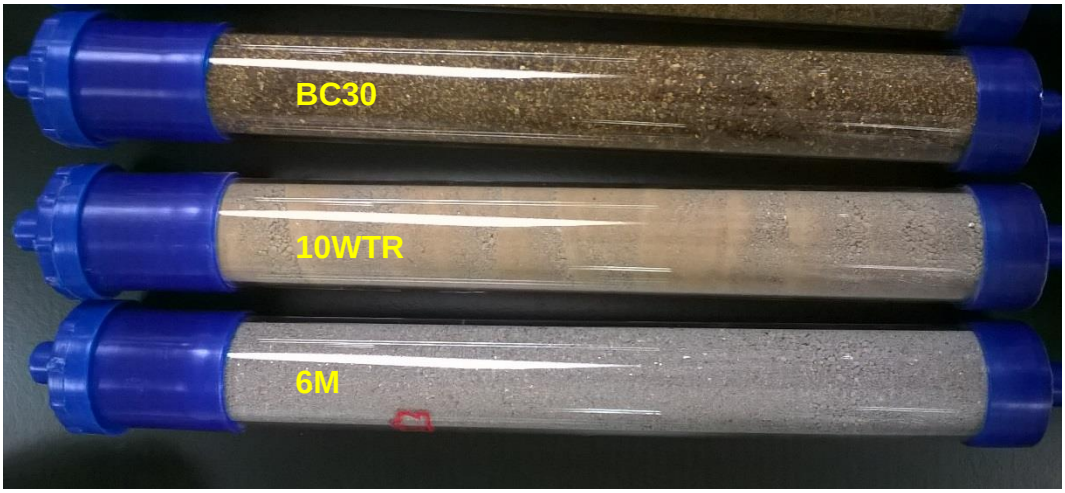

Figure 4.2. 20-cm glass columns filled with different mixtures.

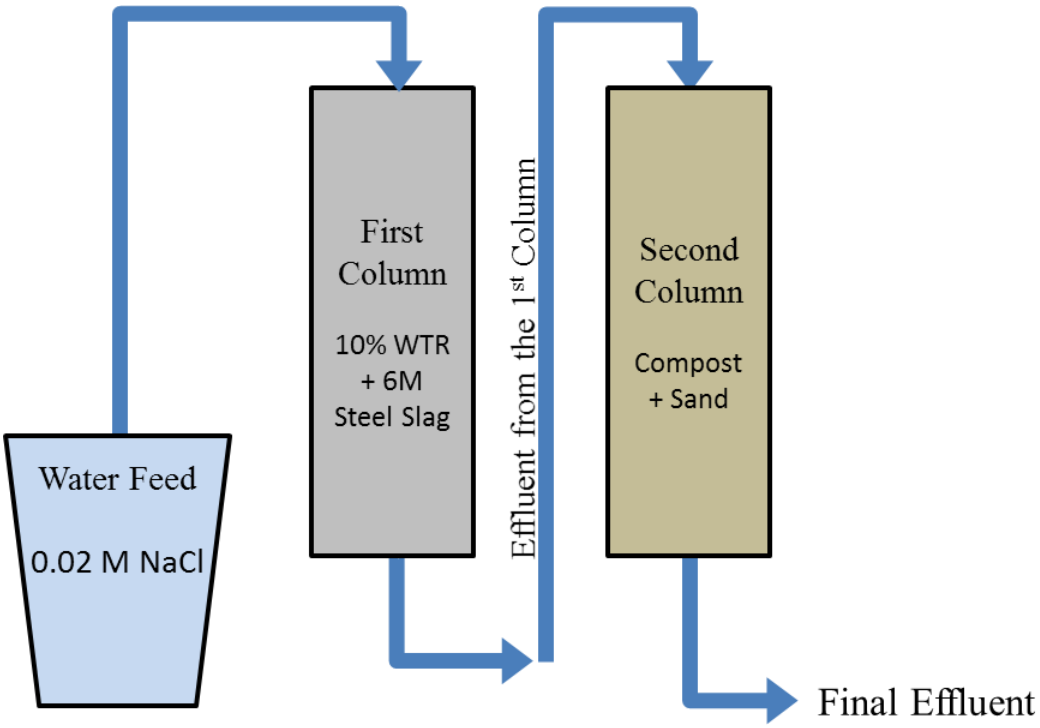

Figure 4.3. Two-columns-in-series setup for CLTs.

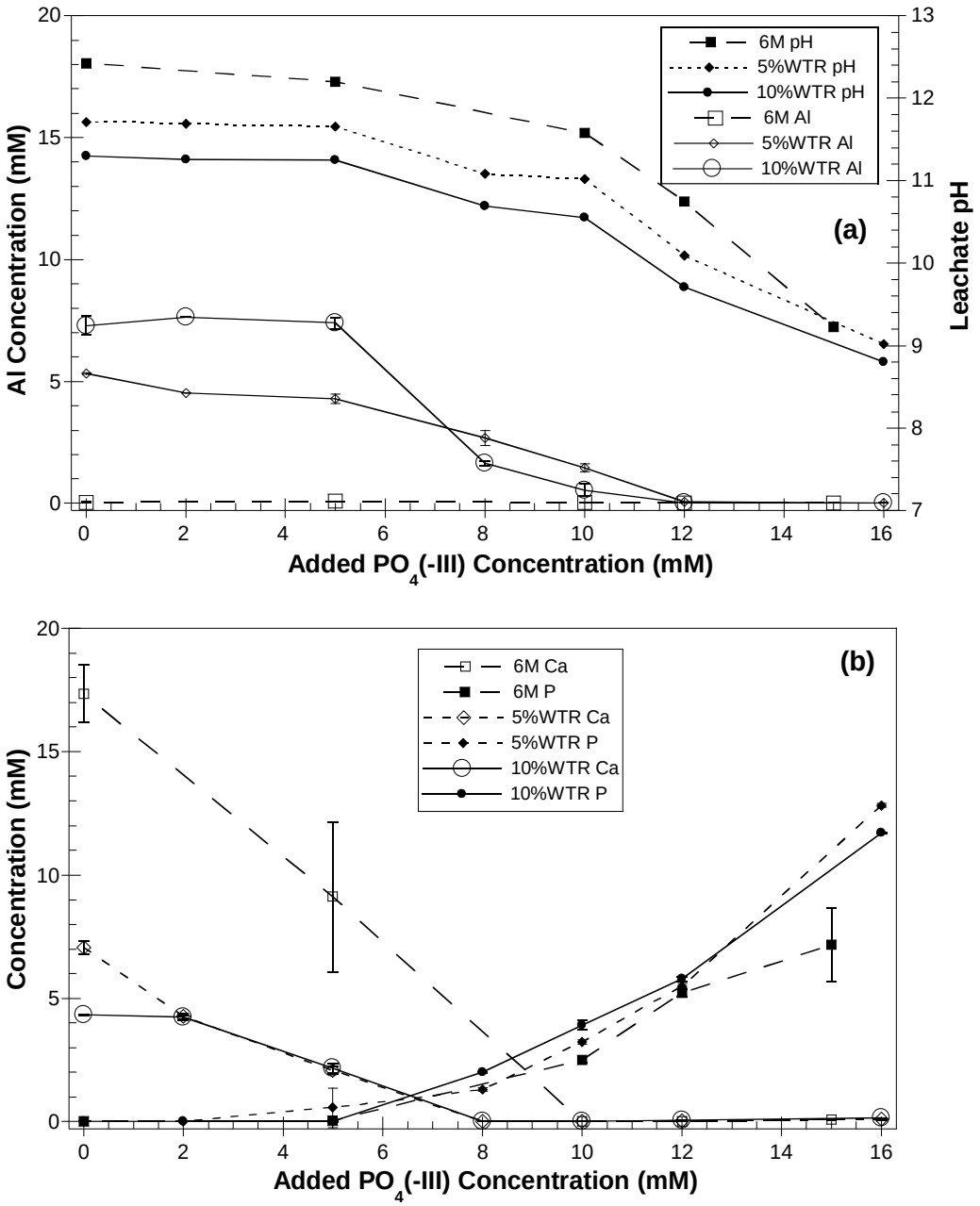

Figure 4.4. (a) Dissolved Al concentrations and leachate pH and **(b)** dissolved Ca and P concentrations for 6M, 5% WTR/6M and 10%WTR/6M against the amount of added NaH_2PO_4 concentration.

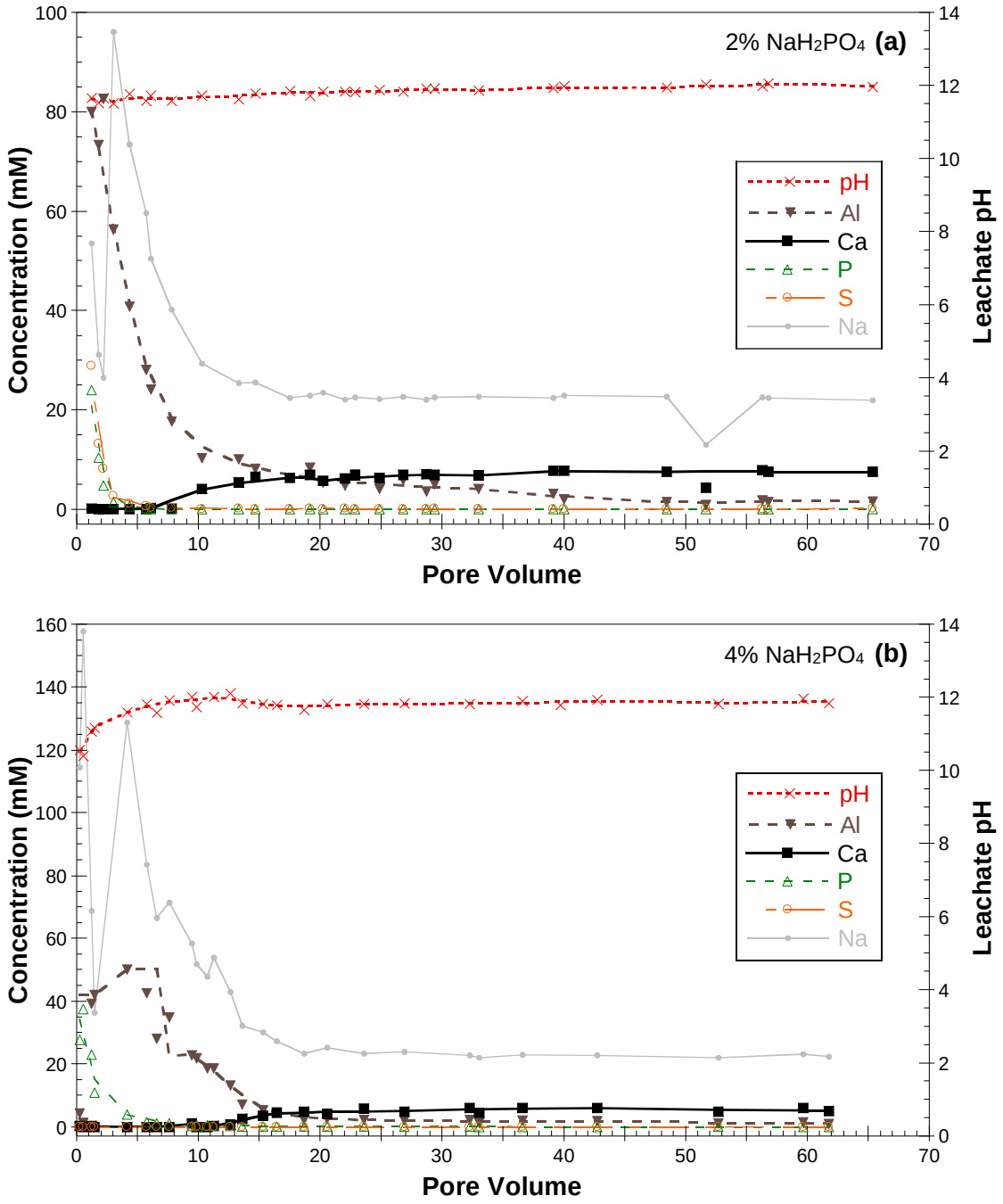

Figure 4.5. Dissolved Al, Ca, Na, P and S concentrations in the leachates from **(a)** 2% NaH_2PO_4- and **(b)** 4% NaH_2PO_4-added 10WTR columns.

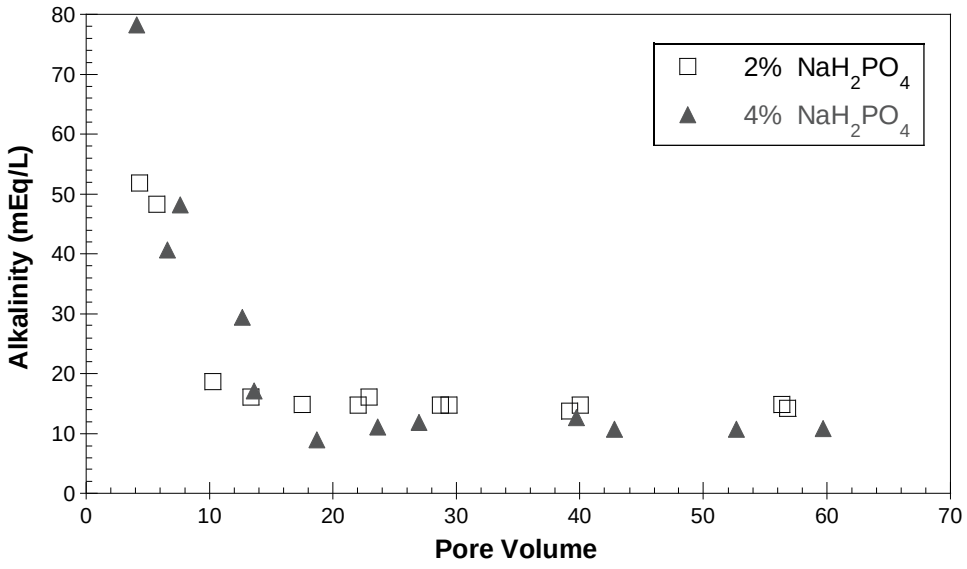

Figure 4.6. Alkalinity and pH measured in the leachates from 2% and 4% NaH_2PO_4-added 10WTR columns.

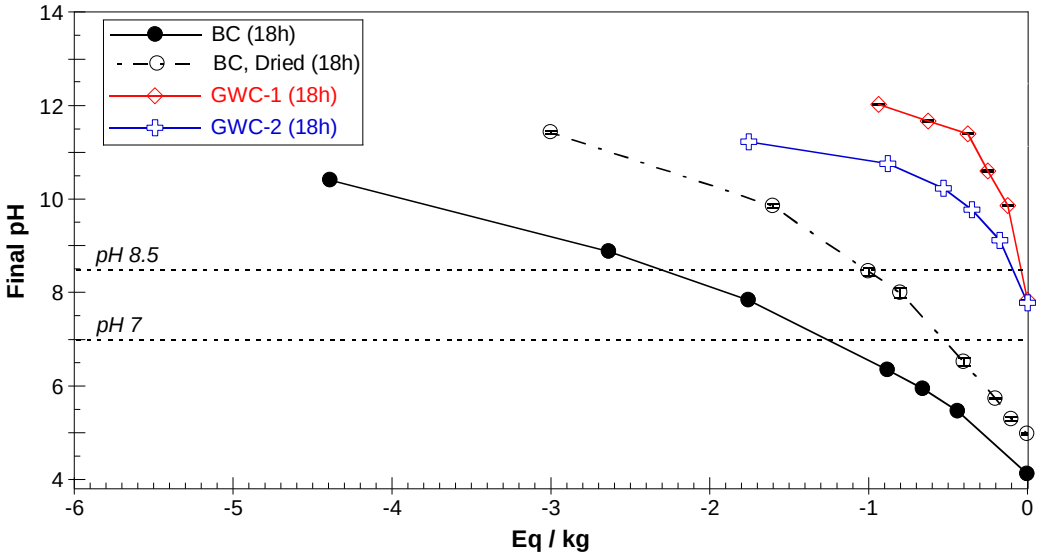

Figure 4.7. Buffering capacity of composts, 6M and 10WTR; Eq/kg values were based on dry weight.

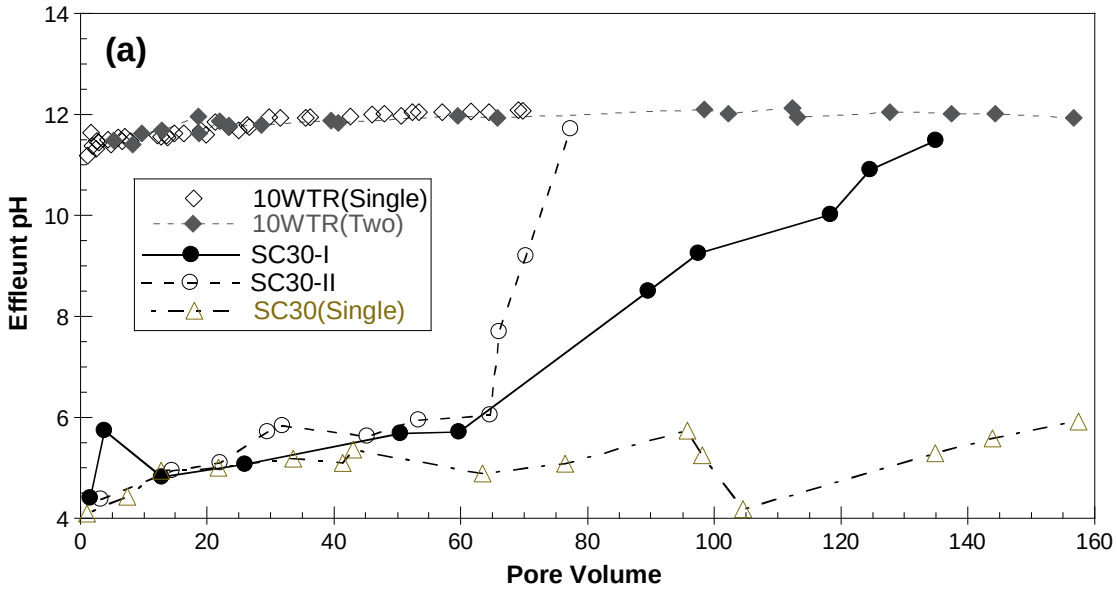

Figure 4.8. Effluent pH values from two-column systems as a function of PV of the first columns; **(a)** 10WTR(Two), BC30-I and BC30-II; **(b)** BC15, BC30 and GWC1; **(c)** 6M, 6M/BC30 and BC30(Single) [1].

[1] : 6M(Single) and 10WTR(Single) were respectively the 6M column and 10WTR column in the one-column system and their data are presented in Chapter 3, previously. 6M(Two) was the first column containing 6M steel slag in the two column system; its effluent was pumped into 6M/BC30. 10WTR(Two) is the combined data from five 10WTR columns that were the first columns containing 10%WTR+90%6M in the Two column systems; effluent of 10WTR(Two) columns was pumped into BC30-I, BC30-II, BC15, BC50 and GWC1. BC30(Single) was a single column system that was using 0.02 M NaCl as the effluent.

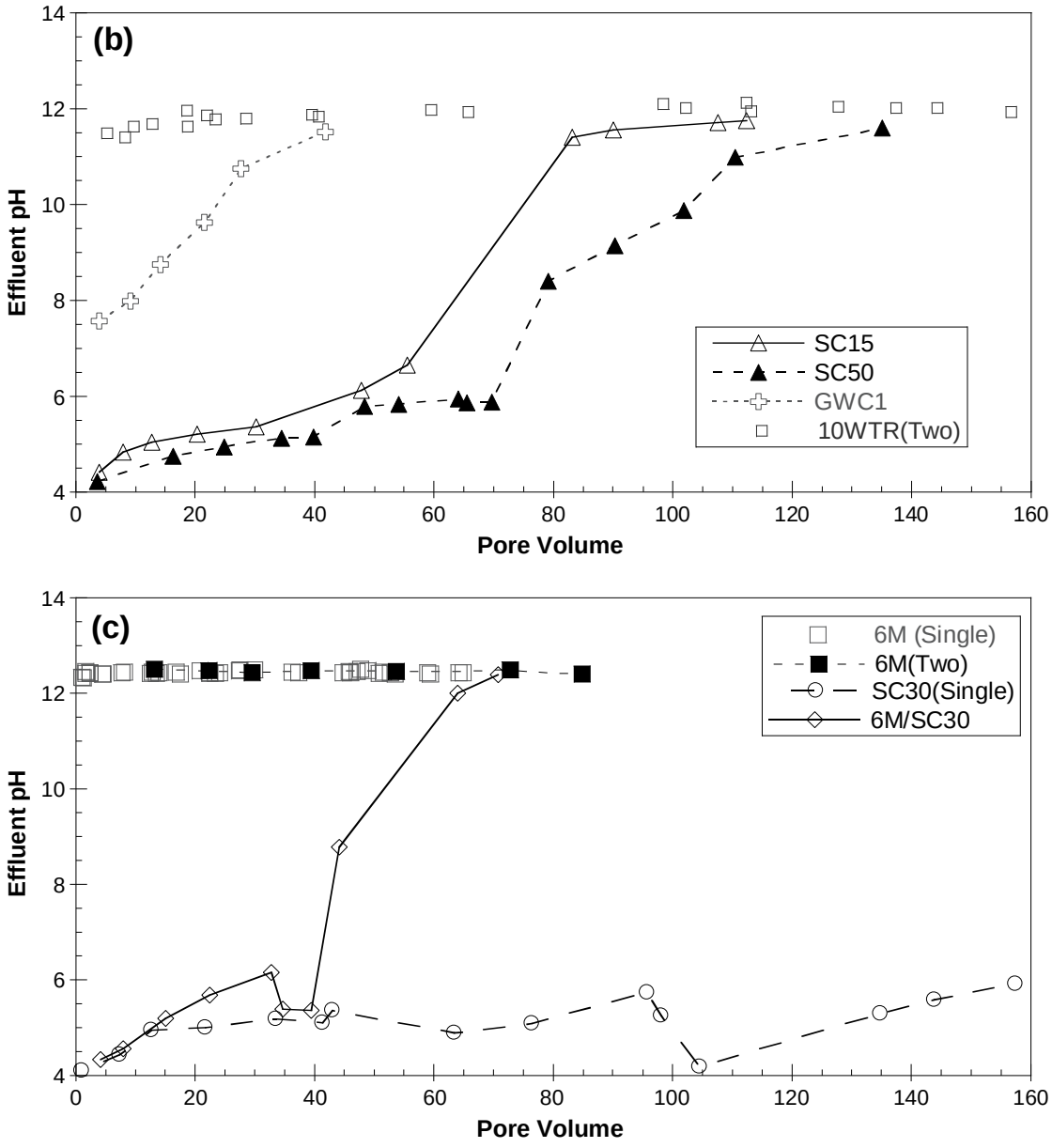

Figure 4.8. (continued)

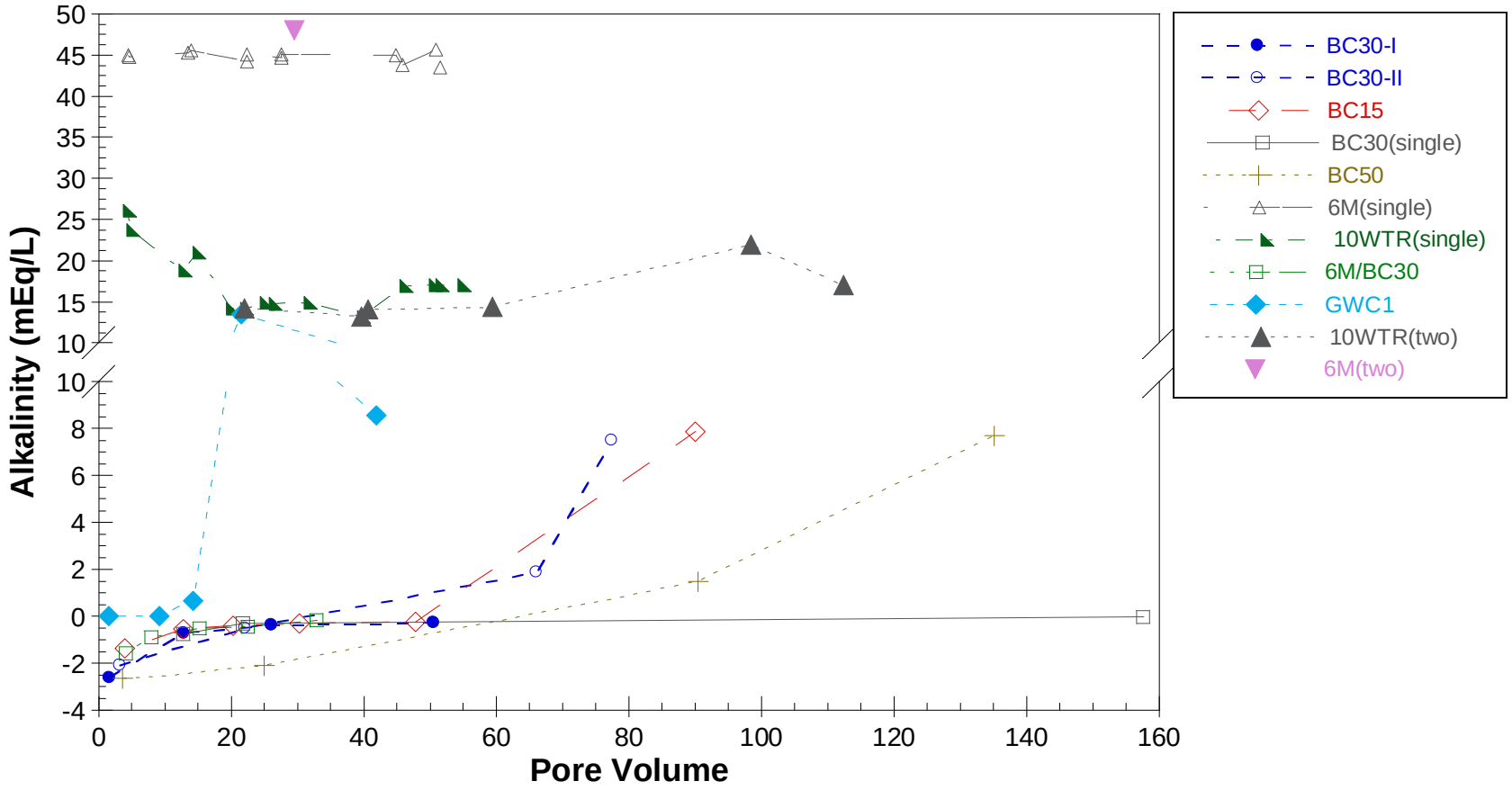

Figure 4.9. Alkalinity in the leachates from first and second columns.

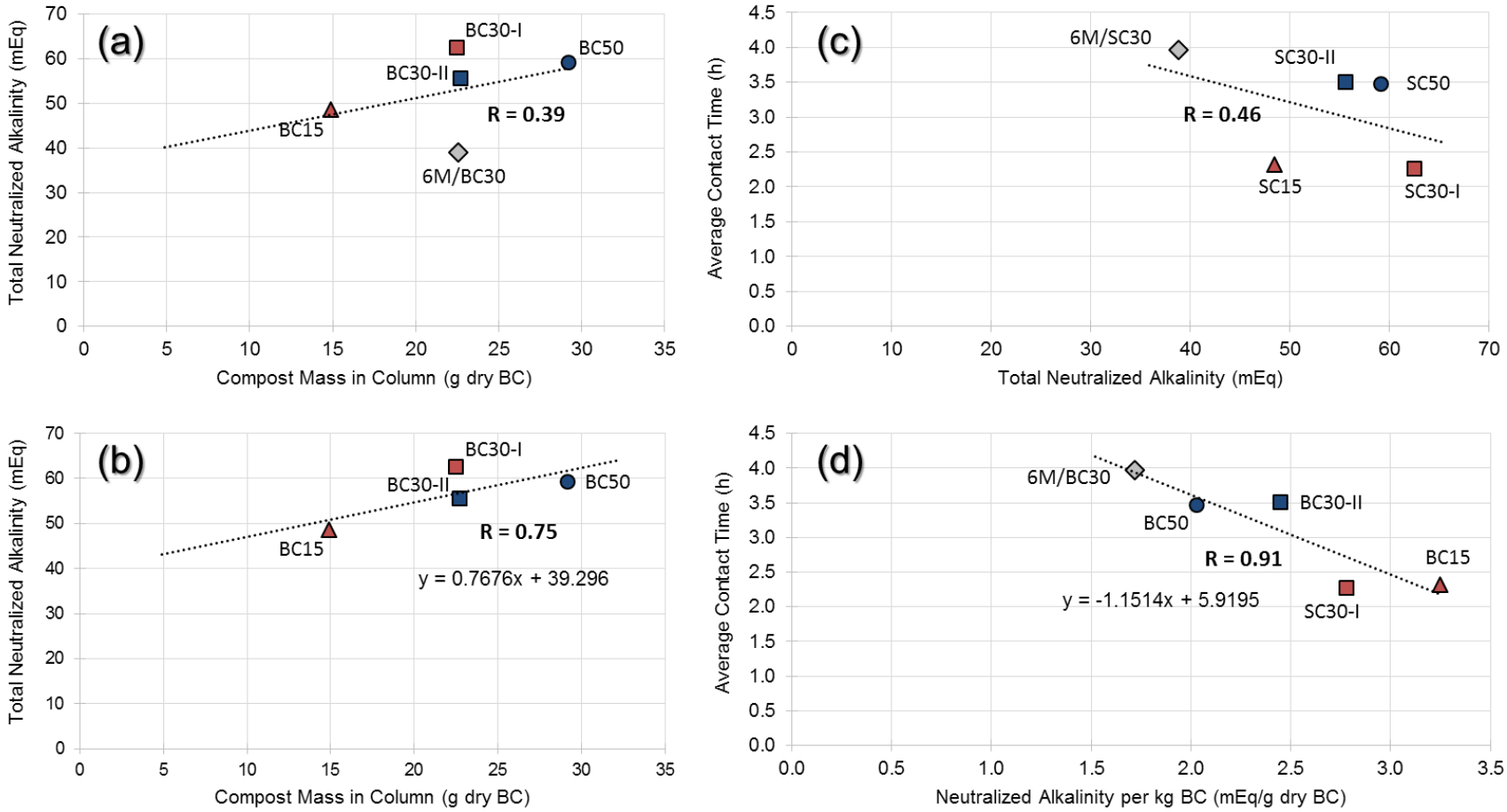

Figure 4.10. Correlations between various parameters calculated for biosolids compost columns.

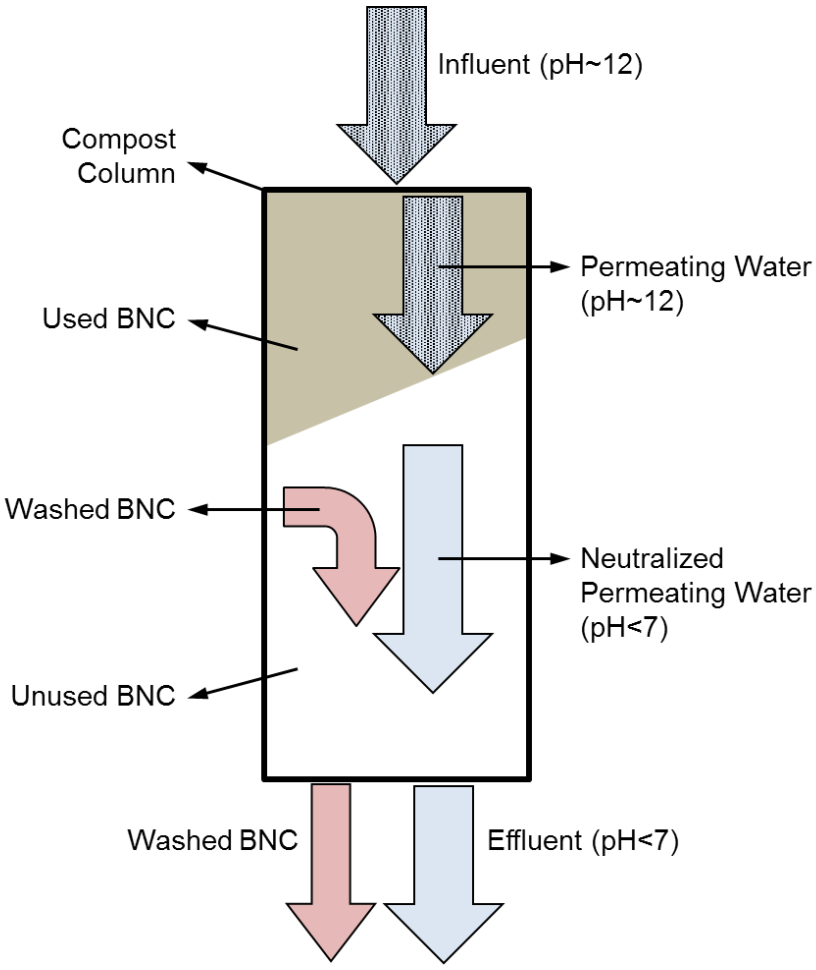

Figure 4.11. Neutralization of influents with high pH inside biosolids compost columns and BNC loss due to water flow.

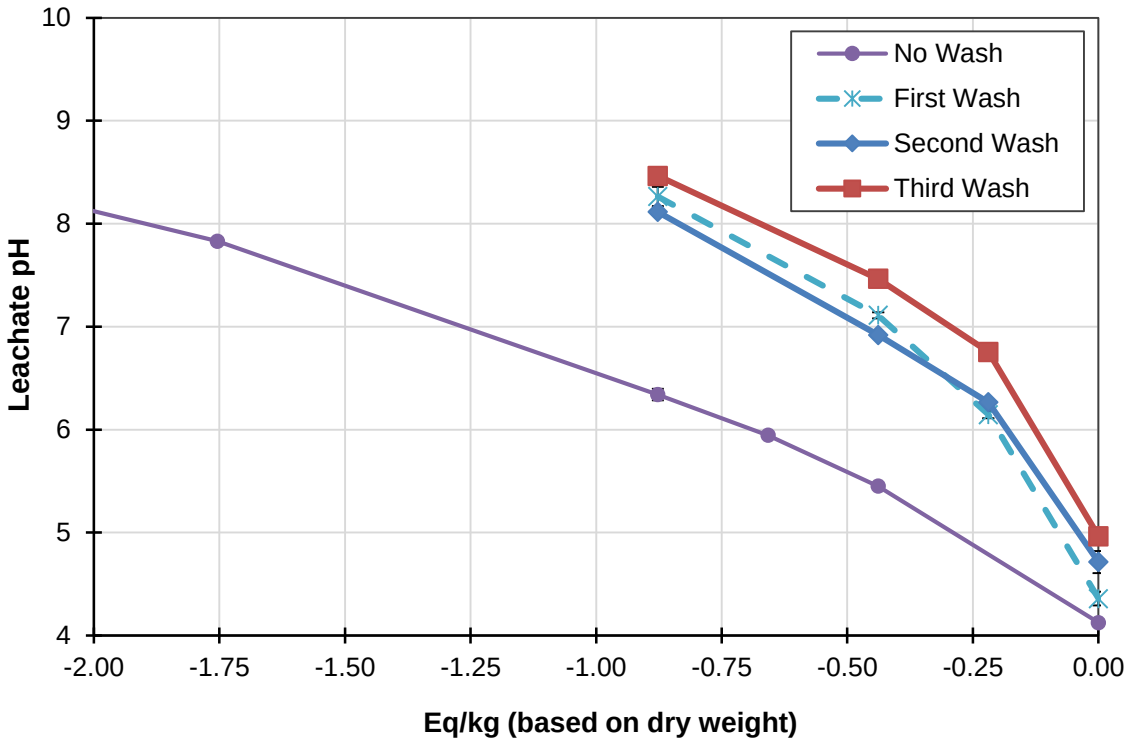

Figure 4.12. Base neutralizing capacities of fresh and washed biosolids composts [1].

[1] **:** Washed biosolids composts were treated with 0.04 M NaCl solution for 18 hours. 0.04 M NaCl was used to simulate the ionic strength of 10WTR leachate.

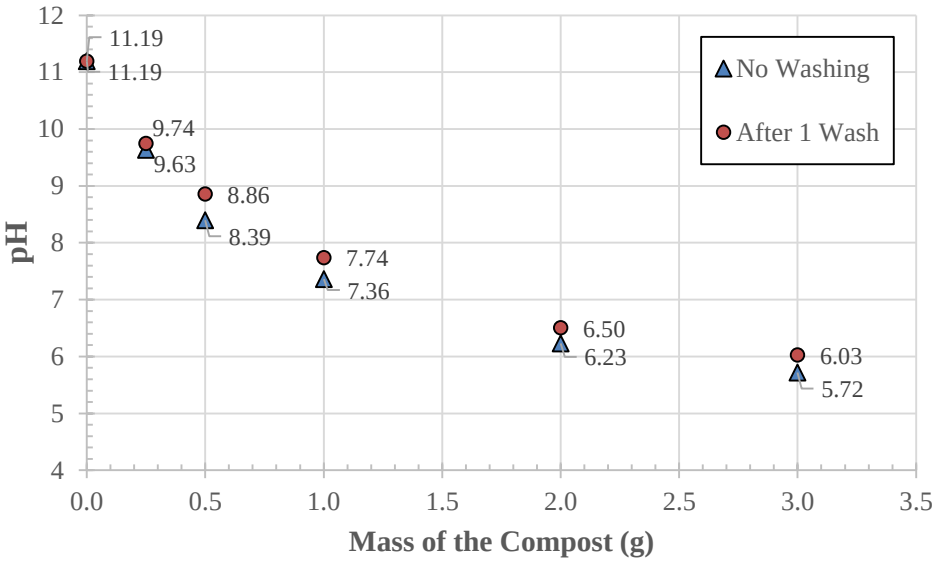

Figure 4.13. The leachate pH values from 18hLTs conducted using 10WTR leachate and different amounts of fresh and washed biosolids compost samples [1].

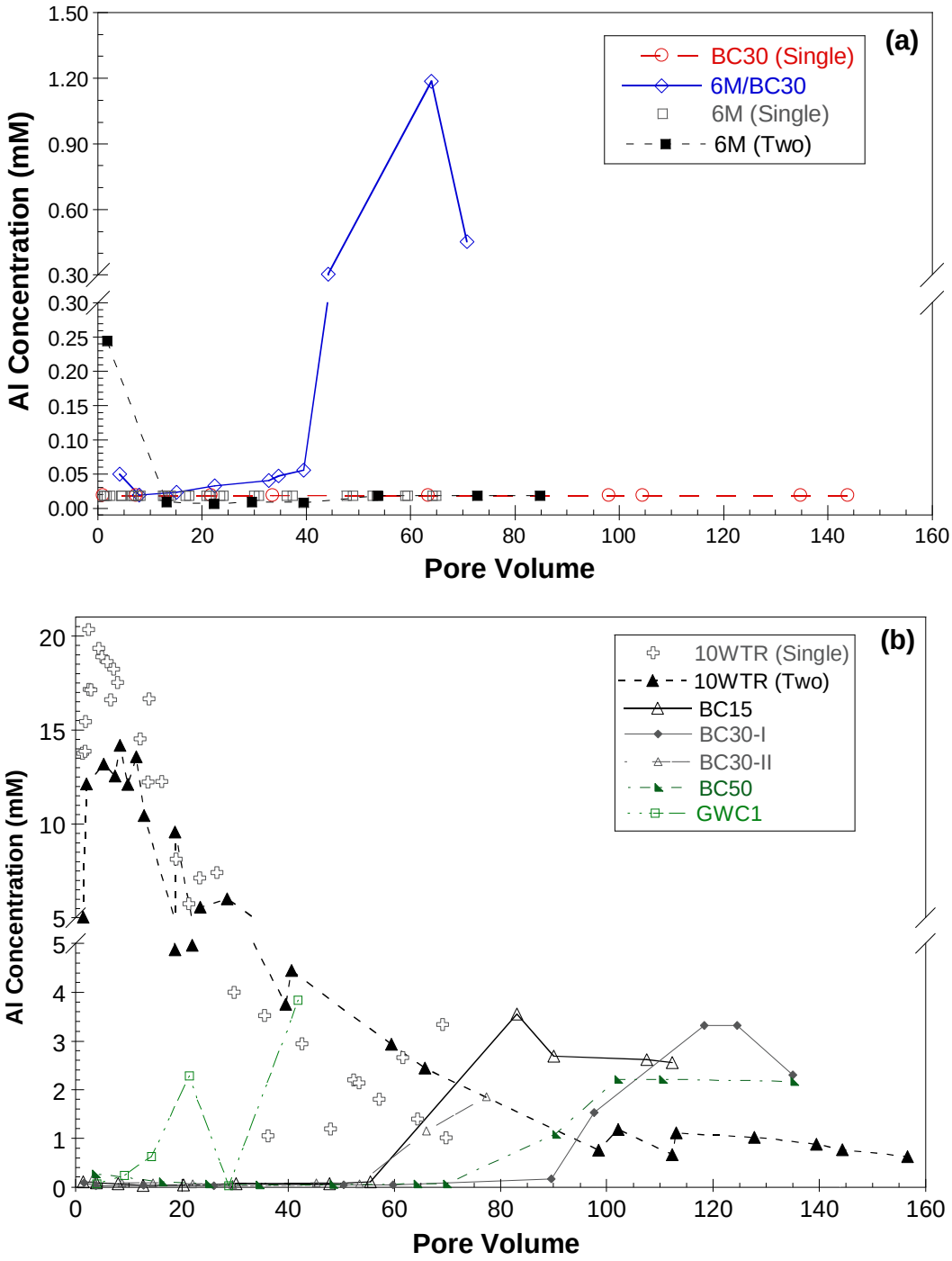

Figure 4.14. Al release from compost columns; **(a)** BC30(Single), 6M/BC30, 6M(single) and 6M(Two); **(b)** 10WTR(Single), 10WTR(Two), BC15, BC30-I, BC30-II, BC50 and GWC1.

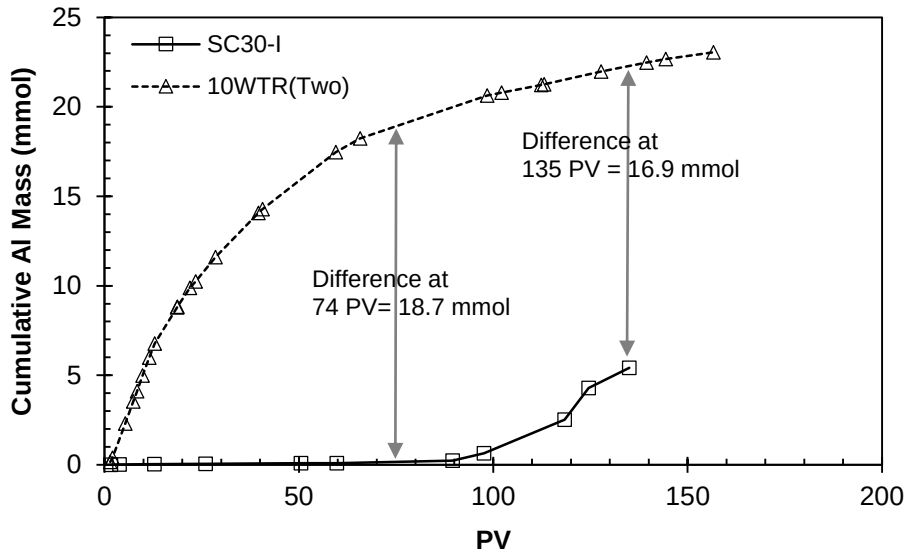

Figure 4.15. The cumulative dissolved Al(+III) mass that was released from 10WTR and BC30-I.

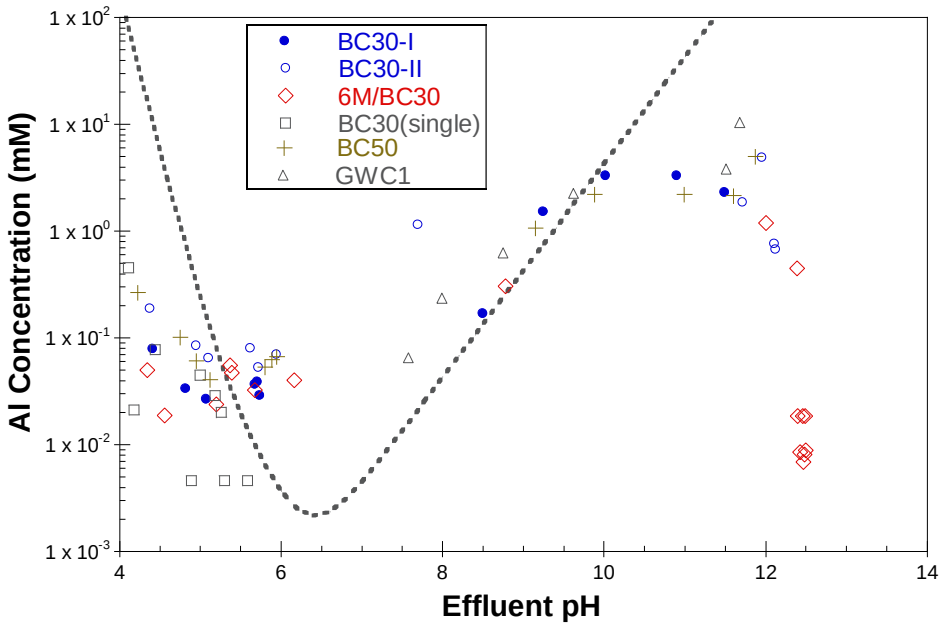

Figure 4.16. Dissolved Al release from compost columns, along with Al(+III) solubility curve for am-$Al(OH)_3$ (I = 0.05 M, 20°C, 1 atm).

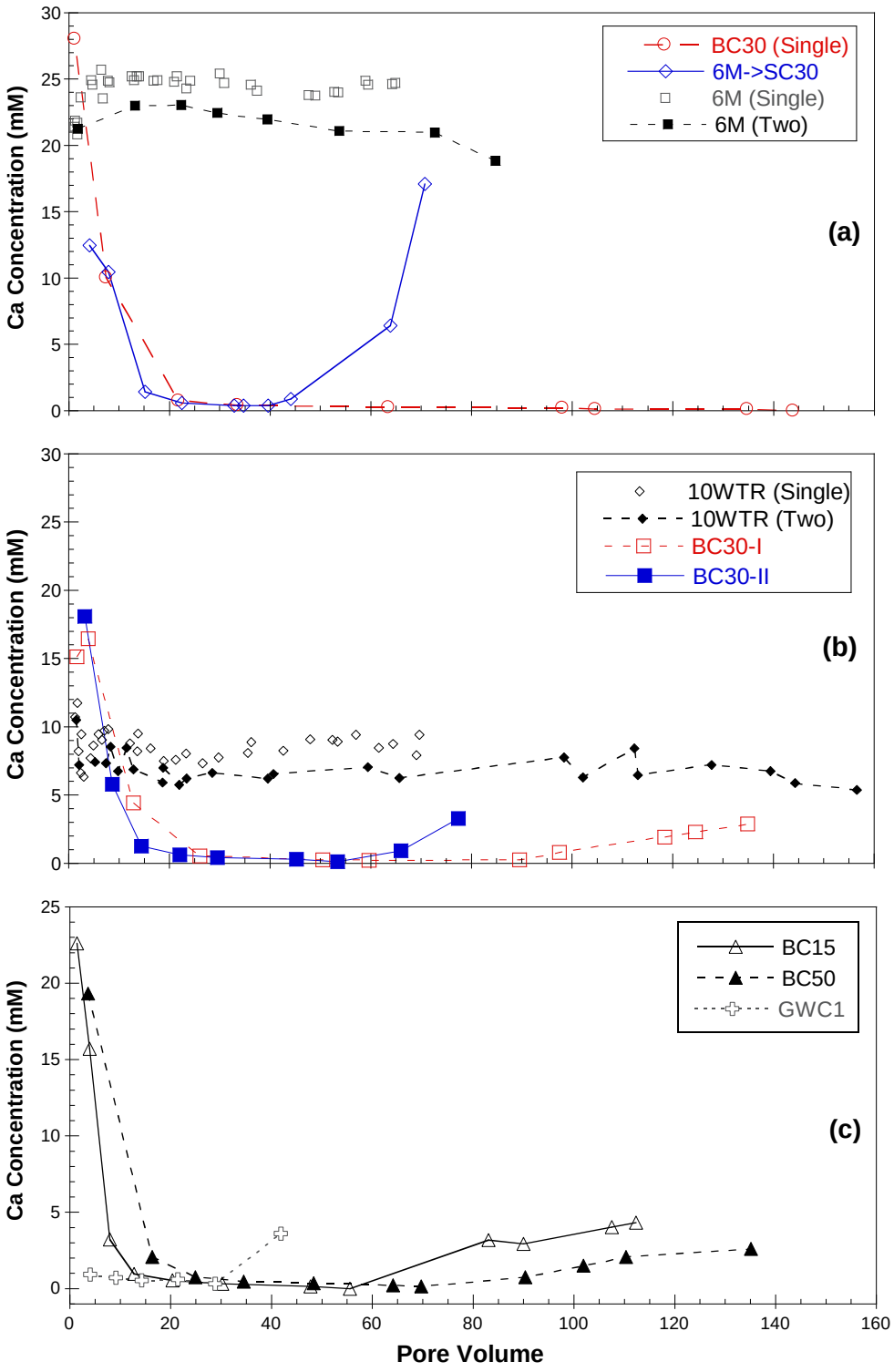

Figure 4.17. Dissolved Ca release from compost columns; **(a)** BC30(Single), 6M/BC30, 6M(single) and 6M(Two); **(b)** 10WTR(Single), 10WTR(Two), BC30-I and BC30-II; **(c)** BC15, BC50 and GWC1.

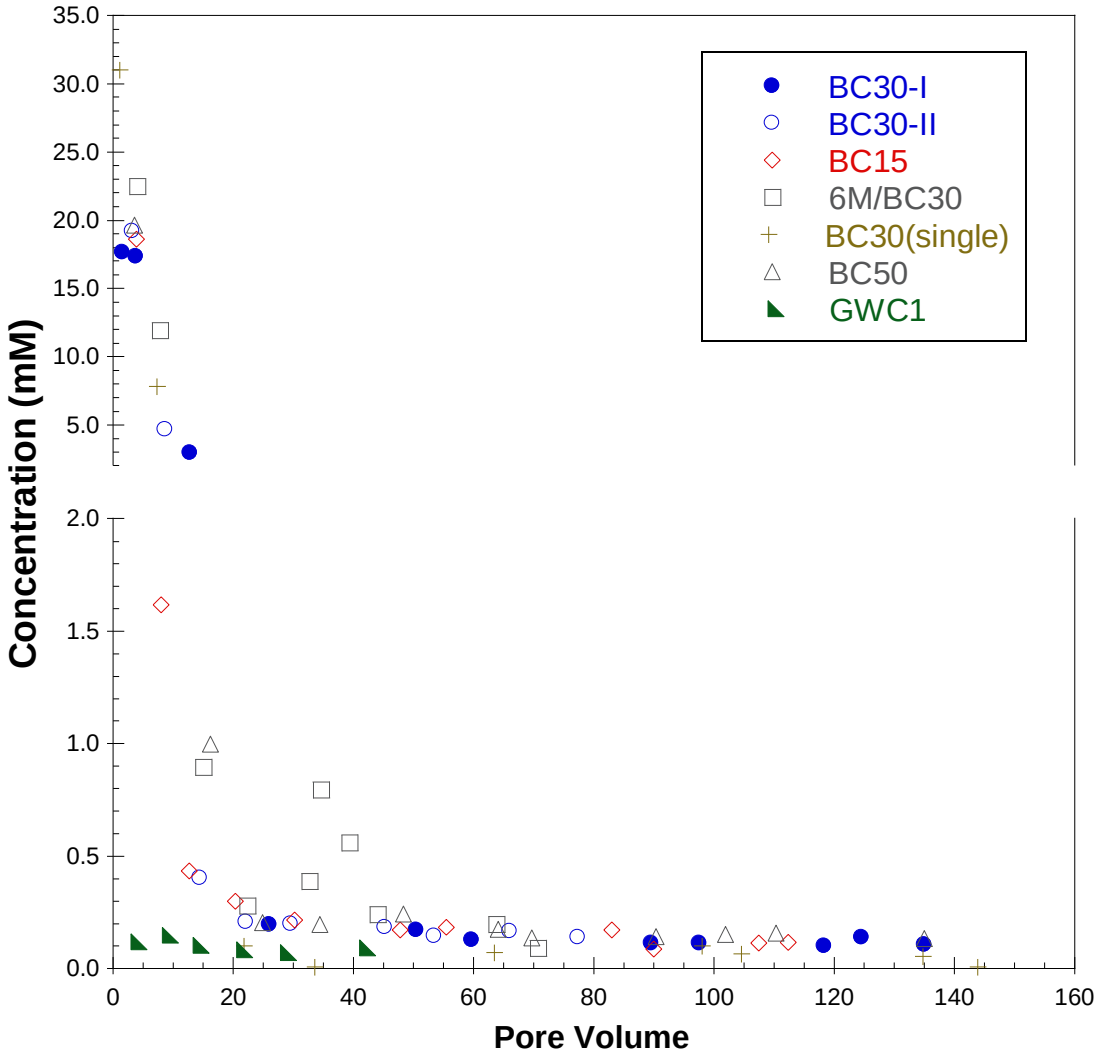

Figure 4.18. Dissolved S release from compost columns.

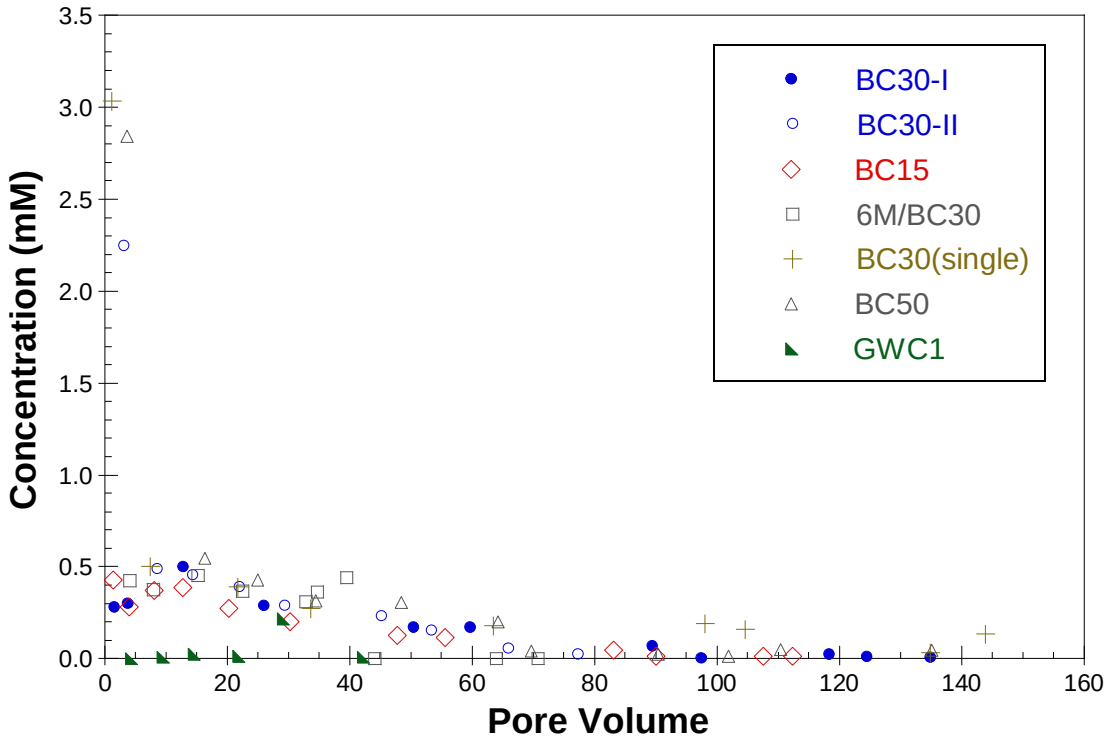

Figure 4.19. Dissolved P release from compost columns.

CHAPTER 5: CONCLUSIONS AND RECOMMENDATIONS

Steel slag is a by-product of the steel-making industry that is produced in increasingly large quantities. However, the high pH levels in seepages of steel slags is a major environmental risk associated to beneficial use of steel slag in large quantities. Steel slag has the capacity to produce highly alkaline leachates (pH>12) over decades mainly due to weathering of its CaO-bearing constituents (Yan et al., 2000; Koryak et al., 2002; Roadcap et al., 2005; Mayes et al., 2006; Riley and Mayes, 2015). Therefore, development of a feasible treatment process that mitigates high alkalinity in the leachates of steel slag is crucial to promote beneficial use of steel slag in road construction.

In the first part of this study, aged basic-oxygen furnace (BOF) steel slag samples were analyzed to characterize their alkalinity producing capacity. Since aging process is imperative to minimize swelling tendency of steel slags and standard practice before utilization in road construction, aged steel slag samples (6 months, 1 year and 2+ years) were used in this study. Leachate alkalinity and Ca(+II) release were determined to be strongly correlated to $Ca(OH)_2$ dissolution for all aged steel slag samples. Furthermore, it was found that prolonged aging periods (1 year and 2+ years) had a small effect on reducing the overall alkalinity producing capacity. Three categories of treatment methods were designed to hinder formation of $Ca(OH)_2$: (1) coating steel slag with bitumen; (2) bathing steel slag in either Fe(+III), Al(+III), or PO_4(-III); and (3) mixing steel slag with an alum-based drinking water treatment residual (WTR). The performance of these methods were evaluated based on reduction in Ca(+II) release, pH, and alkalinity in the leachate of treated slag in batch-type water leach tests; the specifications that yielded the optimum performance levels were determined for each method. 10% (wt./wt.) WTR-addition to steel

slag was determined to be the most successful mitigation method; leachate alkalinity and Ca release were reduced ~70%. Furthermore, the other treatment methods were more complex processes with multiple steps and also more time consuming, whereas WTR addition was simply mixing two solid wastes under dry conditions. One more advantage of WTR addition over others was that its performance appears to be less sensitive to dosage variation.

The second part of the study focused on investigation of the mechanism of alkalinity mitigation effect upon hydration of steel slag in the presence of WTR. Column leach tests were conducted to investigate the mitigation effect under dynamic conditions. Based on the interpretation of calculated saturation indices and the results from SEM and EDX analyses, $Ca(OH)_2$ solubility was found to be not governing Ca^{2+} and OH^- release in WTR-amended slags. Formation of ettringite ($Ca_6Al_2(SO_4)_3(OH)_{12}•26H_2O$) and/or monosulfate ($Ca_6Al_2SO_4(OH)_{12}•6H_2O$) as secondary mineral phases were suggested as the predominant mechanism behind the observed mitigation of alkalinity in steel slag leachates. The results of column leach tests demonstrated that the alkalinity mitigation effect was stable in the long term (70−80 pore volumes) and not significantly affected by changes in particle size and flow rate.

Although WTR addition was found to a reliable mitigation method for the high alkalinity problem in aged steel slag leachates, final effluent pH values were still unacceptably high (>11.5) and the leachates from WTR/6M mixtures were contaminated with high concentrations of dissolved Al(+III). Furthermore, the majority of the alkalinity in the WTR-amended slag leachates was found to originate from $Al(OH)_4^-$ that was acting as a base. High pH levels above 10.5 were found to be required for the alkalinity mitigation

effect to take place in WTR/6M systems. Therefore, residual alkalinity and dissolved Al concentrations in WTR-modified steel slag leachates should be removed without interfering with the high pH levels occurring in the WTR/6M system, in order to maintain alkalinity mitigation effect of WTR addition. It was postulated that a separate treatment process should be employed after the leachate is formed and leaves the WTR/6M system.

The final part of the study tested methods for removing the residual Al(+III) and alkalinity in WTR-amended slag as a separate process. The residual alkalinity in WTR-amended slag leachates was completely eliminated through contact with a biosolids compost with high base neutralization capacity. In an experimental setup where the effluents from a 10% WTR-amended slag column were fed into a second column containing the compost, effluent pH levels below 7 were maintained for 68 pore volumes using ~0.13 kg compost (dry wt.) per 1 kg WTR-amended slag, on average. In addition to removal of alkalinity, the majority of the dissolved Al(+III) and Ca(+II) loads from the 10% WTR-amended slag columns were retained in compost columns until reaching the breakthrough point for the neutralizing capacity of biosolids compost. However, the quality of the leachate at the final stage was impaired by high dissolved P contamination (1−3 mM). The total neutralized amount of alkalinity per kg compost (based on dry wt.) was found to be more strongly correlated to the contact time instead of to the mass of the compost placed inside the columns, suggesting that it is possible to obtain better neutralizing performances at slower pore velocities, which is likely to occur in the field.

This study is the first effort to devise a treatment method to mitigate the alkalinity production capacity of steel slag. Although further investigation is needed, the experimental results demonstrate that complete removal of alkalinity in steel slag leachates

is achievable using only waste by-products. In the author's opinion, the *in situ* mitigation of alkalinity in seepage from steel slag layers is more feasible and appealing compared to the more challenging task of remediation of alkalinity after it is released into the environment and may help to dismiss some of the reluctance for using steel slag among decision-maker circles for future projects. Increasing utilization of steel slag with water treatment residual in road construction will decrease costs and space requirements of landfilling for both of these waste by-products; additionally, decreasing the consumption of natural aggregates will reduce the environmental impact occurred during the excavation of these natural materials. Finally, the treatment methods that were shown to effectively reduce alkalinity in the steel slag leachates (i.e., WTR-modification and/or utilization of BNC in composts) can also be considered to control the seepage from the old steel slag dump sites and from steel slag piles.

5.1. Recommendations for Application

The results of the bench-scale column tests demonstrate that complete *in situ* mitigation of alkalinity in steel slag seepage is possible in a two-step treatment procedure; (1) WTR modification; and (2) contact with biosolids compost. This two-step treatment procedure can be realized in the field in a setup involving construction of a road embankment using WTR-amended aged steel slag and biosolids compost/sandy soil-filled trenches acting as barriers for the leachate from the embankment at each side of the road (Figure 5.1).

Using aged steel slag in road embankment construction is considered to be more suitable compared to using it in construction of other unbound sections of the road (e.g., road base and sub-grade) since in such a configuration the steel slag layer will be at an elevated level that is furthest away from the groundwater table. A drainage system must be installed under

the embankment to ensure that the leachate from the WTR-amended slag embankment is directed to compost barriers at the each side of the road. Direct discharge to surface waters should be avoided especially since the biosolids compost was observed to produce effluents with high concentrations of dissolved P regardless of the influent quality. After the seepage passes through the compost barrier and reaches the boundary between the barrier and surrounding soil, it is believed that the surrounding background soil can cope with the final leachate containing high concentrations of dissolved P and <0.3 mEq/L acidity at pH 4.4−6.1.

Results of the column tests showed partial alkalinity mitigation effect upon WTR addition to aged steel slag was persistent over the long term (157 PV) and that the biosolids compost columns were very effective in maintaining pH levels below 7 and retaining dissolved Ca(+II) and Al(+III) to the point where base neutralization capacity of biosolids-based compost was depleted (68 PV). Based on the combined results of all column tests, mixing ~110 kg WTR per metric ton of steel slag (approximately 21% WTR by volume) is recommended for use in embankment construction. 140 kg biosolids compost (based on dry wt., mixed with 340 kg sandy soil) per metric ton of steel slag is recommended for the barrier construction in order to neutralize alkalinity in the steel slag leachates for 68 PV. Assuming that 1 PV is equivalent of 1 year of leaching in the field (see the discussion in Section 4.4), this configuration should able to maintain leachate pH levels below 7 for 68 years. The design service life for the highways is usually 30 years (Lemer, 1996; Bin-Shafique et al., 2006). The compost/sandy soil mixture placed into the trenches on periphery of the road can be easily replaced with minimum interruption to traffic. If the barrier is frequently maintained replacing the depleted media, the total amount of compost

that has to be used in the barrier for alkalinity mitigation can be reduced. For example, if the compost is replaced every 10 years, the total amount of biosolids compost mass will only be ~20 kg (dry wt.) mixed with 50 kg sand per ton of steel slag used in the embankment. In stormwater management systems, compost is commonly used in bioretention cells. Thus, instead of constructing barriers containing compost, integration of stormwater management system and drainage system of the road can be considered in some locations.

5.2. Recommendations for Future Research

It is important to foster beneficial use of steel slag in construction in order to decrease the amount of landfilled steel slag. Since the turn of the 21st century, steel slag generation significantly increased in parallel to the doubled global annual output of crude steel. Thus, more research on mitigation of alkalinity in steel slag leachates should be conducted to find methods that can minimize associated environmental risks.

The most important parameter for selection of the compost source for this application was considered to be the base neutralizing capacity (BNC) of the compost per unit weight. However, the correlation between BNC of biosolids compost and the number of pore volumes before reaching breakpoint was not well-established. Biosolids compost used in this study had a BNC of 2.0 Eq/kg (18hLT, dry wt.) and the ANC of 10% WTR+90% steel slag mixture was 0.780 Eq/kg (18h+4hLT, dry wt.). On average, 2.6 Eq alkalinity per kg dry compost was neutralized in column tests. It is clear that composts with higher BNC will perform better but a robust method for the selecting most suitable composts and estimating their performance in the field need to be developed. Such investigation should

be expanded to involve testing of different types of composts with high BNC. Biological processes undergoing in the compost may play a role in neutralization of alkaline leachates.

Evidence for significant BNC loss upon submersion of compost was presented, even when the influent was not alkaline. BNC loss due to water flow appeared to be very likely and pore velocity was also an important parameter affecting BNC loss, since the total neutralized amount of alkalinity per kg compost (based on dry wt.) was found to be more strongly correlated to the contact time instead of to the mass of the compost placed inside the columns. The kinetics of BNC loss due to water flow should be defined in order to better establish the correlation between BNC per unit compost mass and neutralization performance.

Particle size may be an important parameter that can affect the porosity of the biosolids compost/sandy soil columns, but only the fraction of biosolids compost below 2.00 mm and sandy soil with a particle size within the range of 0.25 mm−2.00 mm was used in the column leach test study. Porosity, along with influent flow rate, defines the pore velocity of the water flow and the contact time is a function of porosity and pore velocity. The performance of composts with varying particle size ranges can also be investigated.

Significant differences between dissolved Al(+III) and Ca(+II) concentrations in the influents and effluents were evident, but the fates of these cations were not clearly determined. It was proposed that dissolved Al(+III) and Ca(+II) bind to organic matter in the compost and are removed from the solution. However, the total Al(+III) and Ca(+II) in the effluent was not measured, only dissolved. Some Al(+III) and Ca(+II) could be attached to particulate organic matter suspended in the effluent (Besnard et al., 2001; Yin et al.,

2002). Thus, the mass balance should be investigated by measuring the Al(+III) and Ca(+II) accumulated in the column media and dissolved and total concentrations in the leachates. Furthermore, the potential remobilization of Al(+III) and Ca(+II) that was retained on compost should be investigated to determine the appropriate disposal method.

Finally, effects of WTR-modification on trace metal release from steel slag can be investigated. Trace metals, such as Cr and V, can be released in form of oxyanions from steel slags under alkaline conditions (Chaurand et al., 2007; De Windt et al., 2011). Ettringite formation was reported to be effective in immobilization of trace metals such as Cr, As and Se in oxyanion form in the alkaline pH range (Chrysochoou and Dermatas, 2006). During ettringite precipitation, Cr(+VI) can be removed from aqueous solution by substitution of CrO_4^{2-} in place of SO_4^{2-} in the crystal structure (Perkins and Palmer, 2000). Therefore, WTR-modification may reduce trace metal release.

FIGURES

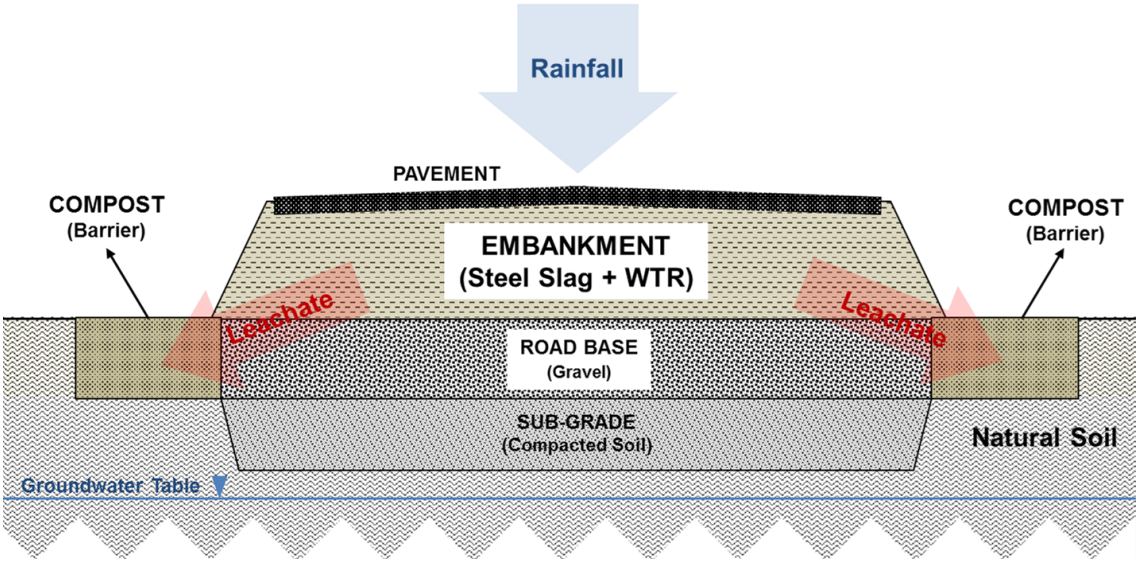

Figure 5.1. The cross-section of a typical roadway in Maryland and the conceptual design for the configuration of alkalinity mitigation system.

REFERENCES

AASHTO (2000). M 145. "Standard Specification for Classification of Soils and Soil-Aggregate Mixtures for Highway Construction Purposes", American Association of State Highway and Transportation Officials (AASHTO), Washington, DC.

AASHTO (2010). M 320. "Standard Specification for Performance-Graded Asphalt Binder", American Association of State Highway and Transportation Officials (AASHTO), Washington, DC.

Ahmedzade, P., and Sengoz, B. (2009). "Evaluation of steel slag coarse aggregate in hot mix asphalt concrete." *Journal of Hazardous Materials*, 165(1–3), 300-305.

Alizadeh, R., Chini, M., Ghods, P., Hoseini, M., Montazer, S., and Shekarchi, M. "Utilization of Electric Arc Furnace Slag as Aggregates in Concrete − Environmental Issue." *6th CANMET/ACI International Conference on Recent Advances in Concrete Technology*, Bucharest, Romania, June 2003, 451-464.

ALS (2006). ALS Code ME-XRF06, "ME-XRF06 Whole Rock XRF Method", ALS USA Inc., Reno, NV, September 14, 2006.

Andreas, L., Diener, S., and Lagerkvist, A. (2014). "Steel slags in a landfill top cover – Experiences from a full-scale experiment." *Waste Management*, 34(3), 692-701.

APHA (2005). *Standard Methods for the Examination of Water and Wastewater*, American Public Health Association (APHA), American Water Works Association (AWWA) and Water Environment Federation (WEF), Washington, D.C.

Arabani, M., and Azarhoosh, A.R. (2012). "The effect of recycled concrete aggregate and steel slag on the dynamic properties of asphalt mixtures." *Construction and Building Materials*, 35, 1-7.

ASTM (2006a). D3987-12. "Standard Practice for Shake Extraction of Solid Waste with Water", ASTM International, West Conshohocken, PA, October 2006, DOI: 10.1520/D3987-06.

ASTM (2006b). D4874-95. "Standard Test Method for Leaching Solid Material in a Column Apparatus", ASTM International, West Conshohocken, PA, May 2006, DOI: 10.1520/D4874-95R06.

ASTM (2007). E70-07. "Standard Test Method for pH of Aqueous Solutions with the Glass Electrode", ASTM International, West Conshohocken, PA, May, 2007, DOI: 10.1520/E0070-07.

ASTM (2008). D7348-08e1. "Standard Test Methods for Loss on Ignition (LOI) of Solid Combustion Residues", ASTM International, West Conshohocken, PA, October, 2008, DOI: 10.1520/D7348-08.

ASTM (2009). D2940/D2940M-09. "Standard Specification for Graded Aggregate Material For Bases or Subbases for Highways or Airports", ASTM International, West Conshohocken, PA, August 2009, DOI: 10.1520/D2940_D2940M-09.

ASTM (2010a). D859. "Standard test method for silica in water", ASTM International, West Conshohocken, PA.

ASTM (2010b). D854-10. "Standard Test Methods for Specific Gravity of Soil Solids by Water Pycnometer", ASTM International, West Conshohocken, PA, March, 2010, DOI: 10.1520/D0854-10.

ASTM (2011). D1067−11. "Standard Test Methods for Acidity or Alkalinity of Water", ASTM International, West Conshohocken, PA, April, 2011, DOI: 10.1520/D1067-11.

ASTM (2012). D698-12. "Standard Test Methods for Laboratory Compaction Characteristics of Soil Using Standard Effort (12 400 ft-lbf/ft^3(600 kN-m/m^3))", ASTM International, West Conshohocken, PA, June, 2012, DOI: 10.1520/D0698-12.

Baciocchi, R., Costa, G., Polettini, A., and Pomi, R. (2009). "Influence of particle size on the carbonation of stainless steel slag for CO2 storage." *Energy Procedia*, 1(1), 4859-4866.

Barbarulo, R., Peycelon, H., and Leclercq, S. (2007). "Chemical equilibria between C–S–H and ettringite, at 20 and 85 °C." *Cement and Concrete Research*, 37(8), 1176-1181.

Barca, C., Gérente, C., Meyer, D., Chazarenc, F., and Andrès, Y. (2012a). "Phosphate removal from synthetic and real wastewater using steel slags produced in Europe." *Water Research*, 46(7), 2376-2384.

Barca, C., Troesch, S., Meyer, D., Drissen, P., Andrès, Y., and Chazarenc, F. (2012b). "Steel Slag Filters to Upgrade Phosphorus Removal in Constructed Wetlands: Two Years of Field Experiments." *Environmental Science & Technology*, 47(1), 549-556.

Barra, M., Ramonich, E.V., and Munoz, M.A. "Stabilization of soils with steel slag and cement for application in rural and low traffic roads." *Proceedings of the Beneficial Use of Recycled Materials in Transportation Application*, RMCR University of Durham, November 13-15, 423-432.

Baur, I., Keller, P., Mavrocordatos, D., Wehrli, B., and Johnson, C.A. (2004). "Dissolution-precipitation behaviour of ettringite, monosulfate, and calcium silicate hydrate." *Cement and Concrete Research*, 34(2), 341-348.

Beesley, L. (2012). "Carbon storage and fluxes in existing and newly created urban soils." *Journal of Environmental Management*, 104, 158-165.

Behnood, A., and Ameri, M. (2012). "Experimental investigation of stone matrix asphalt mixtures containing steel slag." *Scientia Iranica*, 19(5), 1214-1219.

Belhadj, E., Diliberto, C., and Lecomte, A. (2014). "Properties of hydraulic paste of basic oxygen furnace slag." *Cement and Concrete Composites*, 45, 15-21.

Besnard, E., Chenu, C., and Robert, M. (2001). "Influence of organic amendments on copper distribution among particle-size and density fractions in Champagne vineyard soils." *Environmental Pollution*, 112(3), 329-337.

Bin-Shafique, S., Benson, C.H., Edil, T.B., and Hwang, K. (2006). "Leachate Concentrations from Water Leach and Column Leach Tests on Fly Ash-Stabilized Soils." *Environmental Engineering Science*, 23(1), 53-67.

Boesch, D.F., Brinsfield, R.B., and Magnien, R.E. (2001). "Chesapeake Bay Eutrophication." *Journal of Environmental Quality*, 30(2), 303-320.

Bowden, L.I., Jarvis, A.P., Younger, P.L., and Johnson, K.L. (2009). "Phosphorus Removal from Waste Waters Using Basic Oxygen Steel Slag." *Environmental Science & Technology*, 43(7), 2476-2481.

Cetin, B., Aydilek, A.H., and Li, L. (2012). "Experimental and numerical analysis of metal leaching from fly ash-amended highway bases." *Waste Management*, 32(5), 965-978.

Chang, E.E., Chiu, A.-C., Pan, S.-Y., Chen, Y.-H., Tan, C.-S., and Chiang, P.-C. (2013). "Carbonation of basic oxygen furnace slag with metalworking wastewater in a slurry reactor." *International Journal of Greenhouse Gas Control*, 12, 382-389.

Chang, Y.-Y., Song, K.-H., and Yang, J.-K. (2008). "Removal of As(III) in a column reactor packed with iron-coated sand and manganese-coated sand." *Journal of Hazardous Materials*, 150(3), 565-572.

Chaurand, P., Rose, J., Briois, V., Olivi, L., Hazemann, J.-L., Proux, O., Domas, J., and Bottero, J.-Y. (2007). "Environmental impacts of steel slag reused in road construction: A crystallographic and molecular (XANES) approach." *Journal of Hazardous Materials*, 139(3), 537-542.

Chrysochoou, M., and Dermatas, D. (2006). "Evaluation of ettringite and hydrocalumite formation for heavy metal immobilization: Literature review and experimental study." *Journal of Hazardous Materials*, 136(1), 20-33.

Claveau-Mallet, D., Wallace, S., and Comeau, Y. (2013). "Removal of phosphorus, fluoride and metals from a gypsum mining leachate using steel slag filters." *Water Research*, 47(4), 1512-1520.

COMAR (COMAR 26.08.02.033 A(4)). COMAR 26.08.02.033 A(4). "Water Quality Criteria Specific to Designated Uses", the Code of Maryland Regulations (COMAR), Division of State Documents. <http://www.dsd.state.md.us/comar/getfile.aspx?file=26.08.02.03-3.htm>

Damidot, D., and Glasser, F.P. (1993). "Thermodynamic investigation of the CaO.Al2O3.CaSO4.H2O system at 25°C and the influence of Na2O." *Cement and Concrete Research*, 23(1), 221-238.

Dayioglu, A.Y., Aydilek, A.H., and Cetin, B. (2014). "Preventing Swelling and Decreasing Alkalinity of Steel Slags Used in Highway Infrastructures." *Transportation Research Record*, 2401, 52-57.

De Windt, L., Chaurand, P., and Rose, J. (2011). "Kinetics of steel slag leaching: Batch tests and modeling." *Waste Management*, 31(2), 225-235.

Diener, S., Andreas, L., Herrmann, I., Ecke, H., and Lagerkvist, A. (2010). "Accelerated carbonation of steel slags in a landfill cover construction." *Waste Management*, 30(1), 132-139.

Ding, C., Yang, X., Liu, W., Chang, Y., and Shang, C. (2010). "Removal of natural organic matter using surfactant-modified iron oxide-coated sand." *Journal of Hazardous Materials*, 174(1–3), 567-572.

Drizo, A., Comeau, Y., Forget, C., and Chapuis, R.P. (2002). "Phosphorus Saturation Potential: A Parameter for Estimating the Longevity of Constructed Wetland Systems." *Environmental Science & Technology*, 36(21), 4642-4648.

Drizo, A., Forget, C., Chapuis, R.P., and Comeau, Y. (2006). "Phosphorus removal by electric arc furnace steel slag and serpentinite." *Water Research*, 40(8), 1547-1554.

Duchesne, J., and Reardon, E.J. (1995). "Measurement and prediction of portlandite solubility in alkali solutions." *Cement and Concrete Research*, 25(5), 1043-1053.

Edil, T.B. (2006). "Green Highways: Strategy for Recycling Materials for Sustainable Construction Practices". *Seventh International Congress on Advances in Civil Engineering*, Istanbul, Turkey, October 11-13, 2006, Yildiz Technical University.

Emery, J. (1984). "Steel Slag Utilization in Asphalt Mixes." MF 186-1, National Slag Association, Pleasant Grove, UT.

Fällman, A.M. (2000). "Leaching of chromium and barium from steel slag in laboratory and field tests − a solubility controlled process?" *Waste Management*, 20(2–3), 149-154.

Frank, A., Madej, A., Galgan, V., and Petersson, L.R. (1996). "Vanadium poisoning of cattle with basic slag. Concentrations in tissues from poisoned animals and from a reference, slaughter-house material." *Science of The Total Environment*, 181(1), 73-92.

Fruehan, R.J. (1998). *The Making, Shaping and Treating of Steel*, The AISE Steel Foundation, Pittsburgh, PA.

Gabrisová, A., Havlica, J., and Sahu, S. (1991). "Stability of calcium sulphoaluminate hydrates in water solutions with various pH values." *Cement and Concrete Research*, 21(6), 1023-1027.

GHP (2010). "Recycle and Beneficial Reuse Group". The Green Highways Partnership (GHP). <http://www.greenhighwayspartnership.org/index.php?option=com_content&view=article&id=23&Itemid=22> (November 2, 2015).

Glanville, T.D., Richard, T.L., and Persyn, R.A. (2003). "Impacts of Compost Blankets on Erosion Control, Revegetation, and Water Quality at Highway Construction Sites in Iowa." Agricultural and Biosystems Engineering Technical Reports and White Papers, Paper 2, Agricultural and Biosystems Engineering Department, Iowa State University of Science and Technology, Ames, Iowa.

Gleason, D.J. (2013). "Field-scale optimization and evaluation of a recycled materials based stormwater treatment technique." Master of Science, University of Maryland, College Park, MD.

Grubb, D., Wazne, M., Jagupilla, S., and Malasavage, N. (2011). "Beneficial Use of Steel Slag Fines to Immobilize Arsenite and Arsenate: Slag Characterization and Metal Thresholding Studies." *Journal of Hazardous, Toxic, and Radioactive Waste*, 15(3), 130-150.

Gustafsson, J.P. (2012). "Visual MINTEQ v3.0." Royal Institute of Technology, Stockholm, Sweden.

Gustafsson, J.P. (2015). "Visual MINTEQ v3.1." Royal Institute of Technology, Stockholm, Sweden.

Hagvall, K., Persson, P., and Karlsson, T. (2015). "Speciation of aluminum in soils and stream waters: The importance of organic matter." *Chemical Geology*, 417, 32-43.

Hampsoim, C.J., and Bailey, J.E. (1982). "On the structure of some precipitated calcium alumino-sulphate hydrates." *Journal of Materials Science*, 17(11), 3341-3346.

Hendricks, D. (2010). *Fundamentals of Water Treatment Unit Processes: Physical, Chemical, and Biological*, CRC Press, Boca Raton, FL.

Huang, P.M., Li, Y., and Sumner, M.E. (2011). *Handbook of Soil Sciences: Properties and Processes, Second Edition*, Taylor & Francis Group, Boca Raton, FL, USA.

Hue, N.V., Craddock, G.R., and Adams, F. (1986). "Effect of Organic Acids on Aluminum Toxicity in Subsoils." *Soil Science Society of America Journal*, 50(1), 28-34.

Huijgen, W.J.J., and Comans, R.N.J. (2006). "Carbonation of Steel Slag for CO2 Sequestration: Leaching of Products and Reaction Mechanisms." *Environmental Science & Technology*, 40(8), 2790-2796.

Hunter, J.G., Kang, D.H., and Bundy, M. (2014). "Identification of Techniques to Meet pH Standard During In-Stream Construction." Research Report, Office of Policy and Research, Maryland State Highway Administration and National Transportation Center, Morgan State University, Project Number SP109B4D, Baltimore, MD, March 2014.

Hussain, S.I., Blowes, D.W., Ptacek, C.J., and Olding, D. (2014). "Phosphorus Removal from Lake Water Using Basic Oxygen Furnace Slag: System Performance and Characterization of Reaction Products." *Environmental Engineering Science*, 31(11), 631-642.

Inc., A.U. (ALS Code ME-XRF06). ALS Code ME-XRF06. "ME-XRF06 Whole Rock XRF Method", ALS USA Inc., Reno, NV, September 14, 2006.

Iqbal, H., Garcia-Perez, M., and Flury, M. (2015). "Effect of biochar on leaching of organic carbon, nitrogen, and phosphorus from compost in bioretention systems." *Science of The Total Environment*, 521–522, 37-45.

Jagupilla, S.C., Grubb, D.G., and Wazne, M. (2012). "Immobilization of Sb(III) and Sb(V) Using Steel Slag Fines." *GeoCongress 2012*, American Society of Civil Engineers, 3988-3994.

Juckes, L.M. (2003). "The volume stability of modern steelmaking slags." *Mineral Processing and Extractive Metallurgy*, 112(3), 177-197.

Kaufman, H.W., and Kleinberg, I. (1979). "Studies on the incongruent solubility of hydroxyapatite." *Calcified Tissue International*, 27(1), 143-151.

Kerndorff, H., and Schnitzer, M. (1980). "Sorption of metals on humic acid." *Geochimica et Cosmochimica Acta*, 44(11), 1701-1708.

Kim, H. (2010). "Use of inorganic by-product amended compost/manure to sequester metals and phosphorus from diffuse source pollution." Doctor of Philosophy, University of Maryland, College Park, MD.

King, K.W., and Torbert, H.A. (2007). "Nitrate and ammonium losses from surface-applied organic and inorganic fertilizers." *The Journal of Agricultural Science*, 145(04), 385-393.

Koryak, M., Stafford, L.J., Reilly, R.J., and Magnuson, M.P. (2002). "Impacts of Steel Mill Slag Leachate on the Water Quality of a Small Pennsylvania Stream." *Journal of Freshwater Ecology*, 17(3), 461-465.

Kourounis, S., Tsivilis, S., Tsakiridis, P.E., Papadimitriou, G.D., and Tsibouki, Z. (2007). "Properties and hydration of blended cements with steelmaking slag." *Cement and Concrete Research*, 37(6), 815-822.

Kuan, W.-H., Lo, S.-L., Wang, M.K., and Lin, C.-F. (1998). "Removal of Se(IV) and Se(VI) from water by aluminum-oxide-coated sand." *Water Research*, 32(3), 915-923.

KYTC (2012). "Standard Specifications, 400 Asphalt Pavements 12", Section 412 - Stone-Matrix Asphalt (SMA), Kentucky Transportation Cabinet, Kentucky. <http://transportation.ky.gov/construction/pages/kentucky-standard-specifications.aspx>

Lai, C.H., Lo, S.L., and Chiang, H.L. (2000). "Adsorption/desorption properties of copper ions on the surface of iron-coated sand using BET and EDAX analyses." *Chemosphere*, 41(8), 1249-1255.

Lemer, A. (1996). "Infrastructure Obsolescence and Design Service Life." *Journal of Infrastructure Systems*, 2(4), 153-161.

Lewis, D.W. (1992). "Properties and uses of iron and steel slags." *Symposium on Slag National Institute for Transport and Road Research* MF 182-6, National Slag Association, February, 1982. <http://www.nationalslag.org/archive/legacy/nsa_182-6_properties_and_uses_slag.pdf>

Lo, S.-L., Jeng, H.-T., and Lai, C.-H. (1997). "Characteristics and adsorption properties of iron-coated sand." *Water Science and Technology*, 35(7), 63-70.

Lombi, E., Stevens, D.P., and McLaughlin, M.J. (2010). "Effect of water treatment residuals on soil phosphorus, copper and aluminium availability and toxicity." *Environmental Pollution*, 158(6), 2110-2116.

Lothenbach, B., Pelletier-Chaignat, L., and Winnefeld, F. (2012). "Stability in the system CaO–Al2O3–H2O." *Cement and Concrete Research*, 42(12), 1621-1634.

Madrid, L. (1999). "Metal retention and mobility as influenced by some organic residues added to soils: a case study." *Fate and Transport of Heavy Metals in the Vadose Zone*, Selim, H.M., and Iskandar, I.K., eds., Lewis Publishers, Boca Raton, FL, 201–223.

Mäkelä, M., Watkins, G., Pöykiö, R., Nurmesniemi, H., and Dahl, O. (2012). "Utilization of steel, pulp and paper industry solid residues in forest soil amendment: Relevant physicochemical properties and heavy metal availability." *Journal of Hazardous Materials*, 207–208, 21-27.

Manser, A.G.R., and Keeling, A. (1996). *Practical Handbook of Processing and Recycling Municipal Waste*, CRC Press, Boca Raton, FL.

Mayes, W.M., Younger, P.L., and Aumônier, J. (2006). "Buffering of Alkaline Steel Slag Leachate across a Natural Wetland." *Environmental Science & Technology*, 40(4), 1237-1243.

Mayes, W.M., Younger, P.L., and Aumônier, J. (2008). "Hydrogeochemistry of Alkaline Steel Slag Leachates in the UK." *Water, Air, and Soil Pollution*, 195(1-4), 35-50.

Miraoui, M., Zentar, R., and Abriak, N.-E. (2012). "Road material basis in dredged sediment and basic oxygen furnace steel slag." *Construction and Building Materials*, 30, 309-319.

Morar, D., Aydilek, A., Seagren, E., and Demirkan, M. (2012). "Leaching of Metals from Fly Ash–Amended Permeable Reactive Barriers." *Journal of Environmental Engineering*, 138(8), 815-825.

Möschner, G., Lothenbach, B., Rose, J., Ulrich, A., Figi, R., and Kretzschmar, R. (2008). "Solubility of Fe–ettringite ($Ca_6[Fe(OH)_6]_2(SO_4)_3.26H_2O$)." *Geochimica et Cosmochimica Acta*, 72(1), 1-18.

Möschner, G., Lothenbach, B., Winnefeld, F., Ulrich, A., Figi, R., and Kretzschmar, R. (2009). "Solid solution between Al-ettringite and Fe-ettringite ($Ca_6[Al_x,Fe_x(OH)_6]_2(SO_4)_3\cdot 26H_2O$)." *Cement and Concrete Research*, 39(6), 482-489.

Motz, H., and Geiseler, J. (2001). "Products of steel slags an opportunity to save natural resources." *Waste Management*, 21(3), 285-293.

Myers, R.J., L'Hôpital, E., Provis, J.L., and Lothenbach, B. (2015). "Effect of temperature and aluminium on calcium (alumino)silicate hydrate chemistry under equilibrium conditions." *Cement and Concrete Research*, 68, 83-93.

Myneni, S.C.B., Traina, S.J., and Logan, T.J. (1998). "Ettringite solubility and geochemistry of the Ca(OH)2–Al2(SO4)3–H2O system at 1 atm pressure and 298 K." *Chemical Geology*, 148(1–2), 1-19.

Navarro, C., Díaz, M., and Villa-García, M.A. (2010). "Physico-Chemical Characterization of Steel Slag. Study of its Behavior under Simulated Environmental Conditions." *Environmental Science & Technology*, 44(14), 5383-5388.

O'Neill, S., and Davis, A. (2012). "Water Treatment Residual as a Bioretention Amendment for Phosphorus. II: Long-Term Column Studies." *Journal of Environmental Engineering*, 138(3), 328-336.

ODOT (2013). "Construction and Material Specifications, 700 Material Details", 703.01.E, Ohio Department of Transportation, Columbus, Ohio. <http://www.dot.state.oh.us/Divisions/ConstructionMgt/OnlineDocs/Pages/default.aspx>

Ortiz, N., Pires, M.A.F., and Bressiani, J.C. (2001). "Use of steel converter slag as nickel adsorber to wastewater treatment." *Waste Management*, 21(7), 631-635.

Özkök, E., Davis, A.P., and Aydilek, A.H. (2013). "Leaching of As, Cr, and Cu from High-Carbon Fly Ash-Soil Mixtures." *Journal of Environmental Engineering*, 139(11), 1397-1408.

Pa Ho, H. (1975). "Precipitation of phosphate from solution using aluminum salt." *Water Research*, 9(12), 1155-1161.

Pasetto, M., and Baldo, N. (2011). "Mix design and performance analysis of asphalt concretes with electric arc furnace slag." *Construction and Building Materials*, 25(8), 3458-3468.

Perkins, R.B., and Palmer, C.D. (2000). "Solubility of Ca6[Al(OH)6]2(CrO4)3·26H2O, the chromate analog of ettringite; 5–75°C." *Applied Geochemistry*, 15(8), 1203-1218.

Piatak, N.M., Parsons, M.B., and Seal Ii, R.R. (2015). "Characteristics and environmental aspects of slag: A review." *Applied Geochemistry*, 57, 236-266.

Poh, H., Ghataora, G., and Ghazireh, N. (2006). "Soil Stabilization Using Basic Oxygen Steel Slag Fines." *Journal of Materials in Civil Engineering*, 18(2), 229-240.

Pote, P.H., and Daniel, T.C. (2009). "Dissolved Phosphorus in Water Samples." *Methods of Phosphorus Analysis for Soils, Sediments, Residuals, and Waters*, Kovar, J.L., and Pierzynski, G.M., eds., Virginia Tech University, 110-112.

Pratt, C., Shilton, A., Pratt, S., Haverkamp, R.G., and Bolan, N.S. (2007). "Phosphorus Removal Mechanisms in Active Slag Filters Treating Waste Stabilization Pond Effluent." *Environmental Science & Technology*, 41(9), 3296-3301.

Proctor, D.M., Fehling, K.A., Shay, E.C., Wittenborn, J.L., Green, J.J., Avent, C., Bigham, R.D., Connolly, M., Lee, B., Shepker, T.O., and Zak, M.A. (2000). "Physical and Chemical Characteristics of Blast Furnace, Basic Oxygen Furnace, and Electric Arc Furnace Steel Industry Slags." *Environmental Science & Technology*, 34(8), 1576-1582.

Ram, L., Srivastava, N., Tripathi, R., Thakur, S., Sinha, A., Jha, S., Masto, R., and Mitra, S. (2007). "Leaching behavior of lignite fly ash with shake and column tests." *Environmental Geology*, 51(7), 1119-1132.

Riley, A.L., and Mayes, W.M. (2015). "Long-term evolution of highly alkaline steel slag drainage waters." *Environmental Monitoring and Assessment*, 187(7), 463.

Roadcap, G.S., Kelly, W.R., and Bethke, C.M. (2005). "Geochemistry of Extremely Alkaline (pH > 12) Ground Water in Slag-Fill Aquifers." *Ground Water*, 43(6), 806-816.

Said, A., Mattila, H.-P., Järvinen, M., and Zevenhoven, R. (2013). "Production of precipitated calcium carbonate (PCC) from steelmaking slag for fixation of CO2." *Applied Energy*, 112, 765–771.

SCDOT (2007). "Standard Specifications for Highway Construction", 401.2.2.4 Coarse Aggregate, The South Carolina Department of Transportation, Columbia, South Carolina. <http://www.scdot.org/doing/construction_StandardSpec.aspx>

Shen, W., Zhou, M., Ma, W., Hu, J., and Cai, Z. (2009). "Investigation on the application of steel slag–fly ash–phosphogypsum solidified material as road base material." *Journal of Hazardous Materials*, 164(1), 99-104.

Shi, C. (2004). "Steel Slag—Its Production, Processing, Characteristics, and Cementitious Properties." *Journal of Materials in Civil Engineering*, 16(3), 230-236.

Simmons, J., Ziemkiewicz, P., and Black, D.C. "Use of Steel Slag Leach Reds for the Trealtmernt of Acid Mine Drainage ", *National Association of Abandoned Mine Lands Annual Conference*, August 19-22, 2001.

Song, C., Li, M., Xi, B., Wei, Z., Zhao, Y., Jia, X., Qi, H., and Zhu, C. (2015). "Characterisation of dissolved organic matter extracted from the bio-oxidative phase of co-composting of biogas residues and livestock manure using spectroscopic techniques." *International Biodeterioration & Biodegradation*, 103, 38-50.

Sorlini, S., Sanzeni, A., and Rondi, L. (2012). "Reuse of steel slag in bituminous paving mixtures." *Journal of Hazardous Materials*, 209–210, 84-91.

Sparks, D.L. (2003). *Environmental Soil Chemistry*, Academic Press Inc., San Diago, California.

Stumm, W., and Morgan, J.J. (1996). *Aquatic Chemistry: Chemical Equilibria and Rates in Natural Waters*, John Wiley & Sons, Inc., New York, USA.

Stutzman, P.E. (2001). "Scanning Electron Microscopy in Concrete Petrography". *Materials Science of Concrete Special Volume: Calcium Hydroxide in Concrete*, Skalny, J., Gebauer, J., and Odler, I., eds., reprinted from Proceedings of Workshop on the Role of Calcium

Hydroxide in Concrete. Anna Maria Island, Florida, November 1-3, 2000, The American Ceramic Society, 59-72.

Suer, P., Lindqvist, J.-E., Arm, M., and Frogner-Kockum, P. (2009). "Reproducing ten years of road ageing — Accelerated carbonation and leaching of EAF steel slag." *Science of The Total Environment*, 407(18), 5110-5118.

Thomas, J.J., Rothstein, D., Jennings, H.M., and Christensen, B.J. (2003). "Effect of hydration temperature on the solubility behavior of Ca-, S-, Al-, and Si-bearing solid phases in Portland cement pastes." *Cement and Concrete Research*, 33(12), 2037-2047.

Thurman, E.M. (1985). *Organic geochemistry of natural waters*, Martinus Nijhoff/Dr W. Junk Publishers, Dordrecht, the Netherlands

USEPA (1993). "Handbook: Urban Runoff Pollution Prevention and Control Planning." U.S. Environmental Protection Agency, Office of Research and Development, Center for Environmental Research Information, EPA #: 625R93004, Cincinnati, OH, 186.

USEPA (1994). "Land Application of Sewage Sludge." U.S. Environmental Protection Agency, Office of Enforcement and Compliance Assurance, EPA #: 831-B-93-002b, Washington, DC.

USEPA (2000). "Ambient water quality criteria recommendations." Information supporting the development of state and tribal nutrient criteria for rivers and streams in nutrient ecoregion XIV (Eastern Coastal Plain), U.S. Environmental Protection Agency, Office of Water, Office of Science and Technology, Health and Ecological Criteria Division, 822-b-00-022 Washington, DC.

USEPA (2005). "National Management Measures to Control Nonpoint Source Pollution from Urban Areas." U.S. Environmental Protection Agency, Office of Water, EPA #: 841-B-05-0004, Washington, DC, 518.

USGS (2013). "2011 Minerals Yearbook: Slag−Iron and Steel [Advance Release]." van Oss, H.G., ed., U.S. Geological Survey, Survey, U.S.G., Reston, VA, USA, January 2013, 69.61−69.69.

USGS (2015a). "2013 Minerals Yearbook: Slag−Iron and Steel [Advance Release]." van Oss, H.G., ed., U.S. Geological Survey, Survey, U.S.G., Reston, VA, USA, June 2015, 69.61−69.10.

USGS (2015b). "Iron and Steel Slag." Mineral Commodity Summaries, van Oss, H.G., ed., U.S. Geological Survey, Survey, U.S.G., Reston, VA, USA, January 2015, 82−83.

UW (2005). "Standard Operation Procedure: Analysis of Major, Minor and Trace Elements in Soil and Sediment Samples with ICP-OES and ICP-MS", University of Wisconsin - Madison, Soil Testing Laboratory, October 2005. <http://uwlab.soils.wisc.edu/files/procedures/soil_icp.pdf>

van Zomeren, A., van der Laan, S.R., Kobesen, H.B.A., Huijgen, W.J.J., and Comans, R.N.J. (2011). "Changes in mineralogical and leaching properties of converter steel slag resulting from accelerated carbonation at low CO2 pressure." *Waste Management*, 31(11), 2236-2244.

Wang, G., Wang, Y., and Gao, Z. (2010). "Use of steel slag as a granular material: Volume expansion prediction and usability criteria." *Journal of Hazardous Materials*, 184(1–3), 555-560.

Wang, K., He, C., You, S., Liu, W., Wang, W., Zhang, R., Qi, H., and Ren, N. (2015). "Transformation of organic matters in animal wastes during composting." *Journal of Hazardous Materials*, 300, 745-753.

Wang, Q., and Yan, P. (2010). "Hydration properties of basic oxygen furnace steel slag." *Construction and Building Materials*, 24(7), 1134-1140.

Wang, Q., Yan, P., and Feng, J. (2011). "A discussion on improving hydration activity of steel slag by altering its mineral compositions." *Journal of Hazardous Materials*, 186(2–3), 1070-1075.

Wang, Q., Yang, J., and Yan, P. (2013). "Cementitious properties of super-fine steel slag." *Powder Technology*, 245, 35-39.

Wang, X., and Cai, Q.-S. (2006). "Steel Slag as an Iron Fertilizer for Corn Growth and Soil Improvement in a Pot Experiment." *Pedosphere*, 16(4), 519-524.

Warren, C.J., and Reardon, E.J. (1994). "The solubility of ettringite at 25°C." *Cement and Concrete Research*, 24(8), 1515-1524.

Wershaw, R.L., Llaguno, E.C., and Leenheer, J.A. (1996). "Mechanism of formation of humus coatings on mineral surfaces 3. Composition of adsorbed organic acids from compost leachate on alumina by solid-state 13C NMR." *Colloids and Surfaces A: Physicochemical and Engineering Aspects*, 108(2–3), 213-223.

Wintenborn, J.L., and Green, J.J. (1998). "Steelmaking Slag: A Safe and Valuable Product." The Steel Slag Coalition, Association, N.S., November, 1998.

WSA (2013). "Worldsteel Short Range Outlook (SRO) for 2013 and 2014". the World Steel Association (WSA), Brussels, Belgium, 07.10.2013. <http://www.worldsteel.org/media-centre/press-releases/2013/worldsteel-short-range-outlook.html> (October 15, 2013).

WSA (2015). "Crude steel production". *Annual data 1980-2014*, the World Steel Association (WSA), Brussels, Belgium, November 2015. <https://www.worldsteel.org/statistics/statistics-archive/steel-archive.html> (November 20, 2015).

Wu, S., Xue, Y., Ye, Q., and Chen, Y. (2007). "Utilization of steel slag as aggregates for stone mastic asphalt (SMA) mixtures." *Building and Environment*, 42(7), 2580-2585.

Xie, J., Chen, J., Wu, S., Lin, J., and Wei, W. (2013). "Performance characteristics of asphalt mixture with basic oxygen furnace slag." *Construction and Building Materials*, 38, 796-803.

Xu, A., Zhang, H., Yang, Y., Cui, J., He, D.-f., and Tian, N.-y. (2012). "Optimization Study of Calcium Leaching From Steelmaking Slag." *Journal of Iron and Steel Research, International*, 19(4), 34-68.

Yan, J., Moreno, L., and Neretnieks, I. (2000). "The long-term acid neutralizing capacity of steel slag." *Waste Management*, 20(2–3), 217-223.

Yi, H., Xu, G., Cheng, H., Wang, J., Wan, Y., and Chen, H. (2012). "An Overview of Utilization of Steel Slag." *Procedia Environmental Sciences*, 16, 791-801.

Yildirim, I.Z., and Prezzi, M. (2009). "Use of Steel Slag in Subgrade Applications." Joint Transportation Research Program, Indiana Department of Transportation and Purdue University, FHWA/IN/JTRP-2009/32, West Lafayette, Indiana.

Yildirim, I.Z., and Prezzi, M. (2011). "Chemical, Mineralogical, and Morphological Properties of Steel Slag." *Advances in Civil Engineering*, 2011, 13.

Yin, Y., Impellitteri, C.A., You, S.-J., and Allen, H.E. (2002). "The importance of organic matter distribution and extract soil:solution ratio on the desorption of heavy metals from soils." *Science of The Total Environment*, 287(1–2), 107-119.

Zhou, Y.-F., and Haynes, R.J. (2010). "Sorption of Heavy Metals by Inorganic and Organic Components of Solid Wastes: Significance to Use of Wastes as Low-Cost Adsorbents and Immobilizing Agents." *Critical Reviews in Environmental Science and Technology*, 40(11), 909-977.

Zhou, Y., and Haynes, R. (2011). "A Comparison of Inorganic Solid Wastes as Adsorbents of Heavy Metal Cations in Aqueous Solution and Their Capacity for Desorption and Regeneration." *Water, Air, & Soil Pollution*, 218(1-4), 457-470.